SCINTILLATIONS FROM ALPHA TRACKS IN GASES

and

FAST NEUTRONS FROM LOW ENERGY DEUTERON REACTIONS

by

A. Ward

Department of Natural Philosophy

University of Glasgow

Presented as a thesis for the degree of Ph.D.

in the University of Glasgow.

December, 1955.

CONTENTS.

* * * *

APPENDIX.

Preface.

The results of experimental research using scintillation counter techniques are presented in the thesis, which is divided into two parts.

In Part I - "Scintillations from Alpha Tracks in Gases" a description is given of an investigation of the emission of light from the tracks of 5 MeV alpha particles in gases. The light emission is measured by the number of photo-electrons released from the photocathode of photomultipliers rather than the absolute number and wavelength of emitted quanta.

The work described in Part I was done entirely by the author, and the results are original. The experiments performed were intended to cover the main characteristics of the light emission and the results obtained give a fairly clear picture of the mechanism of the process in pure gases and mixtures of gases.

In Part II - "Fast Neutrons from Low Energy Deuteron Reactions in Light Elements", experiments are described in which scintillation

counters were used to investigate the mode of reactions of the type A(d,n)A + p in light elements at low deuteron energies, and the use of these reactions as sources of fast neutrons for scattering and absorption experiments.

Previous to the work described in Part II, very few practical applications had been made of scintillation counters in experiments involving the detection of fast neutrons in the energy range 1 - 15 MeV, due to difficulties inherent in fast neutron spectroscopy. Two techniques developed by the author are described which overcome these difficulties to the extent of allowing quantitative measurements on fast neutrons with comparable precision and greatly improved efficiency in comparison to other techniques.

The interpretation of the results of measurements on fast neutrons by the author is made using the theory of deuteron stripping by Butler (1951) and Bhatia (1952) reviewed by Huby (1953); the concept of the formation and decay of a compound nucleus due to N. Bohr (1937) and discussed by Blatt and Weisskopf (Theoretical

Nuclear Physics and the theory of the effect of Coulomb charge in deuteron stripping by A.H.de Borde, private communication).

In the development of the technique of counting proton recoils in plastic scintillators, described in chapter 1, the author is indebted to Dr. Coon (Los Alamos) for a stimulating discussion during the Nuclear Physics Conference (Glasgow 1954) on his measurements of elastic scattering of fast neutrons using thin crystals of scintillating anthracene. In the application of this technique to the investigation of the reaction $^{11}B(d,n)^{12}C$ (chapter 2) the author was assisted by Dr. P.J. Grant.

The final chapter of the thesis is devoted to a discussion of future experimental research using low energy deuteron reactions in light elements as sources of fast neutrons for scattering and absorption experiments in the light of the work by the author described in the thesis and all known data and current theoretical interpretations.

A method developed by the author to

produce thin deuterium targets is described in the Appendix (section 1). The advice of Dr. J.G. Rutherglen and the assistance of Mr. R. Storey in the construction of the apparatus for making targets is gratefully acknowledged.

The time delay-voltage converter described in section 2 of the Appendix was due entirely to the author, but in the development of the electronic circuit described in section 3 the author was greatly assisted by discussions with Dr. G.W. Hutchinson. Apart from these acknowledgments the work described in the thesis was done entirely by the author and the results obtained are original.

The author is indebted to Professor P.I. Dee for his continued support and encouragement, and many stimulating discussions during the course of the research.

Summary.

Part I.

The emission of light from the tracks of alpha particles in the gases argon, helium, nitrogen and methane has been studied using a photomultiplier.

The specific emission has been measured together with the total number of emitted photons which are produced in the range 3,000 - 6,000 Å. The total number of emitted photons is found to be independent of pressure in the monatomic gases argon and helium but varies with pressure in nitrogen and in mixtures of methane with argon or helium. The variation with pressure is explained in terms of quenching by collision. The lifetime of the excited states responsible for the emission is estimated to be less than 10^{-6} sec. The recombination of ions is shown to play no appreciable part in the production of the photons.

The results of the experiments give a fairly clear picture of the events in a gas, traversed by heavy charged particles, which lead to the emission of visible light.

Part II.

In an introduction the significance of low energy deuteron reactions in light elements as sources of fast neutrons for scattering and absorption experiments, current theories describing the reactions themselves and the limitations of existing fast neutron counting techniques are discussed.

Two scintillation counter techniques for fast neutron counting have been developed by the author and are fully described.

One of these techniques relies on measurements of the energies of recoil protons in hydrogeneous scintillators and has been used to study the reactions $^{11}B(d,n)^{12}C$, $^{2}H(d,n)^{3}He$ and $^{3}H(d,n)^{4}He$ at low deuteron energies. The results of these investigations clearly show that the theory of deuteron stripping successful at high deuteron energies requires modification at low energies. The source of the deviation from theory and the required modification are discussed.

The other technique relies on measurements of neutron times of flight to obtain neutron energy spectra and has been used to measure the inelastic neutron spectrum following scattering of 14 Mev neutrons in aluminium.

In a final chapter, the possible future significance of low energy, high deuteron beam current Cockcroft-Walton accelerators for research using fast neutrons is discussed with reference to the techniques developed and the results obtained by the author and recently by others in this field.

The Appendix contains details of electronic circuits developed and technical data obtained during the research described in the thesis.

PART I.

SCINTILLATIONS FROM ALPHA TRACKS IN GASES

Introduction

Scintillations from gases refers to the emission of light from the tracks of heavily ionising particles in gases. In the experimental work by the author, described in the thesis, alpha particles from polonium were used, because they gave a convenient source of monoenergetic heavy charged particles with an energy of five million electron volts. The effects observed with alpha particles suggest strongly that the numerical results obtained can be extrapolated to higher energies and other types of particles, such as deuterons, protons and mesons.

It has been known since the earliest days of radioactivity that the emission of light in the visible spectrum can be observed in the vicinity of strong radioactive sources in air. The beam in modern machines for the acceleration of heavy particles to high energies, such as high tension accelerators, Van de Graaff generators, cyclotrons and linear accelerators, is often detected by the experimenters observing the faint emission of blue light from the track of the beam in the residual gas of the acceleration chamber. The light emission from

an external beam (i.e. in air at atmospheric pressure) of heavy particles from such a machine is intense.

The emission of visible light from gas atoms excited by electrons is a phenomenon frequently encountered both in and outside research laboratories. One of the most important simple applications of this emission in technology is the detection of leaks in high vacuum systems by observing the change in colour of a discharge tube when a little gas or organic vapour enters the system through the leak.

Owing to experimental difficulties, mainly the high cost of strong sources of heavy particles and the low intensity of the light emission, little experimental research has been done on the emission of visible light from the tracks of heavy charged particles in gases. The development of the modern photomultiplier, with a sensitivity curve

not very different from that of the eye and a far higher detection efficiency for transient light pulses has now made it possible to investigate this emission quantitatively with weak sources of heavy particles. So little had appeared in print on this subject previous to 1953 (Green and Schopper 1952) that when the initial effects, which led to the investigations described here, were first observed it was only after a process of elimination and deduction from observations that the effects were attributed to scintillations from gases. The results obtained by Green and Schopper show that the light emission from nitrogen and argon is equivalent to the emission of approximately 1,000 photons in the visible spectrum (per polonium alpha particle) in so far as the effect of the emission in releasing electrons from the cathode of photomultipliers is concerned. In addition, the above authors found that oxygen did not scintillate appreciably, and that traces of organic vapours reduced the efficiency of light production. The order of magnitude of the total light emission observed by Green and Schopper, (1952)

which is confirmed by the author for nitrogen and argon, and several other gases, indicates that in comparison with liquid and solid scintillating materials (Birks 1953) the gases studied so far have very low efficiencies and have no obvious applications as practical scintillaters in counting experiments. However, so little appeared to be known about scintillations from heavily ionising particles in gases that the subject invited further investigation. Although the research by the author described in the thesis does not comprise a complete and exhaustive study of the effects associated with scintillations from gases, an attempt was made toperform experiments designed to throw light on the initial production of the excited states and their subsequent de-excitation by quenching or by emission of radiation. As a result of the experiments described in part I of the thesis it is possible to construct a simple semi-quantitative picture of the events in a gas or mixture of gases, following the passage of a heavy charged particle, which lead to the emission of light in the visible spectrum from the gas.

SCINTILLATIONS FROM GASES

CHAPTER 1.

The Efficiency of Production of Photons Effective in Releasing Electrons from the Photocathode of Modern Photomultipliers.

A discussion of scintillations from gases when traversed by heavily ionising particles must begin by some remarks on the yield of useful photons observed to be emitted from the gas when a known amount of energy is lost by an ionising particle in the gas. The phrase useful photons should be understood to refer to the fact that since the sensitivity of a photomultiplier to light is appreciable over a restricted region of the spectrum, then only photons with a wavelength in this restricted region can be termed useful in the sense that they are likely to release photo-electrons from the photocathode.

Unlike the human eye, a modern photomultiplier has no means of indicating the wavelength of photons responsible for electron emission from the photocathode, other than the suggestion that if photo-electrons are emitted then the photons responsible for the emission probably lie within the region of wavelengths in which the sensitivity of the photomultiplier is highest.

By interposing absorbers between the photocathode and the scintillator it is clearly possible to arrange

that only light within a very restricted region, e.g. 100 A^{o}, of wavelengths is allowed to reach the photocathode. By keeping this channel width of transmitted wavelengths constant, varying the upper and lower edges and correcting for the known sensitivity of the photomultiplier it would be possible to obtain the true spectrum of the light emitted as scintillations from a gas. (The usual type of wavelength spectrometers which have better resolution require somewhat stronger sources of light than are generally available using radioactive sources such as polonium). This has not been attempted here since the available range of absorbers could not cover the expected spectrum.

While this is regrettable, it has been possible to define a quantity related to the emitted spectrum, which can be measured and which allows quantitative experiments. The symbol N_e will be used here for this quantity which is defined as the number of equivalent photons which are emitted into a solid angle of 4π when an alpha particle loses 5 Mev energy in a gas. The number of equivalent photons is that number of photons of a wavelength at the peak of the sensitivity curve of the photomultiplier which would release the same number

of photoelectrons from the photocathode as the actual light emission when an alpha particle loses 5 Mev energy in a gas.

This quantity N_e will be different when measured using photomultipliers with different spectral response. Experiments will now be described which allowed estimates of Ne to be made for different gases using an E.M.I. photomultiplier, type 5311.

Experimental Procedure

A small tungsten lamp was placed at a distance of 40 yards from the photo-cathode of a photomultiplier. The temperature of the filament was found by measuring the power dissipation in it. From the temperature the spectral distribution from the lamp was deduced on the assumption that it behaved like a black body and that the efficiency of conversion of electric power to radiation was 100%.

Tungsten lamps lose less than 10% of the power they consume in processes other than radiation, and the spectral distribution is the same as a black body of temperature T corresponding to power dissipation W according to the tables of Harrison et al (1948).

The photoelectrons released from the photocathode by the light from the lamp passed with electron amplification through the stages of the photomultiplier to the collector. The collector resistance R and capacity C were adjusted so that $CR \sim 10^{-6}$ sec. The pulses appearing on the collector passed through a cathode follower and were then amplified by an amplifier with a bandwidth of 500 K c/s, T.R.E. type 1008A. The pulses from the output of this amplifier were fed to a discriminator and scaler type 1008. By counting the number of pulses above a fixed pulse height on the scaler when the lamp was moved to various distances from the photomultiplier cathode, it was verified that this measured counting rate varied strictly according to the inverse square of the distance between the lamp and the photomultiplier, and that the straight line when extrapolated passed through the origin at infinity.

The number of counts in the scaler was observed for a known bias in the discriminator and a measured energy dissipation in the tungsten lamp placed at a measured distance from the photomultiplier. Immediately afterwards for the same bias in the discriminator the number of counts in the scaler was observed for a measured number

of alpha particles losing a known fraction of their energy in a gas in close proximity to the photocathode of the photomultiplier. It is easily seen that the equivalent photon emission from the gas is given by

$$N_e = \frac{\theta n}{\epsilon} \cdot \frac{S'}{S} \cdot \frac{E_\alpha}{E} \cdot \frac{1}{M} \quad \ldots\ldots\ldots(1)$$

where n is the number of equivalent photons emitted by the lamp in one second, and is obtained by the cross-integration of the photomultiplier sensitivity curve and the actual emission from the lamp which was found by the method described above. θ is the fraction of the number of equivalent photons produced by the lamp which fell upon the window of the multiplier, ϵ is the efficiency of collection of the light produced by the α -particles in the gas, S'/S is the ratio of the counting rates on the scaler for the α -induced gas emission and the lamp respectively, E/E_α is the fraction of α -particle energy absorbed in the gas, and M is the number of α -particles absorbed per second. For equation (1) to hold it is necessary to keep E so small that rarely does the same α -particle cause the emission of more than one photo-electron from the photocathode. It was verified that this condition was satisfied by

comparing the pulse height distribution from the lamp with that from the α -particles absorbed in the gases. The evaluation of n was facilitated by using a high lamp temperature because the cross integration between the emission spectrum of the lamp and the sensitivity curve of the photomultiplier is more accurate under this condition. To avoid saturation of the photomultiplier from such a bright light D was kept very large and it is believed that n was measured to within a factor of two. For the calculations ϵ was evaluated by blackening the walls of the α -particle chamber and estimating the average solid angle subtended by the photocathode to the gas. Some error in the evaluation of ϵ will remain owing to the fact that the photons from the gases do not all pass normally through the surface of the quartz. Furthermore, the photons passing obliquely into the photocathode are more likely to produce photo-electrons than are those which pass through the surface normally. The photomultiplier used in these experiments had a sensitivity of ten equivalent photons per emitted electron.

The table shows the values obtained for N_e for different gases at atmospheric pressure by substitution of the above measured quantities into equation (1).

For comparison, the corresponding figure for an anthracene crystal is included (Birks 1953).

TABLE I

Gas	Nitrogen	Argon	Helium	Methane	Anthracene Crystal
N_e	150	250	1000	-	9000

Owing to the uncertainties involved these figures should only be taken as a guide in experiments using photo-multipliers with response curves similar to that used by the author. It was found that the scintillations from air produced almost the same counting rate on the scaler as did those from nitrogen. For the compilation of this table it was assumed that in all gases the specific efficiency of photon production varies with alpha particle energy in the same way as the Bragg curve of ionisation.

As a check on the quantitative value of the results given by the experiment described above, the results of a later experiment may be quoted here.

In this experiment, which will be described below, an effort was made to achieve a high efficiency of light collection from the tracks of alpha particles in gases. Under these conditions values of N_e were deduced from measurements of the average pulse height due to scintillations from the gases. The possibility of obtaining an estimate of Ne in this way arises out of several

factors. The values of N_e given in table I suggest that if each photon has an appreciable chance of producing a photoelectron when it passes into the photocathode, a scintillation normally results in the release of several photoelectrons. The corresponding voltage pulses from the photomultiplier can, therefore, be considerably larger than those due to only one electron leaving the photocathode.

. This will only be true if a large fraction of the light emission from the gas is 'collected' by the photocathode and if the electron charge at the collector due to the release of each separate photoelectron does not leak away through the leakage resistor R faster than the average time interval between the emission of each photoelectron. That is, the time constant for decay, CR, of the charge on the collector with capacity C must be much greater than τ the lifetime against decay of the excited atoms in the track of each alpha particle. It will be shown later, in the section describing the experiment, that the lifetime of the excited states responsible for the

scintillations is less than 10^{-6} sec.

The lamp was operated at temperature T. From the temperature T the actual emission spectrum of the lamp was calculated using the usual expression for black body radiation. The brightness of the lamp at this temperature was obtained from the manufacturer's data and expressed in lumens per second. The number of equivalent photons corresponding to this emission was then found by evaluating the overlap integral of the emission spectrum and the spectral response curve of the photomultiplier. In this way the number of equivalent photons emitted by the lamp for a definite number of lumens was obtained. The number of electrons released from the photocathode per equivalent photon was then derived from the sensitivity of the photocathode in microamperes per lumen. The value obtained was one electron per ten equivalent photons. Clearly this value could have been measured in the laboratory using the procedure of the previous experiment; it is perhaps to be regretted that this was not done. Since each of these photomultipliers were tested separately by the manufacturers this may not have been too important a source of error.

Where $\underline{t}$ is the transparency as defined above,

ϵ is the efficiency of light collection by the photocathode,

E/E_α is the fraction of energy lost by a polonium alpha particle in the gas,

V_o is the mean pulse height due to one photoelectron,

V_E is the mean pulse height due to a scintillation corresponding to an energy loss E.

N_e is given by $N_e = \frac{V_E}{V_o} \cdot \frac{E_\alpha}{E} \cdot \frac{1}{\epsilon t}$ ..... (2).

The values of N_e obtained by inserting the measured quantities into equation 2 indicate that the relative efficiencies of the gases given in the above table are correct to $\sim 5\%$ and the absolute efficiencies to within $\sim$ 50%, which is consistent with the systematic errors involved in both experiments.

Conclusions.

It is concluded that the values given in the above table for the relative efficiencies of the scintillations from different gases are accurate, that it is very unlikely that the absolute efficiencies are wrong by more than a factor of two, and there is indirect evidence that t = 10%.

It is clear from the values given in table I and the value of the transparency t that it is possible to arrange that the scintillation from an alpha particle in a gas very rarely results in the emission of more than one photoelectron from the photocathode by collecting a sufficiently small fraction of the total light emitted. When such an arrangement is used it is possible to state without reservation that the counting rate in a scaler recording pulses above a given voltage height on the collector is directly proportional to the number of photons emitted per alpha particle track in a gas, provided the number of alpha particles remains constant.

This conclusion is essential for the interpretation of several of the experiments to be described below.

CHAPTER 2.

The Specific Emission as a Function of the Velocity of the Particle.

In the previous chapter experiments were described which allowed a measurement of the total light emission from the track of an alpha particle in a gas, in terms of equivalent photons.

In this chapter experiments are described which allowed the variation of the emission of light from the track of an alpha particle in a gas to be measured. The measurements described here of $\frac{dNe}{dE}$ are in fact measurements of a quantity proportional to $\frac{dNe}{dE}$, the value of the constant involved is obtained by equating the whole area under the curve to the values given in the table of the previous chapter. Therefore, the absolute value (in terms of equivalent photons) of the specific emission curve is known only to within the accuracy of the values given in the table for the total emission. The error in the shape of the curve for the specific emission is very much less and was determined by the errors involved in the experiments described in this chapter.

Experimental Procedure.

Figure 1 shows an apparatus designed to measure the variation of light emission along the track of an α -particle as it slows up and stops in the gas. A clean polonium source was made from stock solution by deposition on silver and waxed on to a lead block at the top of the chamber. The particles travelled down the mid-section, passed through a thin aluminium window into a small chamber 3 mm in depth and were finally stopped in a piece of clean crystalline quartz

forming the bottom plate of the chamber. The gas to be investigated was introduced into the chamber through a copper pipe and the light produced along the α -particle tracks passed through the crystalline quartz and was detected by an E.M.I. photomultiplier type 5311 placed immediately below. No liquid paraffin or similar usual coupling medium was inserted between the quartz and the glass envelope of the photomultiplier in case the ultra-violet emission from the gas might be converted to visible photons which would have produced spurious counts in the multiplier. The photomultiplier was followed by an amplifier, discriminator and scaler. Air at known pressure introduced into the mid-section provided variable absorption in the path of the α -particles, while the aluminium window served as a vacuum seal and also prevented light from the mid-section reaching the photomultiplier. This method of absorption was adopted in preference to the use of foils in order to avoid the possibility of light from the room reaching the photomultiplier between readings. It had previously been found that if this occurred a temporary increase resulted in the noise current

from the photo-cathode having the same pulse height distribution as the signals due to photon emission from the gas in the chamber. Crystal quartz was observed to scintillate feebly under α -particle bombardment, but the necessary correction for this effect was determined by introducing methane (a non-scintillating gas) into the chamber and repeating the observations. To estimate the range distribution of the particles reaching the chamber, as the pressure of air in the mid-section was varied, separate experiments were made with a ZnS screen above the quartz.

A determination of the specific emission of photons by helium under α -particle bombardment is shown in figure 2 , and for comparison the Bragg curve of ionization. Since the polonium source was weak it was not possible to collimate the α -particles and the spread in the α -particle ranges had a half-width of 5% of the mean range. The variation of emission along the track in air was found to be similar to that for helium.

Conclusions

It is concluded from these experiments that the specific ionisation and the specific emission

follow each other as the velocity of the alpha particle varies along the track.

It is clear that any value which the shape of the curve in fig.2 has is determined by the degree of linearity between the counting rate in the scaler and the light emission from the gas. It was arranged using the values of N_e given in the table of the previous chapter that the probability of any one alpha particle causing the release of more than one photo-electron from the photocathode was very small. Under this condition the variation of counting rate in the scaler is a true reflection of the variation of light emission along the track of the alpha particle.

Only two gases were investigated, air and helium. These two were specifically chosen because they each belong to one of the two main groups of scintillating pure gases, and it was thought necessary to observe whether there was any difference in specific emission between gases belonging to the two groups. No difference was observed between the curves for air and helium. This classification of the scintillating gases into two groups will be discussed later in the chapter describing the effects observed when the pressure of the scintillating gas is varied.

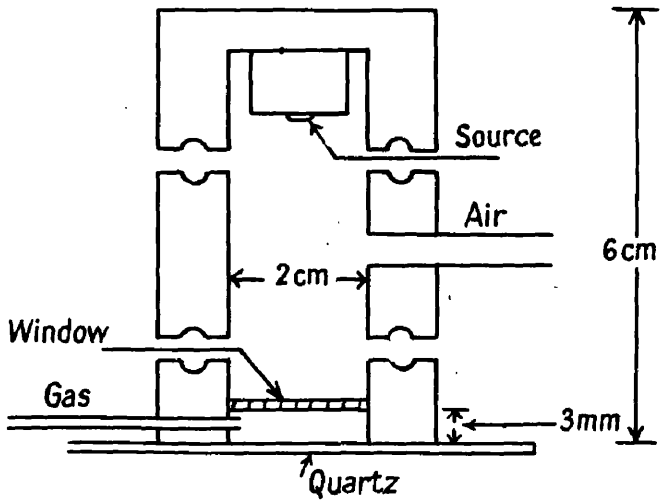

Fig.1.

Apparatus for measuring the specific excitation.

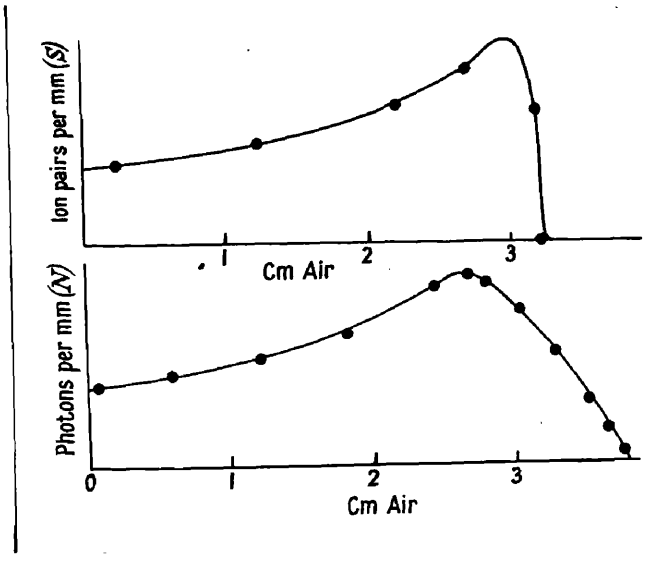

Fig.2.

Specific excitation as a function of alpha particle range in helium.

CHAPTER 3.

The Origin of the Light Emission Observed as Scintillations from Gases.

In the experiments described in the previous chapter it was shown that the specific excitation varies with velocity in the same way as the specific ionisation. This similarity can arise in two ways, either the light emitted from the track comes from the recombination of ions or from the de-excitation of atoms excited by the passage of the alpha particle. In both these cases it is to be expected that the observed variation of specific excitation as a function of velocity should follow closely the specific ionisation. That this should be so for the former is trivial, but if it can be shown that the origin of the light is from the latter then direct evidence has been obtained for a source of energy loss by a heavy charged particle in a gas which does not involve ionisation. The simple model for the Bragg curve of specific ionisation predicts that the specific excitation should be identical to the specific ionisation. There is, in fact, no real difference between the two since the ions are atoms excited into the continuum of energy levels above the binding energy of the electron to the nucleus.

The possibility that the light observed as

scintillations arises from the recombination of excited ions cannot be overlooked, however, so an experiment was performed to find out how much, if any, of the light in a scintillation from an alpha particle track in a gas comes from the de-excitation of atoms directly excited by the passage of the alpha particle. This experiment is described below.

Experimental Procedure.

An apparatus was constructed in which alpha particles from a strongly collimated source of polonium passed through approximately 3 cms. of gas. At right angles to the track of the alpha particles a photomultiplier was placed and by a slit arrangement it was possible to restrict the "view" of the photomultiplier to the gas in the immediate vicinity of the alpha particle tracks. Again at right angles to the alpha particle tracks, but also at right angles to the photocathode of the photomultiplier, two electrodes were placed in the gas. These electrodes, one on either side of the tracks, were out of the "view" of the photomultiplier. This arrangement is shown in figure 3.

The pulses from the photomultiplier were amplified by a 1008 amplifier, and at the output they

had a duration of $2 \cdot 10^{-6}$ sec. These output pulses from the amplifier were fed into a discriminator and scaler. The counting rate in the scaler was directly proportional to the light emission from the gas.

When a voltage difference was applied to the two electrodes in the gas, a current was obtained which, for a sufficiently large voltage, was observed to show little increase for further increase of applied voltage to the electrodes. Under these conditions the current collected by the electrodes was very nearly equal to the rate of production of ions by alpha particles in the gas. That is little recombination of ions occurred in the immediate vicinity of the alpha particle tracks.

When the gas was removed from the chamber the counting rate in the scaler fell to less than 1% of the counting rate when the gas was present and when the alpha particles were blocked off by an obstruction the electrode current fell to zero at high gas pressures.

The experiment consisted of observing the change in counting rate in the scaler when the gas was present and the applied voltage on the electrodes was varied.

No change in counting rate was observed in the scaler when the applied voltage to the electrodes was removed completely. This was observed when the gas was air and also for helium, the two gases investigated. The initial applied voltage was sufficient to achieve almost 100% collection of ion pairs formed in the gas by the alpha particles.

Conclusion.

It is concluded that the origin of the light detected as scintillations from gases is not the recombination of ion pairs produced in the gases by the alpha particles. The result of this experiment shows that the two effects; production of ion pairs and emission of quanta are quite separate in the sense that one does not follow from the production of the other. Each effect results independently following the primary loss of energy by an alpha particle in a gas.

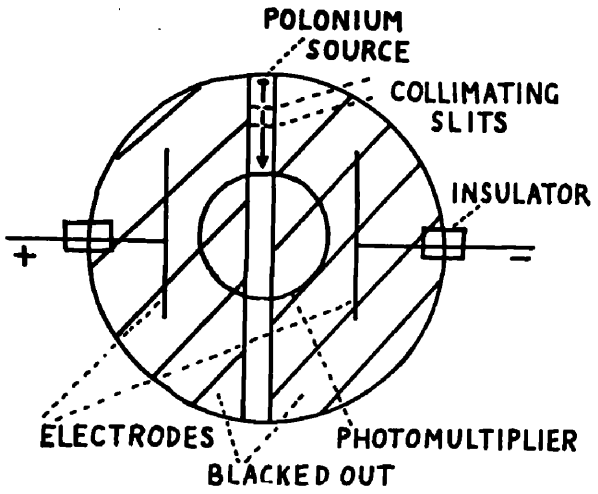

Fig.3.

Apparatus for estimating the contribution to the observed light emission due to recombination of ions.

CHAPTER 4.

The Lifetime of the Excited States against Emission.

The wavelengths of the light observed as scintillations in these experiments have not been investigated. The spectral response curve of the photomultiplier falls to a very low value or zero beyond the limits of the visible region of the spectrum. It, therefore, seems very probable that the scintillations counted in these experiments consisted of photons with wavelengths in the visible region.

The upper limit in the infrared is due to the work function of the oxide film of the photocathode, and the lower limit in the ultraviolet is determined mainly by the absorption of the glass envelope of the photomultiplier used. In the far ultraviolet the sensitivity of photomultipliers has not been investigated and it is necessary to take into account a possible deviation from the simple picture described above for the sensitivity curve of a photomultiplier.

Light emission from a gas such as helium is very likely to be of two main types, far ultraviolet and visible or near visible. This can be inferred

from the level structure of excited states of atomic helium. The photons in the visible spectrum must result from transitions between very highly excited states, with the eventual emission of a far ultraviolet photon as the atom returns to the ground state. Only a small proportion of the true emission can be expected to have wavelengths in the region of sensitivity of the photomultiplier. This argument is indicated by the simplified level structure of helium, shown in figure 4 . However, the photons in the far ultraviolet region of the spectrum may, when they are absorbed by the glass envelope of the photomultiplier, cause the glass to fluoresce or phosphoresce with the resultant emission of photons in the visible spectrum. If this process of conversion of photons to longer wavelengths by the glass has a high efficiency the contribution of the far ultraviolet emission from the gas to the scintillation as observed by the photomultiplier may be sufficiently large to compete with the emission of "visible" photons by the gas atoms.

It is well known that the far ultraviolet emitting levels in helium have lifetimes of the order 10^{-4} sec., while there is theoretical and experimental evidence that the lifetime of "optical" transitions

are of the order 10^{-7} 10^{-8} sec. Any process of conversion of wavelengths can only lengthen the observed lifetime. Therefore, any experiment designed to measure the lifetime of the excited states responsible for the light in a scintillation from helium gives information on the probable wavelengths of the light emission which effects the photomultiplier.

A very simple experiment has been performed and is described below which made it possible to discriminate between the two widely spaced possible values for the lifetime stated above.

Experimental Theory and Procedure.

This method of estimating the effective lifetime against radiation of the excited states responsible for a scintillation from a gas is based on the following argument.

Consider the emission of N_e equivalent photons from a gas due to the passage of an alpha particle through the gas. On the average these photons will release of the order $N_e/10$ photoelectrons from the photocathode of the type used in these experiments. Each of these photoelectrons will cause a cascade of electrons through the dynode stages of the photomultiplier

and eventually each cascade will produce a negative voltage edge on the collecting anode. When CR the leakage time constant of the collecting anode is very much less than the time interval between these edges the output from a broad band amplifier attached to the collecting anode will consist of Ne/10 separate pulses, with an average height V_o say, and when CR is very much longer than the above time interval the output from the amplifier will be one large voltage pulse of a height equal to $\frac{Ne}{10} \times V_o$. This condition can be expressed by the relations

$$CR << \tau \quad Ne/10 \text{ small pulses of height Vo} \quad \ldots(1)$$

$$CR >> \tau \quad 1 \text{ large pulse of height } \frac{Ne}{10} \times V_o \quad \ldots(2)$$

Clearly these relations make it possible to make experimental observations which can discriminate between two widely different possible values of τ by choosing a suitable value of CR and observing whether one large pulse or several small pulses results from increasing the number of photons emitted from a gas for each alpha particle passing through it. This technique is only possible if N_e is greater than unity. The values of Ne given in the table in the first chapter show

that this is the case for 5 Mev alpha particles in several gases including helium.

The experimental procedure adopted here was as follows. The gas being investigated was enclosed in a pressure tight box with a glass window. Alpha particles from a polonium source enclosed in the box produced scintillations from the gas. The photons composing the scintillation from each alpha particle traversing the gas at pressure p passed through the glass window and were detected by the photomultiplier. The voltage pulses on the collecting anode of the photomultiplier with a value of CR equal to $2 \cdot 10^{-6}$ sec., were amplified without distortion by a broad band amplifier. A scaler counted all of these pulses above a voltage bias V on a discriminator attached to the output terminal of the amplifier.

By removing the gas chamber and allowing a little light from a tungsten lamp to fall on the photomultiplier it was possible to observe a plateau in the graph of counting rate N in the scaler against voltage bias V in the discriminator. This plateau was interpreted as being due to counting all the pulses

resulting from single electrons being released from the photocathode by photons from the tungsten lamp. The value of V at which the counting rate N was one half of the counting rate on the plateau was equated to V_o as defined above. The lamp was then removed and the gas chamber replaced. The experiment then consisted of observing the plateau for different pressures of gas and plotting the average pulse height against the pressure p. The average pulse height was again taken as being the value of V at which the counting rate in the scaler was one half the value on the plateau.

It was found that the average pulse height from air, argon, and helium coincided with V_o at low pressures but rose with no indication of flattening off as the pressure increased. The counting rate approached but did not exceed the number of particles per second leaving the polonium source in the gas chamber. These results are shown in figure 5.

Conclusions

It is concluded that the effective lifetime of the excited states responsible for the emission

of the photons in a scintillation from alpha particles in these gases is $\sim 10^{-6}$ sec. This interpretation is supported by a comparison of the values of N_e which can be calculated from the results in figure 5 , and compared with those given in the table in the first chapter, by allowing for the solid angle of acceptance of the photocathode to the gas. It has already been stated in the first chapter that the values of N_e obtained in this way are in good relative agreement and the absolute values agree reasonably well.

In the particular case of helium it is further concluded that the far ultraviolet emission contributes little to the scintillation as observed by the photomultiplier.

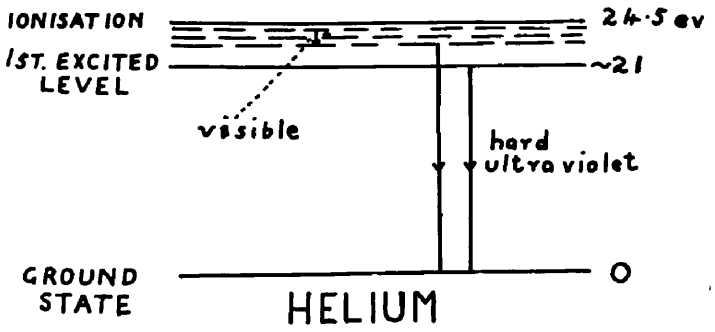

Fig.4.

Simplified level structure of helium, indicating "visible" and ultraviolet transitions.

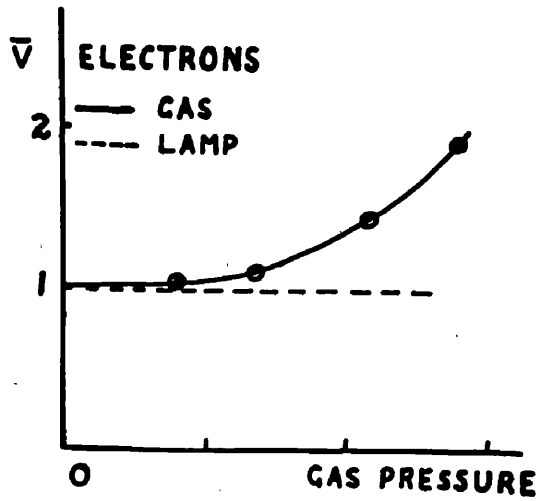

Fig.5.

Effect of pressure on the average pulse height due to scintillations compared with the average pulse height due to single photons from a tungsten lamp.

CHAPTER 5.

The Variation of Efficiency with Pressure.

It was found that the amount of light emitted from nitrogen, for the same amount of α -particle energy absorbed, varied with the pressure. This variation is shown as the broken line in figure 6 . An almost identical curve was obtained for air. This curve was obtained using a chamber whose dimensions were small compared with the range of the α -particles from a bare source of polonium, at the highest pressures used. The efficiency of collection of the light emitted was low to avoid the possibility that one α -particle might cause the emission of more than one photo-electron from the photo-cathode. As has already been explained, this allows N the counting rate on a scaler following a pulse-height discriminator to be taken as directly proportional to the number of photons emitted from the tracks of the α -particles. It can be seen from figure 6 that N increases linearly with pressure, below 10 cm Hg, but above this value the curve flattens off.

Factors which might be thought to be responsible for the form of this curve include oxidation of the source, de-excitation on the walls

of the chamber, self-absorption by the nitrogen and the emission of densely ionizing short range particles by the source. The effects of such factors were examined by turning the source away from the multiplier, changing radically the shape of the chamber and painting it inside, introducing an air gap between the chamber and the photo-cathode, and covering the source with an aluminium foil of stopping power equivalent to a pressure of 10 cm of air. None of these control experiments were found to affect the observed variation of N with pressure. In addition, the same curve was obtained by plotting the increase in the current flowing through the photomultiplier as the pressure was varied.

It is natural to attribute the saturation with pressure of the observed variation of photon emission to de-excitation of excited molecules (quenching) by collision with unexcited molecules. The application of the simple theory of optical quenching to this problem leads to the result that N (the counting rate in the scaler, which is proportional to the rate of emission of quanta from the gas) varies with pressure according to the relation

$$N = Kp(1 + kp)^{-1}, \quad \ldots\ldots\ldots \quad (1)$$

where $kp = n_c \tau / n_o$, (2), τ is the lifetime of the excited states involved, n_c is the number of collisions per second in the gas, n_o is the mean number of collisions before quenching occurs and K is a constant independent of pressure. According to equation (1) there should be a linear dependence between N^{-1} and p^{-1}. The experimental observations are in approximate accord with this result, but there is some indication that processes other than collision quenching may also have to be taken into account in order to explain the pressure variation precisely. However, by assuming that most of the variation with pressure of the photon emission from the optically excited states is due to quenching an approximate value for n_o can be obtained from equation (2).

The value of n_o obtained in this way for the diatomic gas nitrogen is of the order unity when is taken to be of the order of 10^{-8} second. It is interesting to note that similar values for are found for the quenching of the mercury resonance line by organic vapours (Mott and Massey 1949).

It had already been found that the light output from the monatomic gases argon and helium

increased linearly with pressure up to one atmosphere, the highest pressure used. Therefore as a further test of the simple theory outlined above, the variation with pressure of the light output from argon or helium was investigated when they contained small concentrations of methane, which is known to quench by collision excited states in argon (Curran and Craggs 1949).

The results for argon-methane mixtures are shown as the full lines in figure 6 . Similar results were obtained for helium-methane mixtures. It was verified that methane did not appreciably absorb the photons from argon or helium by separate experiments in which a chamber containing methane was interposed between the gaseous scintillator and the photomultiplier. If the value of τ for the argon excited states is taken to be of the order 10^{-8} second, n_0 for collisions of excited argon molecules with methane is again of the order unity. It can be seen that at low pressures the curves rise above the straight line for pure argon, suggesting that at low pressures the relatively long-lived ultra-violet emitting metastable argon states are contributing.

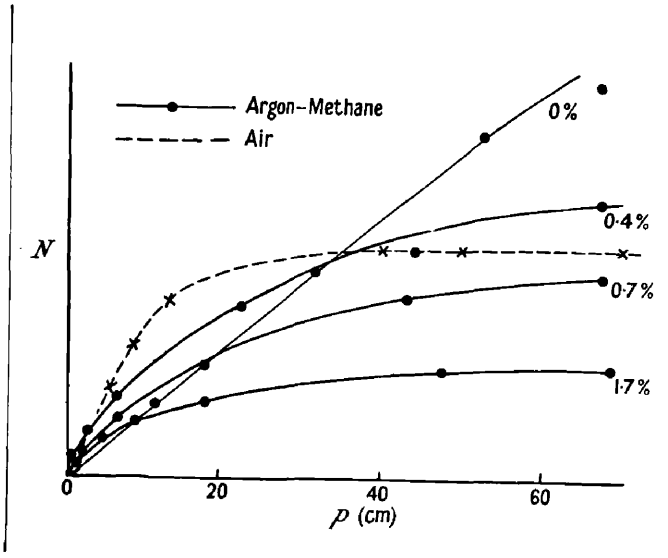

Fig.6.

Variation of efficiency with pressure in air, pure argon and mixtures of argon and methane.

Some Remarks on the Light Emission from Alpha Tracks in Gases.

The results of the experiments described in the previous chapters make it possible to construct a simple picture of the main events in a gas which lead to the emission of light, following the absorption of a heavy charged particle.

The similarity observed between the specific emission and the specific ionisation (chapter 2) suggests that the specific emission is a function of speed. Although it is probable that the primary excitation includes a contribution from delta rays it is natural to attribute most of the primary excited levels to direct excitation by the alpha particle. Both sources of excited levels lead to a specific emission curve similar to the specific ionisation as a function of heavy particle speed. The light emission from the tracks of mesons, protons, deuteron, tritons and other heavy charged particles in gases can, therefore, be deduced from the results obtained in the experiments described here (In this connection it is of interest to note that these results have been used by others,

to estimate the contribution to the glow in the night sky due to Cosmic rays).

The estimates of the total efficiency of light production given in chapter 1 show that as practical scintillators the gases investigated have too low an efficiency for most practical purposes. Krypton, the most efficient gas found so far, has however been used by Boicourt and Brolley (1954) to measure the energy distribution of fission recoils. In this practical application the efficiency was increased by converting, in a thin plastic scintillator, some of the emission in the ultraviolet into visible light. The radiative lifetime is probably 10^{-8} sec., and it seems probable that some further applications of gas scintillators will be made in experiments requiring short coincidence resolution times.

The result of the experiment described in chapter 3 appears to indicate that the light observed from the gas comes from the vicinity of the track and not from de-excitation on the walls of containers. This conclusion adds weight to the interpretation in terms of quenching by collision, of the variation of efficiency with pressure described in chapter 5. This interpretation of the results of these experiments

implies that the amount of visible light observed from pure monatomic gases such as helium, neon, argon and krypton is the maximum which can be obtained from these gases, whereas the visible light observed from pure diatomic gases such as nitrogen and oxygen is reduced by self-quenching by collision. Thus at low pressures, where self-quenching is small, the efficiency of nitrogen gas is greater than that of helium, but at atmospheric pressures helium is more efficient than nitrogen. The effect of polyatomic impurities in gases is in general a reduction of the visible light emission from the gases, probably because the light emission observed from the pure gases is likely to be lost if the energy of excitation is transferred by collision to a polyatomic molecule which has many competing ways in which it can get rid of its excitation energy, only a few of which will result in the emission of visible light.

However, the fraction of the total energy of the heavy charged particle absorbed which is emitted as visible light is very small (chapter 1), and the level structure of the atoms of most gases show that much of the energy must be emitted eventually as very hard ultra-violet light. (This can be compared with

the ultra-violet emission from fluorescent lamps which is allowed to strike material painted on the inner wall which then fluoresces with the emission of visible light). It seems probable that the efficiency of a gas may be increased very much by the addition of sensitising agents (which have yet to be found) which will pick up the energy of excitation by collision and subsequently emit visible light. An indication of this effect (at low pressures helium-methane) is seen in the results of chapter 5, but methane is not suggested as a suitable sensitiser.

It does, however, seem probable that a search would reveal suitable gas sensitisers which would increase the overall efficiency of production of visible light from the tracks of heavy charged particles in pure gases, the process being analogous to those occurring in the well known mixtures of liquid and solid scintillating materials.

PART II.

FAST NEUTRONS FROM LOW ENERGY DEUTERON REACTIONS

Introduction.

The table on the following page shows all the observed and energetically possible reactions of the type A(d,n)A + p in light elements up to carbon. The table has been compiled from data in the reviews of Ajzenberg and Lauritsen (1952, 1955) of reactions in light elements. The Q values for the reactions are given in the table only for the ground state transition and for neutrons leaving the final nucleus in the first and second excited levels. The neutron spectra from these reactions have been measured using nuclear emulsions to detect emitted neutrons (see Huby 1953). The accurate Q values given in the table are not derived from the results of such measurements, but from reaction data leading to what are assumed to be the same levels of the final nucleus (A + p). This data has been obtained by precision measurements of nuclear masses, magnetic analysis of energies of recoil or associated charged particles and precise measurements of gamma ray energies using pair spectrometers. The accuracy in the Q values obtained from direct measurements of neutron

spectra is about a factor of at least ten less than that in the values given in the table, but within this experimental error the neutron energies observed correspond to the known energy levels and ground state of the light nuclei

$A(d,n)A + p$

Reaction	$H^2(d,n)He^3$	$^3H(d,n)He^4$	$Li^6(d,n)Be^7$
Q_m(Mev)	3·27	17·58	3·375
Q_1(Mev)			2·945
Q_2(Mev)			1·275

Reaction	$Li^7(d,n)Be^8$	$Be^4(d,n)B^{10}$	$^*Be^{10}(d,n)B^{11}$
Q_m(Mev)	15·02	4·36	12·369
Q_1(Mev)	12·1	3·64	10·129
Q_2(Mev)	10·8	2·62	7·909

Reaction	$B^{10}(d,n)C^{11}$	$B^{11}(d,n)C^{12}$	$C^{12}(d,n)N^{13}$
Q_m(Mev)	6·472	13·724	-0·281
Q_1(Mev)	4·572	9·30	-2·65
Q_2(Mev)	2·24	6·05	-3·78

Reaction	$C^{13}(d,n)N^{14}$
Q_m(Mev)	5·371
Q_1(Mev)	3·05
Q_2(Mev)	1·4

Apart from the identification of the reactions, measurements of neutron spectra do not readily give further information on the reaction modes.

This information is obtained more readily by an analysis of the yield curves and angular distributions of the reaction products at different deuteron energies. In the case of the two lightest nuclei these can be measured by counting recoil nuclei, but the only practical method at higher A values is by detecting the emitted neutrons directly in a fast neutron spectrometer which has sufficient energy resolution to allow the analysis of several neutron groups from each reaction. The most successful method used previously for such measurements employed nuclear emulsions which have a very low efficiency and require a long time (6 months) spent in the analysis of recoil proton tracks before the required results are available.

The results of such measurements and of similar measurements on reactions of the type A(d,p)A + n at high deuteron energies have

recently been reviewed by Huby (1953). Essentially what is observed at high deuteron energies above the Coulomb barrier of the target nucleus is that the shapes of the angular distributions are characteristic of the spin and parity change involved in the transition between the initial ground state of the target nucleus and the level or ground state of the final nucleus. They vary slowly with deuteron energy and are similar in different reactions involving the same spin and parity changes. In addition, the yield curve where it has been measured varies monotonically with incident deuteron energy.

This characteristic behaviour of the angular distributions and yield curves has been observed not only for A values greater than one, but also in the hydrogen reactions, at deuteron energies well above the Coulomb barriers, but it is only recently that the hydrogen reactions have been recognised as forming part of a general description for deuteron reactions in light elements, (Fairbairn 1954, Butler 1951). Before

discussing the current interpretation of these results (which have led to a new conception of the reaction mode involved) it is useful to consider the reaction mode which was originally thought to be applicable to these reactions before measurements of the angular distributions.

The earlier interpretation of nuclear reactions is due to Bohr, N, (1936, 1937), and is described as the formation and decay of a compound nucleus formed in this case by deuteron capture. That is, the reaction A(d,n)A + p is thought to proceed as follows

$$A + d \longrightarrow (A + d)^{*} \longrightarrow (A + p) + n$$

Compound Nucleus.

The compound nucleus $(A + d)^{*}$ is formed by the deuteron entering the target nucleus A and sharing its energy with the nucleons in A, with the formation of an excited level of the nucleus (A + d). The energy of excitation of the compound nucleus is determined by the incident energy and the binding energy of the deuteron in the compound nucleus. The level of the new

nucleus $(A + d)^*$ is formed by the interplay of nuclear forces between the nucleons. If, in the energy of excitation region involved, several levels overlap then the population density is determined by the natural configurations of nucleons in the nucleus $(A + d)^*$ in this energy region. Once formed the compound nucleus can decay through the entrance channel (elastic scattering) or it can decay by any other exit channels which are energetically possible. In medium and heavy nuclei, low energy products in the various exit channels which lead to highly excited levels of the final nucleus are interpreted in terms of the evaporation model. This statistical model is used because of the very large number of energy levels observed at high energies of excitation in heavy nuclei. In the extreme case of a continuous distribution of available exit channels, the level density problem has been shown theoretically by Weisskopf (Blatt and Weisskopf, 1952, p.370) to be analogous to the energy distribution of molecules in a gas and it seems possible to

describe the distribution in energy of low energy products in terms of an equivalent nuclear temperature T(Mev). In light nuclei, for transitions to discrete levels of the final nucleus, which in practice refers to low lying levels with fairly large energy separation, the relative intensity of reaction products in the different exit channels can be interpreted in terms of separate matrix elements governing the transition between the level in the compound nucleus $(A + d)^*$ and the final level. These matrix elements involve the energy of the transition and the spin and parity changes involved. The angular distribution of the reaction products in each exit channel are specified and characteristic of the same spin and parity changes.

Thus the compound nucleus picture of the reaction mode predicts that the yield curve for reactions of the type $A(d,n)A + p$ in light elements for varying deuteron energy can show fairly rapid fluctuations as different levels of the compound nucleus $(A + d)^*$ are formed, or

as the excitation energy approaches the optimum value for the formation of a particular level. In addition, the shapes of the angular distributions can vary wildly as the deuteron energy varies and for different target nuclei even though the spin and parity changes involved between the initial and final nuclei are the same.

The experimental results at high deuteron energies are not readily compatible with these conclusions and have led to a theory by Butler (1951) and Bhatia (1952) which is called Deuteron Stripping. The theory of Butler, which usually gives the same numerical results as the theory of Bhatia, is more amenable to a qualitative description, and can be stated as follows -

The neutron and proton in the incident deuteron have kinetic energy and momentum due to their internal motion within the deuteron and due to the kinetic energy of the deuteron as a whole. The energy spectrum of neutrons and protons approaching the target nucleus is, therefore, continuous. Protons or neutrons approaching the target nucleus with the required angular

momentum and energy can be captured and form excited levels of the target nucleus; the excess energy being carried away by the neutron or proton which is observed from the reaction. Thus, the process allows the investigation of proton and neutron capture reactions leading to levels in the final nucleus less than the binding energy, in contrast to the situation using free protons or neutrons which can only lead to the investigation of levels above the nucleon binding energy. It is clear that the partial widths of the levels in the final nucleus and statistical factors involving the spin changes in going from the initial to the final nucleus partly determine the relative intensity and absolute yield of the emitted neutrons or protons. The angular distribution of the neutrons and protons are determined by the angular momentum of the captured proton or neutron in addition to smaller effects due to the internal motion and the kinetic energy of the incident deuteron. The shapes of the angular distributions are,

therefore, independent of the possible spins and parities of the nucleus (A + d) (since it is not formed) and depend only on the spins and parities of the initial and final nuclei. This reaction mode predicts that the yield should vary monotonically with deuteron energy, and that the angular distributions can be the same for different nuclei and for different emitted particles (neutron or proton) if the spin and parity changes involved are the same.

The shapes of almost all of the angular distributions observed at high deuteron energies can be fitted much better by a particular value of l the angular momentum of the captured nucleon than by any other value. From this value of l, the spin and parity of the level of the final nucleus $(A + {}^{n}_{p})$ can often be deduced, and in principle the partial widths of these levels can be obtained, using Butler's (1951) theory, from the absolute partial cross sections observed experimentally.

However, Huby (1953) has pointed out that values of the partial widths obtained in this way

vary with the deuteron energy employed, and that this may be due to the fact that the deuteron stripping theory (Butler 1951, Bhatia 1952) used at high deuteron energies completely ignores the possible effects of Coulomb charge on the incident deuterons and on the emitted nucleon (proton). To obtain the correct values of the partial widths, and so exploit deuteron stripping at high deuteron energies to the full, it appears to be necessary to modify the existing theory to include the effects of Coulomb charge

The purpose of current experiments at low deuteron energies is, therefore, two fold. Firstly, there are far more low energy Cockcroft-Walton accelerators giving deuterons of energy up to ~1 Mev for low energy experiments than there are Van de Graaff and cyclotrons for high energy studies. It is, therefore, of some importance to discover whether the results at low energies can be used with the same profit as those at high energies in nuclear spectroscopy. Secondly, it seems probable that if a successful

theory is developed for low energy experiments, where Coulomb charge effects are larger then the accuracy in the Coulomb correction at high energies, should be good, and correct values for partial widths obtained.

However, it is only in the last five years that deuteron stripping has become recognised as the predominant reaction mode at high energies, rather than compound nucleus formation and decay. Until recently, almost all of the experiments performed, using low energy accelerators, were studies of gamma radiation following proton capture. This statement excludes the two hydrogen reactions. The reaction $^{2}H(d,n)^{3}He$ has been studied since the nineteen thirties, while the reaction $^{3}H(d,n)^{4}He$ has been studied vigorously as tritium became more generally available in the last ten years. The main reason behind this study of the hydrogen reactions was that it was thought (and still is) that since the structure of the reacting nuclei are relatively simple,

more would be gained in terms of fundamental theory from a study of them rather than heavier nuclei.

The hydrogen reactions are not viewed here, from this approach. Instead, the results of measurements on them are related by the author to the general problem of how to describe the modes of reactions of the type A(d,n)A + p in light elements at low deuteron energies, where Coulomb effects may be large.

At the time of the beginning of the research of the author described here, there were no measurements of angular distributions and yields from the reactions A(d,n)A + p at low deuteron energies apart from the hydrogen reactions. This was partly because of the factors stated above, but also because of the lack of accurate, but fairly quick, techniques for measuring angular distributions and partial cross sections in these reactions. At the time of writing, there is a much greater interest in the reactions, and papers have been published recently which show

the results of experimental measurements (Green et al 1955, Ihsan 1955) at low deuteron energies and theoretical attempts (Austern and Butler 1954, Yoccoz 1954, Grant, I.P., 1955) to modify the original deuteron stripping theory to include Coulomb charge effects.

As a result of the work by the author, described in chapters 1 - 4, and recent results by others, it is beginning to be recognised that the interpretation of the angular distributions at low energies cannot be made simply in terms of the original deuteron stripping theory successful in fitting the shapes at high energies. The required modification to the Butler and Bhatia stripping theories to fit the observed results is large, and no completely successful theoretical treatment has yet been put forward, and it seems probable that several years will elapse before sufficient experimental data accumulates for this to be possible.

However, even this fact is some progress in a hitherto unexplored field, and the author has been able to draw some tentative conclusions

from a few chosen experiments (chapters 1 - 4) on the probable amount and character of the effect of Coulomb charge on deuteron stripping reactions and the interpretation of these reactions at low deuteron energies. These conclusions are discussed in chapter 5. In chapter 1 a description of a simple, but accurate and reliable, fast neutron spectrometer is given, which was developed by the author primarily to allow investigations of these reactions without the long delay associated with nuclear emulsion technique. The aim of the research by the author, described in chapters 2, 3 and 4, was to open up and extend our knowledge of deuteron reactions in light elements at low deuteron energies, by experiments on the reactions $^{11}B(d,n)^{12}C$, $^{2}H(d,n)^{3}He$ and $^{3}H(d,n)^{4}He$. At the beginning of each chapter, or embodied in the chapter, the previous results related to these reactions and their interpretation by the author are given in detail.

Since the experimental research by the author, described in chapters 6, 7, 8 and 9, is related to the use of the reactions A(d,n)A + p at low deuteron energies as sources of fast neutrons for scattering and absorption experiments, the rest of this introduction is devoted to a discussion of the significance of these reactions in this sense.

The table given at the beginning of the Introduction shows that the reactions A(d,n)A + p are sources of fast neutrons in the energy range 1 - 15 Mev, using deuterons of a few hundred Kev. These reactions can be compared with other sources of neutrons in current use, which are mainly fission reactions

in fast reactors, photo-neutron sources, and reactions of the type $A(p,n)A^1$ in light elements.

The neutron flux from fast reactors is intense, but the energy distribution decreases very rapidly with increasing neutron energy. Photo-neutron sources are usually fairly weak, have a low neutron energy, and a very high gamma ray background.

The most convenient sources of fast neutrons are the reactions $^7Li(p,n)^7Be$ and $^3H(p,n)^3He$. The first reaction was originally thought to be a line source of neutrons, but later work (see Ajzenberg and Lauritsen) has shown that there are two Q values, - 1·645 Mev and - 1·21 Mev, and that the relative intensities vary with proton energy. The tritium reaction is now recognised as a standard line source of fast neutrons using fast protons from Van de Graaff accelerators (Freeman 1953). However, one of the practical considerations which is likely to prove of considerable significance in the development of fast neutron sources is the cost of the accelerating machine which is much greater

for a Van de Graaff than it is for a high beam current Cockcroft-Walton accelerator of a few hundred Kev, and many such machines have either been constructed or are under construction in various laboratories. The cross sections in the deuteron reactions are comparable with that of the proton-tritium reaction. The beam current of a Van de Graaff is of the order 5 μA, while deuteron beam currents are of the order 10 m.a. in modern machines run at several hundred KeV. The value of the Gamow penetration factor in targets with atomic numbers of the order 5 is 10^{-1} —— 10^{-2} at deuteron energies of a few hundred Kev. Apart from the two hydrogen reactions which are single line sources of neutrons, the other reactions have several high energy lines and often a continuum at low neutron energies, and emit gamma radiation of several Mev. The ratio of the number of neutrons in high energy well separated lines to the rest of the radiation is usually of the order five or ten to one. Thus, provided fast neutron counting techniques are available which can cope

with backgrounds of this nature and order of magnitude, low energy deuteron reactions in light elements can become very convenient line sources of neutrons over the whole energy range 1 - 15 Mev.

The apparent charge independence of nuclear forces and the dual nature of protons and neutrons in nuclei means that for most experiments using fast neutrons there are corresponding experiments using fast protons. The experiments of Fermi and Marshall (1947) and Havens et al (1949, 1951) supported by the theory of Schwinger (1948) and Foldy (1951, 1952) show that the contribution to the total cross section of fast neutrons, due to a spin-independent interaction between orbital electrons and the Coulomb field associated with the concept of the neutron existing as a dissociated proton-pion pair, is of the order 10^{-6}. The calculations of Schwinger and Foldy also predict that the contribution to the total cross section due to the interaction of the intrinsic dipole moment of the neutron with the Coulomb field of the heaviest nuclei is also of the order 10^{-6}. The

results of experiments using fast neutrons, therefore, reflect very accurately the effects of specifically nuclear forces, and in experiments which aim to investigate nuclear interactions results obtained using fast neutrons are much more easily interpreted and made use of than those obtained using fast protons which contain the effects of Coulomb charge. Unfortunately the same argument shows that the experimental difficulties in fast neutron experiments are greater than in the corresponding experiments using charged particles. Fast neutrons can only be produced and detected using charged particles or gamma rays from associated nuclear reactions which are influenced by the long range electromagnetic forces which are the basis of all existing experimental techniques. The division of labour between the use of charged particles and neutrons in many experiments is currently determined by whether the effect of Coulomb charges introduce greater uncertainties and increase the difficulty of observing nuclear effects in comparison with the uncertainties and difficulties

associated with existing fast neutron experimental techniques.

The purpose of the technique described in chapter 7 is to exploit the speed and high efficiency of scintillation counters for experiments on neutrons which require good energy resolution. The technique uses the time of flight of neutrons to discriminate between them and gamma rays, and to allow measurements of neutron energies. In contrast to the use of a single plastic scintillator as a fast neutron spectrometer, described in chapter 1, the time of flight technique is intended for measurements of neutron energy distributions which are continuous. That is, it is intended for measurements of the low energy neutrons from scattering experiments on medium and heavy nuclei rather than measurements of the high energy well separated discrete neutron groups in experiments on light nuclei. As has been already mentioned, it is thought that the energy distribution of such low energy products may be described by the Evaporation Model. The purpose of the experiment described in chapter 8 was to apply this time of

flight technique in an investigation of the reaction A (n,n^1)A using a beam of 14 Mev neutrons from the reaction $^3H(d,n)^4He$, and, in particular, to measure the low energy distribution of inelastic neutrons for comparison with the predictions of this model.

During the course of this research, a similar experiment was done by Graves and Rosen (1953) using nuclear emulsions to measure the inelastic neutron energy distribution. After the experiment, the results of a completely independent investigation of the same reaction, using an almost identical time of flight technique, were published by O'Neill (1954).

In chapter 8 these results are compared satisfactorily with those observed by the author, and it seems that time of flight techniques of this type have some advantages in possible energy resolution and speed of obtaining results in these experiments. The time of flight technique described is not so easy to use in practice as the single plastic scintillator, described in chapter 1. The success of the technique in

achieving a low statistical error depends on the use of multi-channel time delay analysis in the millimicrosecond region, which required the extension of existing electronic circuits. The circuits used and their mode of operation are given in the Appendix. In chapter 6 of the thesis is a description of some experiments on the reaction $^{127}I(n,2n)^{126}I$. This investigation essentially followed as a biproduct of the search for the reaction $^{3}H(d,\gamma)^{5}He$, described in chapter 5, but it is included here as an example of the use of fast neutrons for the production and investigation of isotopes and for the practical value of knowing the characteristics of the activity induced in sodium iodide crystals by fast neutrons.

Recently, and quite independently of the research by the author described in the thesis, there have been several interesting developments in the interpretation of fast neutron scattering and absorption experiments, which suggest that the neutron energy region 1 - 15 Mev is of particular significance, and

that sources of neutrons and fast neutron spectrometers in this energy region have considerable future value in research in low energy nuclear physics. In chapter 9, these developments, and possible future trends in this field, are discussed in relation to the scintillation counter techniques and data developed and obtained in the course of the research by the author, described in the thesis.

The Appendix contains a section, giving details of the method of producing thin deuterium targets developed primarily for the investigation of the reaction $^{2}H(d,n)^{3}He$, described in chapter 3.

At the beginning of each chapter in the thesis, there is a detailed analysis and critical review of the results of previous experiments by others which are related to the research by the author described in the chapter.

CHAPTER I.

The Single Plastic Scintillator as a Fast Neutron Spectrometer.

The technique described in this chapter was developed by the author primarily for measurements of absolute yields and angular distributions of high energy neutron groups from reactions of the type A(d,n)A + p in light elements. Apart from indirect measurements on recoil nuclei in the reactions $^{2}H(d,n)^{3}He$ and $^{3}H(d,n)^{4}He$, the reactions can only be fully investigated by direct measurements on the emitted neutrons. Any fast neutron spectrometer intended for such measurements must be capable of resolving neutron groups in the energy range 1 - 15 MeV., separated by a few MeV., in the presence of gamma radiation with quantum energies of several MeV., resulting from the de-excitation of product nuclei. For absolute yields at

different deuteron energies and relative measurements at different angles, the absolute counting efficiency and variation of efficiency with neutron energy must be known accurately, since

the reaction energy includes the incident, deuteron energy and centre of mass effects are large, causing considerable variation of observed neutron energy at different angles.

The only suitable nuclear reaction which allows these criteria to be satisfied and gives convenient charged particles for detection is elastic scattering by protons. The theoretical calculations of Hamilton (1949) for radiative capture of neutrons by protons in the energy region 1 - 15 Mev suggest that the ratio of inelastic to elastic scattering is of the order 10^{-4}. There appears to be no experimental observations of radiative capture by protons reported for neutrons in this energy range. The absorption of fast neutrons by hydrogen in transmission experiments is interpreted as being due to elastic n-p scattering, and precision values for the cross section have been measured in this way by Storrs et al (1953), Fields et al (1953), Hafner et al (1953) and Rose et al (1952) at neutron energies E_n(lab) of 1·32 Mev, 2·5 Mev, 4·75 Mev, and 14·1 Mev, respectively with errors

less than 0·1%. Less accurate values over the continuous energy range 3 - 12 Mev have been obtained by Nereson and Darden (1953), which lie on the smooth curve predicted by the theory of Biedenharn and Rose (1949). The theoretical curve decreases monotonically with increasing energy, varies roughly as E_n^{-1} in this energy region, and is expressed as a function of four parameters describing the total scattering in terms of the sum of triplet and singlet interaction. The best values of these parameters are discussed by Blatt and Weisskopf, p.70, and it seems possible to calculate the total n-p cross section at any energy in the range 1 - 15 Mev to well within an error of 1% using the theoretical curve and the precision values from the transmission experiments at a few energies.

The angular distribution of recoil protons has been measured by Walt and Barschall (1953), and Armstrong et al (1953) at neutron energies of 1 Mev and 14 Mev. To within the experimental error of 5% at the higher neutron energy the angular distribution is isotropic in

centre of mass, and the theory of Biedenharn and Rose suggests that within this energy region the angular distribution should be isotropic corresponding to s wave scattering. Assuming that this is strictly true, the energy spectrum of recoil protons in lab. is, therefore, flat. To within 0.1% the neutron and proton masses are equal; therefore, a single neutron group of energy E_n results in a flat distribution of recoil protons up to an energy of E_n. For several neutron groups the proton spectrum consists of several plateaus and abrupt steps. All fast neutron spectrometers relying on n-p scattering measure the neutron spectrum by observations on this energy distribution of recoil protons, and avoidance of effects produced by gamma rays. The three charged particle techniques used to observe recoil protons are nuclear emulsions, proportional counters and scintillation counters.

In nuclear emulsions, the tracks of recoil protons are easily distinguished from electron tracks due to gamma rays by the difference in grain density. If the incident direction of neutrons which entered the plates is known, the

number and range of recoil protons lying within a specified angular cone around this direction can be measured. A plot of the number of these "knock-on" protons against the range gives a peaked spectrum, each peak corresponding to a neutron group. Using the range-energy relation of protons in the emulsion and the n-p scattering cross section the neutron energy distribution can then be obtained from these results. The efficiency of neutron detection is extremely low, due to the thinness of the plates in comparison with neutron mean free paths of the order of several inches, and this implies long machine running times during which drift may occur. Much more significant though, is the extremely long time which elapses (6 months) for the analysis of the plates before results are obtained and the delay in initial setting up of experiments. The nuclear emulsion is probably the best technique to use to establish the fact that a reaction exists, but it is too time-consuming for investigations requiring a large number of measurements. Coincidence measurements are, of course, impossible.

Proportional counters filled with a high concentration of methane have too low an efficiency for most experiments, due to the low nuclear absorption of a gas. This low efficiency results in very poor statistics, while wall effects greatly reduce the inherently high resolving power.

Proportional counters filled with gases with no hydrogen have been used to detect recoil protons from a thin hydrogeneous radiator bombarded by a parallel beam of fast neutrons. By collimating the recoil protons the pulse spectrum from the counter, when corrected for n-p cross section in the radiator, gives the incident neutron spectrum. The resolution achieved depends mainly on the thickness of radiator used. For a radiator with a total transparency for fast neutrons of 10^{-3}, the energy spread in recoil protons of 10 Mev is 10%. Collimation may reduce the effective efficiency to 10^{-5}. Any increase in energy resolution results in a roughly proportional decrease in efficiency. While the technique has been used by Nereson and Darden (1953), using neutrons from the Los Alamos fast reactor,

the efficiency is too low for an investigation of the reactions A(d,n)A + p.

A fast neutron spectrometer using hydrogeneous scintillators and measuring the pulse height distribution of recoil protons in the scintillator has been described by Beghian et al (1952). This method uses a second scintillation counter with a sodium iodide scintillator to detect slow neutrons following "knock-on" n-p collisions in the first (hydrogeneous) scintillator. By counting only the pulses from the fast neutron counter, which are in coincidence with pulses in the slow neutron counter (due to gamma rays following slow neutron capture in iodine or sodium), a single peak with a low pulse height tail is observed for a single neutron group. By using delayed coincidence between the pulses it is possible to avoid observing gamma rays due to Compton scattering. This method is only one of many possible variations of double scattering and coincidence technique which aim at a mechanical differentiation of the recoil proton pulse height

distribution in hydrogeneous scintillators. Unfortunately, these methods introduce severe practical difficulties associated with the calculation of the absolute neutron counting efficiency and the variation of efficiency with neutron energy for yield and angular distribution measurements, the mechanical movement of two counters, and complication of electronics. Also the reduction in efficiency makes coincidence measurements between gamma rays and associated neutrons almost useless due to the very low counting rates. No results on nuclear reactions beyond the measurement of neutron energies have been reported using these methods. These measurements of neutron energies can usually be obtained much more accurately by other means, if they are significant. For these reasons, double scattering and coincidence techniques have been neglected in the development of a method of measuring the recoil proton spectrum in hydrogeneous scintillators.

The method described here uses plastic scintillators because they are easily machined and polished, the efficiency is less likely to

change due to impurities, and in combination with a du Mond photomultiplier type 6292, the complete unit is compact, light and permanently sealed.

The basis of the method is very simple. A thickness of plastic scintillator is chosen, such that electrons which pass right through it produce a pulse which is smaller than that produced by "knock-on" protons for the lowest energy group of neutrons in the neutron spectrum which is being investigated. The pulse height distribution from the plastic scintillator, when exposed to a flux of radiation containing several high energy groups of neutrons and high energy gamma radiation, consists of several edges and plateaus at large pulse heights and a rising tail of very small pulses. Each edge and plateau corresponds to a single high energy neutron group and the rising tail of small pulses includes electrons from the absorption of gamma radiation (mainly by the carbon present in the plastic). The observed pulse height distributions for high energy neutrons from the reactions $^{11}B(d,n)^{12}C$ and $^{3}H(d,n)^{4}He$ are shown in figure 1. The plastic used was polystyrene and 2·5% terphenyl-

butadiene, and was 7 m.m.s. in depth by $1\frac{1}{2}$" diameter, surrounded by magnesium oxide and sealed to the glass of a du Mond photomultiplier 6292 by silicon oil.

The non-linear response of organic scintillators to protons means that the shape of the observed pulse height distributions for a single neutron group are not exactly rectangular, but are more peaked towards lower pulse heights. Also the half value at the edge of each plateau occurs at pulse heights which do not vary linearly with neutron energy. By measuring the pulse heights at half values of plateaus in the pulse height distributions due to neutrons from the reactions $^{2}H(d,n)^{4}He$, $^{11}B(d,n)^{12}C$ and $^{3}H(d,n)^{4}He$ with energies of approximately 2·5, 9 and 13, and 14 Mev respectively, and from electrons due to Compton scattering of gamma rays from standard sources of ^{137}cesium, ^{22}sodium, ^{60}cobalt, with gamma ray energies of ·663, ·511 and 1·27, 1·12 and 1·32, the response curve of this plastic scintillator has been measured and is shown in figure 2. A comparison of these results with

the ranges of protons and electrons in the plastic (calculated from the tables of Aaron et al (1953) shows that, although the fluorescence efficiency of the scintillator is less for protons than it is for electrons, it is always possible to select a suitable thickness of plastic since the ranges of recoil protons are $\sim 10^{-2}$ x range of fast electrons, while the fluorescence efficiencies differ only by a factor of 2 - 3 in this energy region. The possibility of carbon recoils being counted is reduced to vanishing by the following factors. The total cross section of fast neutrons in carbon observed by Nereson and Darden (1953) does not rise above that for hydrogen by more than a factor of about three over the energy region 1 - 15 Mev. The results of Coon (private communication) for elastic scattering in carbon show that about 80% of the neutrons are scattered at angles less than 25°. The maximum energy of a carbon recoil is $\frac{1}{3.5}$ the incident neutron energy, and they probably carry an effective charge greater than unity, but even on the assumption of unit charge the linear relation between pulse height and range shows that the pulse heights due to

recoil carbon nuclei are trivial.

Birks (1953) has suggested on theoretical grounds that the relation

$$\left(\frac{dL}{dE}\right)_{\text{Heavy Particles}} = \left(\frac{dL}{dE}\right)_{\text{Electrons}} \times \frac{1}{1 + a\,dE/dx}$$

between the specific fluorescence $(\frac{dL}{dE})$ and the specific ionisation $(\frac{dE}{dx})$ should hold for all types of organic scintillators, where $\underline{a}$ is a constant for any particular scintillator. The numerical integration of this relation, using the range-energy curves of Aaron et al (1949), gives the full lines in figure 2, using a best value of $\underline{a} = 0{\cdot}0175$ $(\text{Kev/mg/cm}^2)^{-1}$ to fit the experimental points for the plastic scintillator. Very recently Storey (private communication) has measured the response curve of this plastic scintillator for several Mev alpha particles, and the results indicate that the light output is proportional to range which is consistent with the above relation and the value of $\underline{a}$ obtained from figure 2.

The theoretical pulse height distribution $(\frac{dN}{dL})$ due to recoil protons from a single neutron

group can be derived from the equation for $\frac{dL}{dE}$, since

$\frac{dN}{dL} = \frac{dN}{dE} / \frac{dL}{dE}$ and $\frac{dN}{dE}$ is constant due to s wave scattering.

The full line in figure 3 is the theoretical curve for a = 0·0175, and can be compared with the experimental points for the neutron group from the reaction $^{2}H(d,n)^{3}He$. It can be seen that at high recoil proton energies the pulse spectrum becomes effectively flat.

The chemical constitution of the plastic scintillator used is effectively $(CH)_n$ and the density is 1.1 gm./c.c. The n-p scattering cross-section in the energy range 1 - 14 MeV can be calculated accurately from the theoretical expression of Biedenharn and Rose, using a triplet scattering range of 2.10^{-13} cms. These quantities were used to derive the curve shown in figure 4 for the efficiency of n-p scattering in a plastic scintillator 1 cm. diameter x 1 cm. depth. For comparison figure 4 also shows the efficiency of gamma ray scattering in the same plastic, which has been calculated from the theory by Heitler

(Quantum Theory of Radiation, p.223).

The actual analysis of the experimental pulse height distributions to obtain the number of neutrons in each energy group depends on the particular experiment, and is illustrated by the descriptions given in the succeeding two chapters. Essentially, the plateaus and edges are subtracted, and the rectangular shape of the recoil energy spectrum is constructed using the response curves in figure 2. The absolute flux of incident neutrons is then obtained using the curve in figure 4. In practice the known relation between the response curve for electrons and protons allows the identification of neutron energies by comparison with Compton edges from convenient sources of gamma rays, which are very convenient in the preliminary setting up of experiments.

The energy resolution is of the order 10% at high energies and the technique is limited to the investigation of reactions with neutron groups separated by at least this amount. An examination of the table at the beginning of the introduction shows that most of the discrete

high energy neutron groups from the reactions $A(d,n)A + p$ can be investigated using this technique.

The energy resolution is limited mainly by the efficiency of light production in the known organic scintillators.

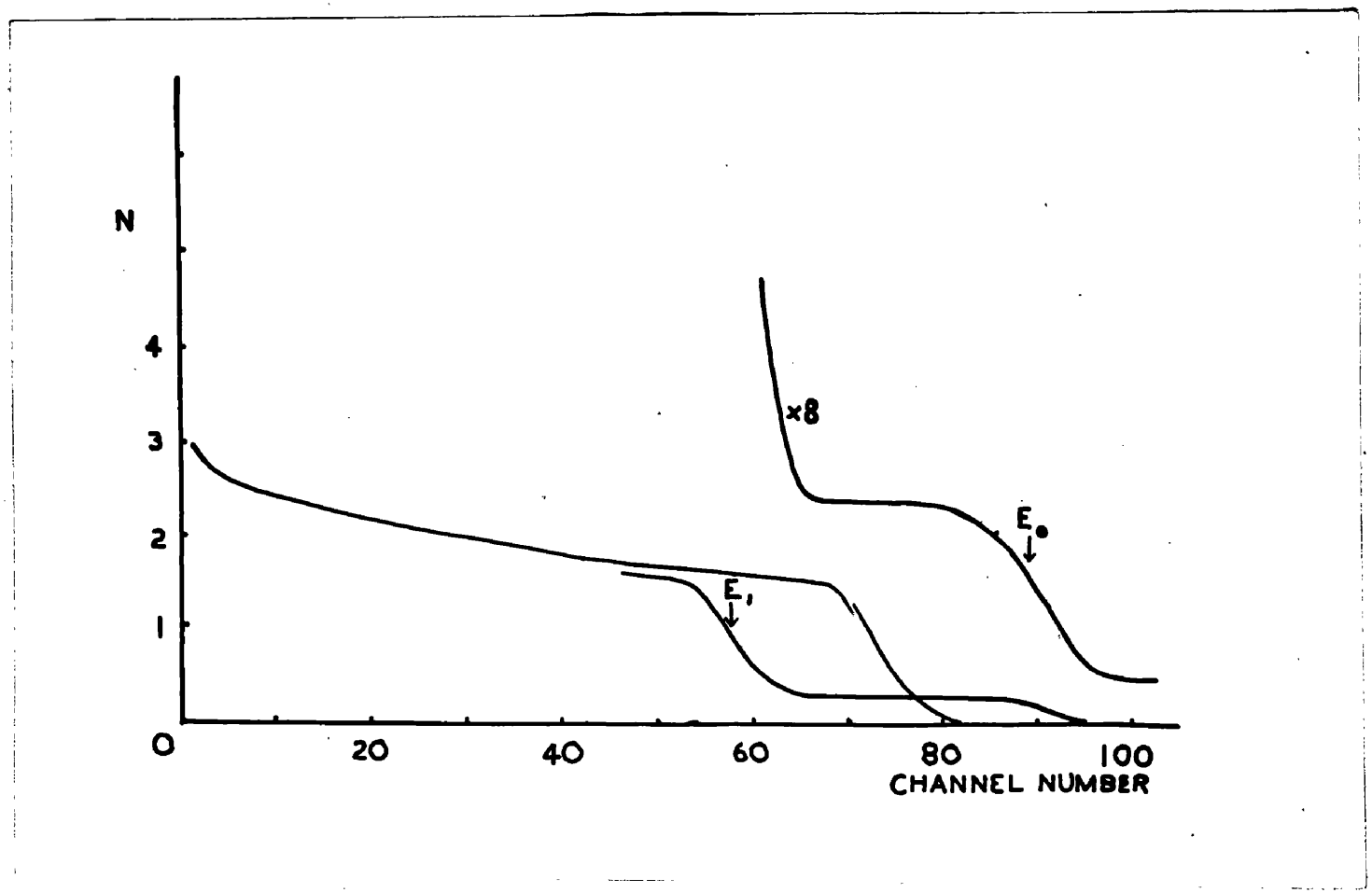

Fig.1.

Pulse height distributions obtained using a plastic scintillator to detect neutrons from the reactions $^{11}B(d,n)^{12}C$ E_0 and E_1 . The edge due to 14 Mev neutrons from the tritium reaction is displaced twenty channels to the left.

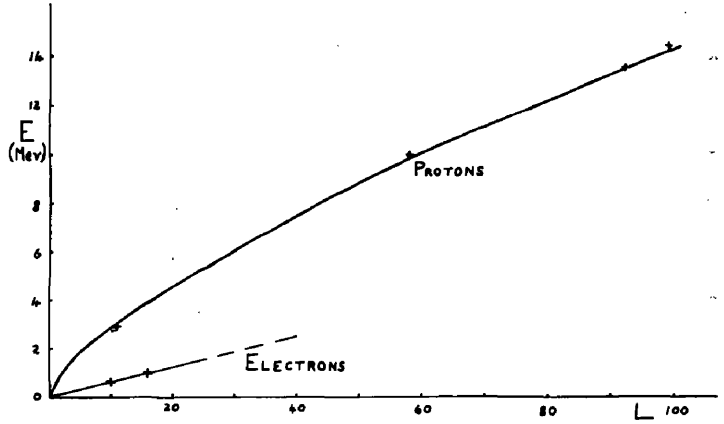

Fig.2.

Reponse curve for Plastic scintillator

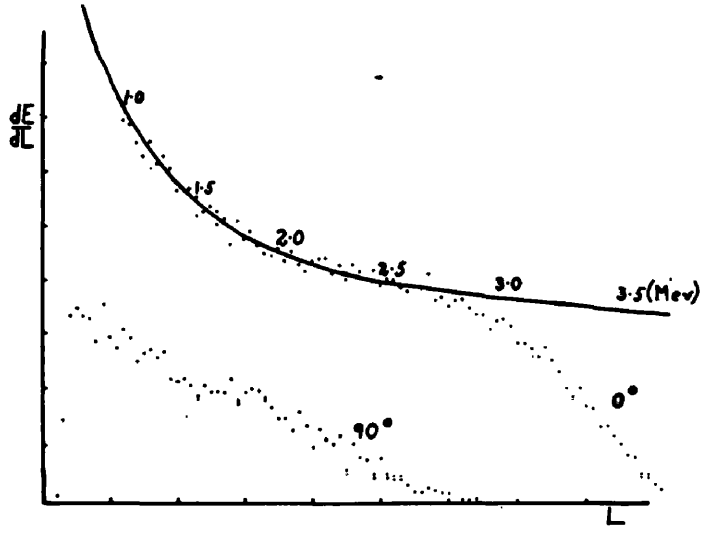

Fig.3.

Theoretical and Experimental Distributions.

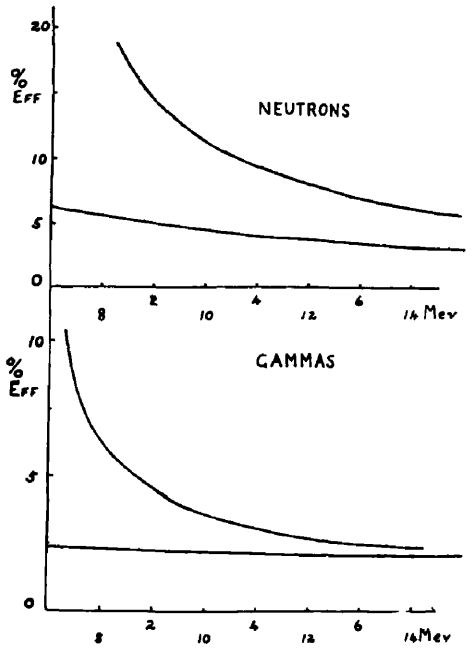

Fig.4.

Efficiency of Plastic scintillator for neutrons and gamma rays

CHAPTER 2.

The Reaction $^{11}B(d,n)^{12}C$.

The energies and intensities of the neutron groups emitted in the reaction $B^{11}(d,n)C^{12}$ have been studied by Gibson (1949) and Johnson (1952). The angular distributions of the emitted neutrons have not so far been very thoroughly examined, owing to the experimental difficulties involved, in particular the lack of a reliable neutron spectrometer.

The experiments described in this chapter and the next two were carried out to investigate the modes of reactions of the type A(d,n) A + p at low deuteron energies and hence, possibly, to indicate the directions in which the present theory requires modification. The main requirement was, therefore, to measure the neutron angular distributions as precisely as possible, since an analysis of these is expected to give information on this problem. This was done using the single plastic scintillator technique, described in the previous chapter. ^{11}Boron was chosen because targets were available and the large separation between the high energy groups

made the analysis more accurate.

A target of separated B^{11}, on a backing of 1/32" copper, was bombarded with currents of a few microamperes of deuterons from a high tension accelerator operated at 600 KV. The angular distributions were measured using the apparatus shown in figure 5, which is a copy of that used by Rutherglen et al (1954), the neutron detector being substituted for a γ-ray detector.

The neutron detector consisted of a piece of plastic scintillator, approximately 4 cm. in diameter by 0·7 cm. thick, together with a Du Mont photomultiplier type 6292 for detection of the light emission from recoil protons in the plastic. Optical contact between the scintillator and the photo-tube was made by a thin film of silicone grease, while the scintillator was surrounded with tightly packed magnesium oxide to improve the efficiency of light collection.

Pulses from the photomultiplier, after amplification, were fed into a 100-channel pulse height analyser, Hutchinson and Scarrott (1951). Preliminary experiments with neutrons from the

boron reaction $^{3}H(d,n)^{4}He$, $^{2}H(d,n)^{3}He$ and gamma rays from standard sources established the response curve described in chapter 1, and gave confidence in the identification of neutron groups in the observed pulse height distributions.

The pulse-height distribution at each angular position was recorded, measurements being taken for a definite number of counts in a fixed monitor counter. This procedure removes possible errors due to inhomogeneity or deterioration of the target. Measurements at the different positions were taken in a random order, and afterwards repeated in the reverse order, thus minimising the effects of any slow changes in the electronic part of the apparatus.

A block of lead, $\frac{1}{2}$" thick, was inserted between the target and the detector to absorb the β -particles from the decay of ^{12}B formed in the reaction $^{11}B(d,p)^{12}B$. If not absorbed, these electrons, which could pass right through the scintillator, produced a strong peak in the region corresponding to a neutron energy of about 4 Mev.

The overall detection efficiency of the phosphor for a given energy-group is very closely independent of the direction of observation relative to the incident deuteron beam. The effective solid angle of detection varies with direction (due to centre-of-mass motion) in the same way as the measured neutron energy E_n while the intrinsic detection efficiency of the phosphor (which is proportional to the n-p scattering cross-section) varies as E_n^{-1} over the small energy-range involved.

The monitor consisted of another plastic scintillator similar to the first. For monitoring purposes no lead was inserted between the target and the detector, since the electron-produced peak from the mirror reaction can be used to help the monitor stability. A discriminator set below the pulse-height corresponding to the electron pulses (but above that corresponding to the background of neutrons from the D-D reaction) resulted in a counting rate almost independent of small variations in either the gain on the monitor amplifier system or the discriminator threshold.

Resolved neutron groups from the reaction $^{11}B(d,n)^{12}C$.

A typical spectrum from this reaction is shown in the upper half of figure 6. It will be seen that the groups corresponding to the ground state and first excited state of C^{12} at 4·43 Mev are well resolved.

Neutron-Gamma Coincidences from the Reaction $^{11}B(d,n)^{12}C$.

The spectrum of pulses from the neutron counter was measured in coincidence with pulses due to gamma rays above 2·5 Mev detected in a sodium iodide crystal (2" diameter x 1½" long) mounted on a second du Mond 6292 photomultiplier. The observed spectrum from the neutron counter taken immediately after the singles spectrum is shown in the bottom half of figure 6. A comparison of the two spectra confirms that the second plateau in the singles spectrum is in coincidence with gamma radiation above 2·5 Mev energy. The spectrum in the gamma counter was measured in coincidence with pulses from the neutron counter due to protons of energy greater than 7 Mev, and was consistent with that expected from a 4·4 Mev gamma ray. The number

of coincidences observed was much greater than could be attributed to random coincidences. These experiments confirm that the 9 Mev neutron group in the singles spectrum leaves the final nucleus of ^{12}carbon in an excited level at 4.4 Mev.

Intensities.

The relative intensities of the groups to the ground and first excited states of C^{12} were determined from the areas under the separated spectra. After correction for the detection efficiency of the phosphor, using the values for the n-p scattering cross-section given by Blatt and Jackson (at a bombarding energy of 600 Kev)

$$I_{4.43}/I_o = 2.3 \pm .5 \quad (\theta = 90^o).$$

This figure is close to that obtained by Gibson (1949) at a bombarding energy of 0.9 Mev.

The absolute intensity (thick target yield) was determined at 600, 500 and 400 Kev. After correction for the effect of the lead absorber the integrated yields for the ground-state and first excited state groups are:

Deuteron energy in Kev.		400	500	600
Yield per 10^{10} deuterons ($\pm$20%)	ground state	9·4	41·5	190
	1st excited state	24	108	530

A logarithmic plot of these results is shown in figure 7, which also shows (dotted line) the Gamow curve calculated from the theory in the table of Mattauch (1946).

Angular distributions.

(a) Ground-state group.

Figure 8 shows the angular distribution of the neutron group leading to the ground state of C^{12}. The average error of any point on the curve is 1.5 - 2%.

The most important of the possible systematic errors was an instrumental anisotropy due to misalignment of the target spot. This was determined by means of the reaction F^{19} (p, α, γ)O^{16} at 340 Kev, where the γ-radiation is known to be isotropic, and found to be less than 1%.

The curve represents the best fit that can be obtained to the experimental points by superposing a stripping curve for $l_p = 1$ (calculated by the theory of Bhatia et al, using a nuclear radius $R = 5{\cdot}4 \times 10^{-13}$ cm) on an assumed incoherent isotropic background.

It will be noted that the experimental points show the anomalous dip at low forward angles which has been previously observed in some other stripping reactions. (Huby 1953).

(b) Excited-state group.

Figure 9 shows the angular distribution of the neutron group leading to the first excited state of ^{12}C. It is seen to be very closely symmetrical about the 90° position, a result which is normally characteristic of compound nucleus formation and not of the stripping mechanism. The experimental distribution is best fitted by the expression $W(\theta)=1 + 0{\cdot}41(\pm {\cdot}03) \cos^2 \theta$ (full curve). After correction for the finite angle of acceptance of the detector the result $W_0(\theta)=1 + 0{\cdot}45(\pm .04)\cos^2\theta$ is obtained.

Comparison with recent results.

Since these results were obtained, the results of similar experiments have been published by Green et al (1955) on the reactions $^{9}Be(d,n)^{10}B$, $^{13}C(d,n)^{14}N$ at 860 Kev and Ihsan (1955) on the reaction $^{11}B(d,n)^{12}C$ at 870 Kev. Ihsan's results at 870 Kev (using nuclear emulsion technique) are shown by a separate symbol in figures 8 and 9 for comparison with those observed here at 600 Kev. These results, and those observed in the experiments by the author described here, are discussed in chapter 5.

The zeros of the theoretical curves drawn using the deuteron stripping theory of Bhatia in figures 8 and 9 are at ordinate values of 3.5 and 4 respectively.

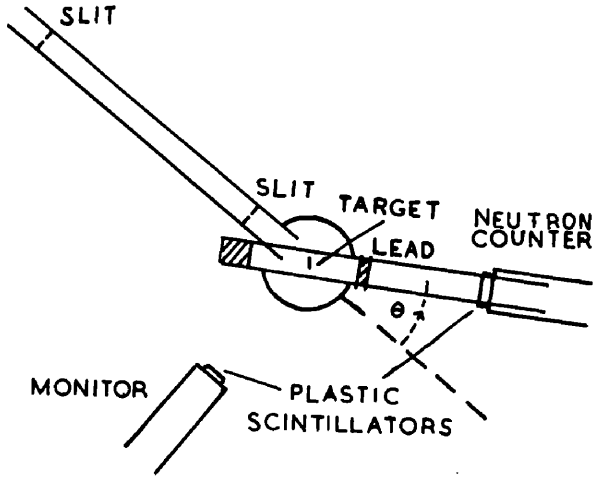

Fig.5.

Angular distribution apparatus.

Fig.6.

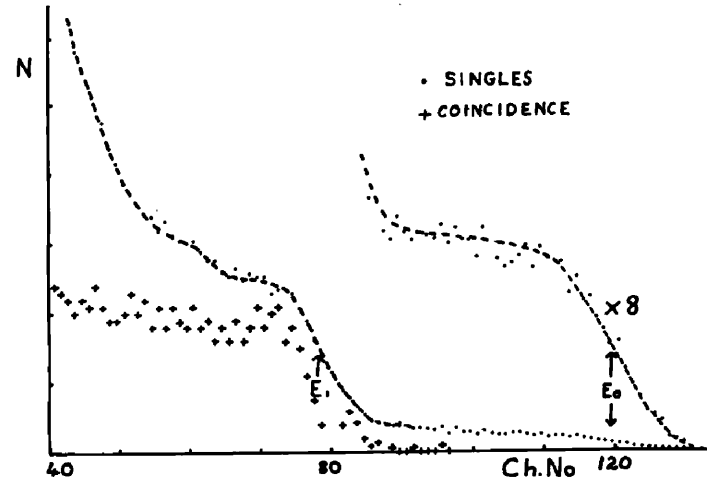

Reaction $^{11}B(d,n)^{12}C$ + (4.4 Mev)

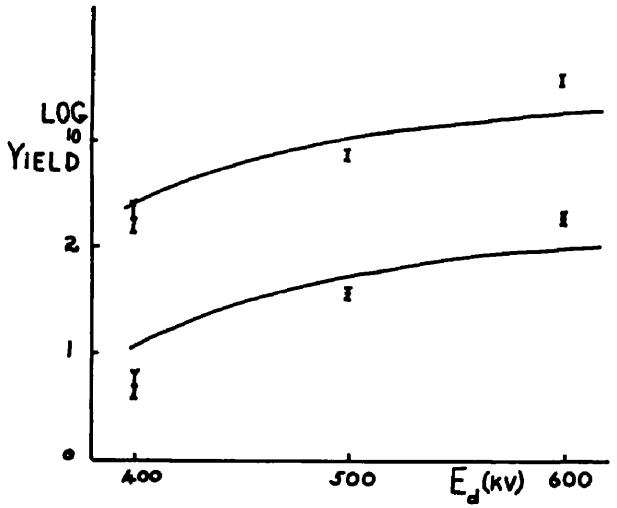

Yield curve and Gamow factor $^{11}B(d,n)^{12}C$.

Fig.7.

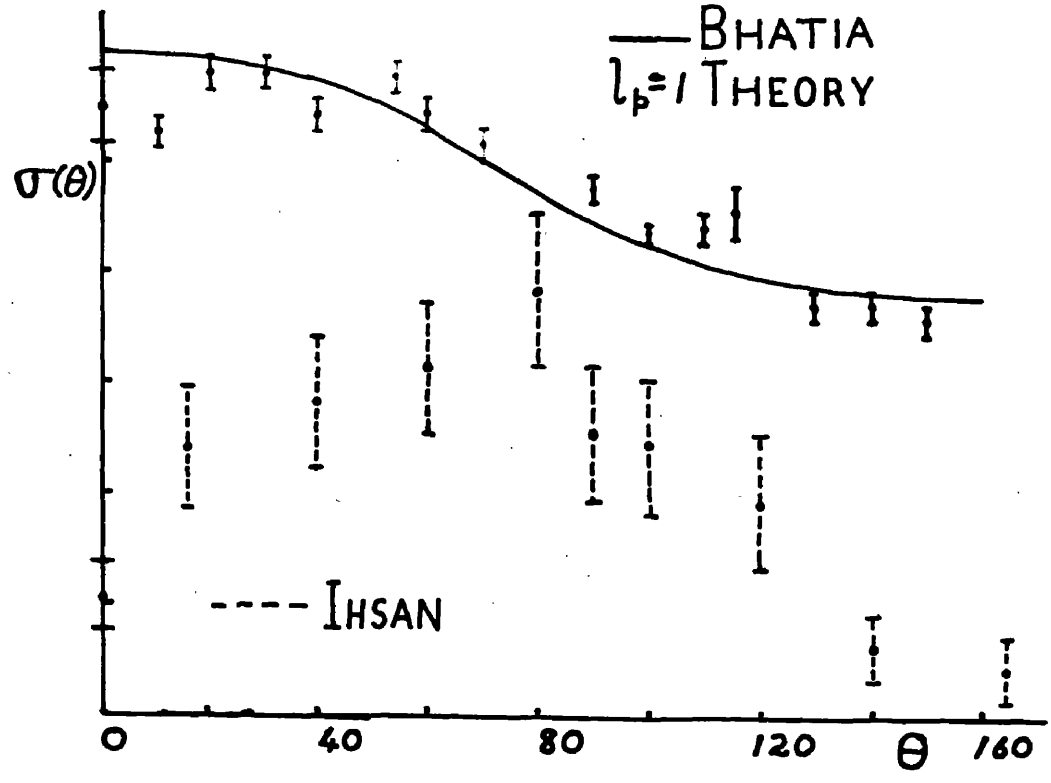

Fig.8.

Angular distribution ground state transition

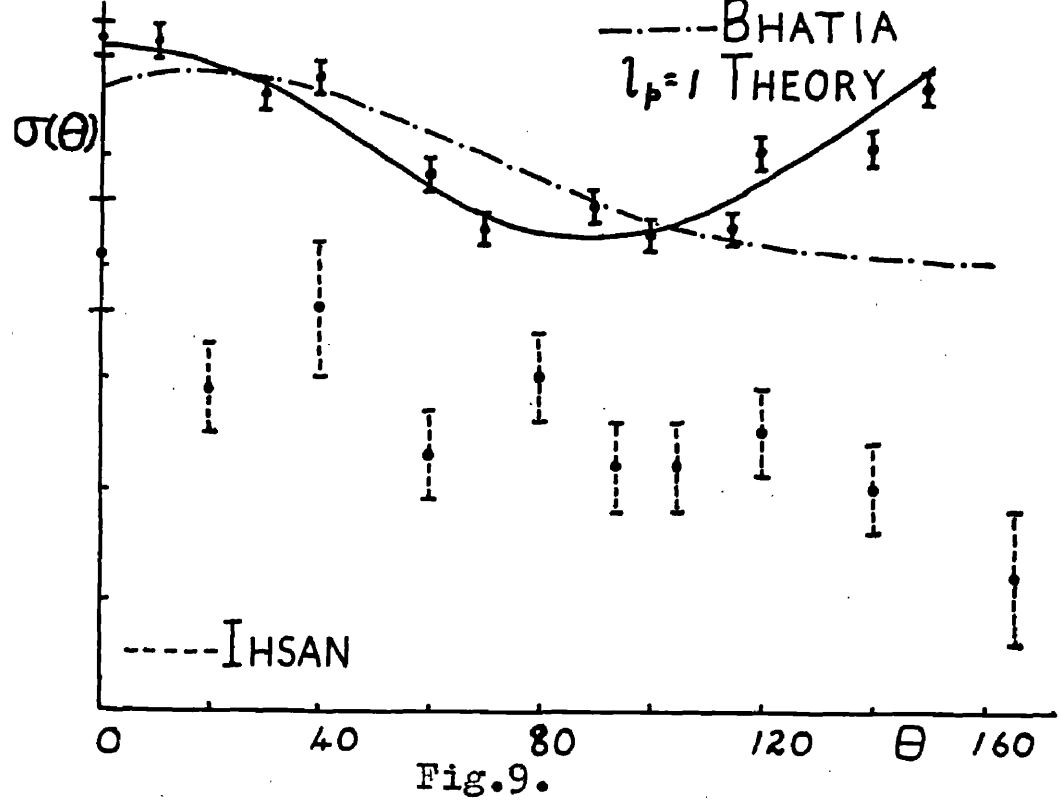

Fig.9.

Angular distribution excited state transition $^{11}N(d,n)^{12}C^*$

CHAPTER 3.

The Angular Distribution of Neutrons from the Reaction $^2H(d,n)^3He$.

The integrated yield in the reaction $^2H(d,n)^3He$ has been measured by Arnold et al (1954) and Preston et al (1954) at values of E_r up to 250 Kev. (E_r is the reaction energy in centre of mass). At higher deuteron energies the yield has been measured by Bennett et al (1946) and by Hunter and Richards (1949). The yield curve obtained from these experiments is very well fitted by the Gamow Coulomb barrier function. The angular distributions have been measured by Bennett et al (1946), Hunter and Richards (1949), Bartholdson (1950), Baker and Waltner (1952), Elliot et al (1953) and Preston et al (1954), at energies $E_r < 250$ Kev, and at higher deuteron energies by Bennett et al, Hunter and Richards and Freemantle (see Fairbairn 1954). The shape of the distribution observed by Freemantle at $E_r = 9{\cdot}5$ Mev has been fitted fairly well by the simple Butler (1951) deuteron stripping theory modified by Fairbairn (1954) to allow for identical reacting nuclei, but not for

Coulomb charge effects. This theory predicts too high an assymetry ratio for the reaction at lower deuteron energies, and gives no indication for the rapid reduction in this ratio as the deuteron energy falls below the Coulomb barrier E_b.

At energies $\lesssim E_b$ the cross section has been expressed by the empirical relation

$$\sigma(\theta_c) = 1 + A\cos^2\theta_c + B\cos^4\theta_c \quad \text{(in centre of mass)}.$$

Preston (1954) has pointed out that the values of A + B measured by Elliot et al (1953) and Preston et al (1954) lie on a smooth curve as a function of deuteron energy which does not pass through the earlier results of other investigators. The earlier results were all made using fast neutron counters of various types, while Preston et al and Elliot et al used proportional counters to detect recoil ^{3}helium nuclei. In contrast to the early measurements of A + B the values of Preston et al and Elliot et al do not lie near the well established curve of values of A + B for the mirror reaction $^2H(d,p)^3H$ Q = 4·04 Mev, but are approximately 40% larger.

Preston et al measured A + B values for this reaction at the same time as the measurements for the neutron reaction, and found values in good agreement with earlier values.

The purpose of the experiments by the author described below was to measure the angular distribution of neutrons from the reaction $^{2}H(d,n)^{3}He$ at deuteron energies near those used by Preston et al ($200 < E < 450$ Kev) by counting neutrons directly. By doing this, it was hoped to establish whether or not there is any significant difference between the neutron and proton reactions and, if so, whether this result can be used to indicate the effect of Coulomb charge in modifying deuteron stripping theory.

The single plastic scintillator technique, described in chapter 1, was used to measure the angular distributions.

In the experiments, thin deuterium targets were used. These targets were preapred by bombarding blocks of silver, 2 mm. x 1 cm. x 3 cm, with deuterium in a 50 Kev accelerating tube built for this purpose. The technique

and the characteristics of the targets are fully discussed in the Appendix. The targets used in the experiments described here had a calculated thickness of ± 30 Kev, and depth in the silver of 55 Kev, at incident bombarding energies E_i on the surface of the silver of 500 and 400 Kev (see Appendix). The reaction energies Ed corresponding to these incident energies were, therefore, 445 ± 30 Kev and 345 ± 30 Kev.

The deuterium targets were transferred from the 50 Kev accelerating column and mounted in the apparatus shown in figure 10. The incident bombarding deuteron beam passed through two slits and entered the silver over an area of 0·2 mm. x 1 cm. Neutrons from the reaction $^{2}H(d,n)^{3}He$ were detected by a single plastic scintillator (1 cm. diameter x 0·7 mm.) mounted on a du Mond 6292 photomultiplier, and rotated at a distance of 10 cms. from the target.

The angular anisotropy of the apparatus was measured by mounting a very thin source of ^{137} cesium in the same position as the deuterium target, and was found to be less than 2%.

The reaction was monitored by counting protons from the mirror reaction $^{2}H(d,p)^{3}H$ in a thin (1 mm.) plastic scintillator, mounted in a fixed position at 90° to the deuteron beam. Protons from the target were allowed to pass along an evacuated tube, 14 cm. long, before emerging from a thin mica window and entering the plastic.

Counting rates of 10^{4} per 5 minutes per 5μA of deuteron current at 445 Kev were observed from the targets in agreement with the estimate of the yield based on the amount of deuterium inserted into the lattice at 50 Kev.

After 50μA hours at 500 Kev the yield of protons from silver originally containing no deuterium was less than 1% of the yield from a deuterium target.

A large background of 25% was encountered during the experiments and is attributed to deuterium build up on the surface of the slits and walls of the apparatus. This was kept to a minimum by using very thin metal for the slits and lining the inside wall between the slits with thin copper foil. The rise in temperature of

the thin metal under bombardment by stray deuteron beam assists in the escape of deuterium. After about 100 μA hours bombardment the background did not appear to change appreciably for further bombardment. It was established that, provided the beam current reaching the target did not vary by more than 20%, the background did not fluctuate by more than 10% of its mean value, which corresponded to a 2·5% error in counting neutrons and trivial error in counting protons. These low values were only achieved by avoiding changes in deuteron energy.

Neutron Spectrum.

The pulse height distributions, background subtracted, observed at 0° and 90° from the neutron counter are shown in figure 3 of chapter 1. The edges of the observed distributions were consistent with the response curve of chapter 1.

Angular Distributions.

The angular distribution of neutrons from a deuterium target bombarded at 500 Kev (which corresponded to a reaction energy of 445 $\pm$ 30 Kev) is shown in figure 11.

The two symbols used to show results at different angles refer to the application of two separate cut off values in the pulses height distribution of recoil protons. In addition to these measurements, ten separate observations were made at 0° and 90°, and the average values found are shown by a third symbol in figure 11. [×]

Similarly, observations were made at 0° and 90° for an incident energy of 400 Kev (= 345 ± 30 Kev), and these are shown in figure 11, joined by a line with a $\cos^2\theta$ variation. [×]

Errors on Values of A + B.

The values of n_c = number of neutrons emitted per unit solid angle in the centre of mass frame of reference, were obtained using the equation

$$n_c = \frac{1}{kK} \cdot \frac{E}{E - E1} \cdot \frac{1}{E\,\theta_E} \cdot \frac{1}{f_E} \cdot N$$

at centre of mass angle θ_c corresponding to laboratory angle θ, where

N = number of counts recorded by the neutron counter at each angle (background subtracted) above the cut off voltage in the pulse height distribution.

E = neutron energy in lab. at lab. angle θ.

E^1 = proton energy in the thick plastic scintillator corresponding to the cut off in the pulse height distribution (0·5 Mev and 0·85 Mev).

σ_E = n-p cross section at energy E.

f_E = correction factor between 98% 100% which occurs in the relation = $Kf_E.E.$

Ω = solid angle of the detector in the centre of mass frame

and kK is independent of θ.

The errors associated with the values of A + B were arrived at by the following considerations. The error in A + B is divided into two - the error, both systematic and random in the measurement of $N(0^o)/N(90^o)$ and the error in calculating $\frac{n_c(0^o)}{n_c(90^o)}$ using the equation given above relating n_c to N.

The systematic error in $N(0^o)/N(90^o)$ was the angular anisotropy of the apparatus, which was estimated to be 1·5%. The random error in $N(0^o)/N(90^o)$ was taken as the standard deviation observed in the mean value of the ratio for all the observations at each energy; these were observed to be 2% and 3% at E_i = 500 and 400 Kev. The total errors in the ratios

$N(0^{\circ})/N(90^{\circ})$ were, therefore, 3.5% and 4.5%.

The errors in the three values of $n_c(0^{\circ})/nc(90^{\circ})$ due to the multiplying factor

$$\frac{1}{k\,K} \cdot \frac{E}{E - E^{1}} \cdot \frac{E}{E \cdot \sigma_{\epsilon}} \cdot \frac{1}{fE}$$

are essentially due to errors in the values of E and E^{1}, and their contribution to the total error is shown in the following table. The values of A + B given have been corrected for finite angular resolution due to the apparatus (5°) and Coulomb scattering (5°).

Error in measured values of $\frac{n_c(0^{\circ})}{n_c(90^{\circ})}$ = 1 + A + B.

E_d(Kev)		445±30	345±30
$\frac{N(0^{\circ})}{N(90^{\circ})}$	Background plus Statistics	2%	3%
	Apparatus anisotropy	1.5%	1.5%
E^{1}		1%	2%
E		4.5%	4%
Total Error in 1 + A + B		9%	10.5%
Error in A + B		12%	15%
A + B		2.3±0.27	2.0±0.28

Conclusions.

Within the experimental error the values of A + B observed by the author and shown in figure 12, together with previous results by others, (the dotted line is the curve for the proton reaction) are consistent with those of Preston et al (1954) and are not in agreement with those of previous workers who counted neutrons directly.

Even if the incident energy is equated to the reaction energy the values of A + B observed for the neutron reaction are significantly higher than those for the proton reaction. The small drop below the values of Preston et al may be due to an underestimate of the target depth in the silver in the calculation in the Appendix. This is also suggested by the larger value of the ratio A/B observed by the author. In figure 11 the dotted line at 445 Kev is the curve for A/B = 1 which is suggested by the results of Preston et al, while the full line is drawn for B = 0. At 360 Kev Preston et al observed A/B = 3 and the ratio increases rapidly with decreasing energy.

The descriptions of the experiments given by previous workers who counted neutrons directly have been carefully studied to see whether it is possible to give any reason for the lower values of A + B observed by these authors.

Baker bombarded a copper plate to "saturation" with 50 Kev deuterons to produce a deuterium target, then observed the angular distribution of neutrons from this target for the same incident energy of 50 Kev, using nuclear emulsion technique. It is, therefore, surprising to find that Baker expected the reaction energy to be as much as 50 Kev. If a lower reaction energy is used, Baker's point in figure 12 moves away from the proton reaction curve towards the values of Elliot et al. Bartholdson used a heavy ice target and counted neutrons using a BF_3 proportional counter surrounded by a paraffin moderator. While the use of a thick target must introduce a larger error, the most likely source of a systematic error would seem to be the variation

of the efficiency of the neutron counter with neutron energy. Bennet et al used deuterium gas targets separated from the vacuum by a thin aluminium foil (1.4 mg./cm^2) which corresponds to an energy loss of 300 Kev in deuterium passing through the foil (which was under pressure) for an incident energy of 800 Kev. The neutrons were counted using a quartz fibre electroscope, which was only sensitive near the silvered quartz fibre since the applied voltages were less than required for saturation. This neutron counter is likely to have large end effects due to loss of ionisation produced by higher energy protons. The authors realised this and state that the effect will be to reduce the observed assymetry ratio. Bennett et al appear to have been more concerned with the large scale variation of the angular distributions observed between E_d = 300 Kev and 1·8 Mev. It seems probable that the neutron counter used was less sensitive to higher neutron energies than was allowed for in obtaining the values of A + B.

Hunter and Richards also used gas targets

with a somewhat thinner foil(δE = 150 Kev at E = 600 Kev). The neutron detector was a shielded long counter, which was believed to have a flat response to different neutron energies. As in the case of Bennett et al, Hunter and Richards were mainly interested in the changes in the angular distribution over the large deuteron energy region of 0.49 Mev — 3.6 Mev.

Apart from the point in figure 12, due to Baker, which appears to be due to a mistake in interpretation of results, the only suggestion which can be put forward to explain the discrepancy between the results of previous workers who counted neutrons directly, and those derived here, is that the variation of efficiency of neutron counting with neutron energy of the neutron counters used was not known accurately.

In chapter 5 the results obtained in the experiments described in this chapter are discussed in relation to the problem of the description of deuteron reactions at low energies near and below the Coulomb barrier and the effect of Coulomb charge.

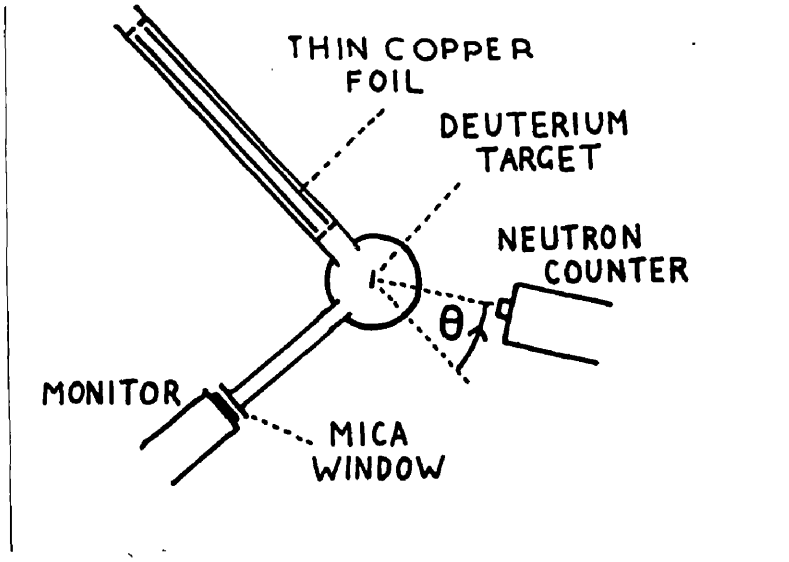

Fig.10.

Angular distribution apparatus.

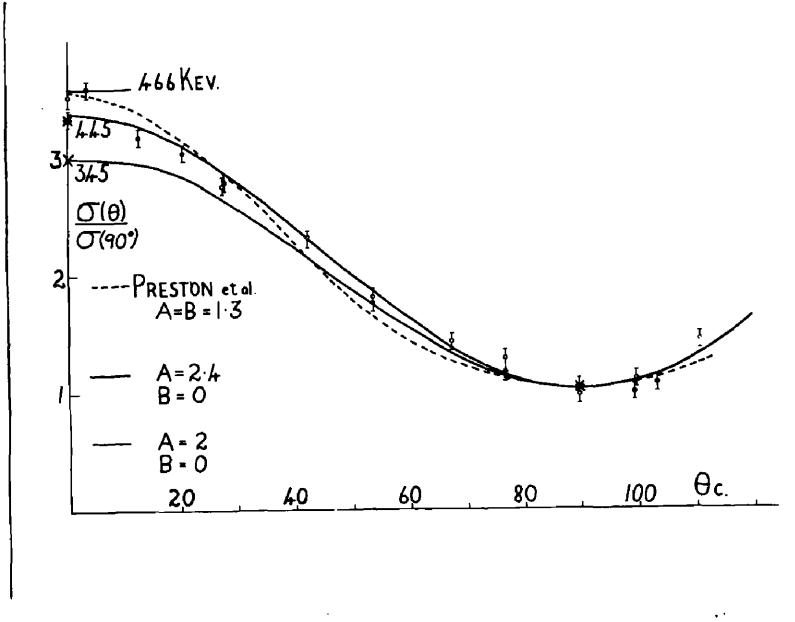

Fig.11.

Angular distribution of neutrons from the reaction $^{2}H(d,n)^{3}He$ Ed = 445 Kev.

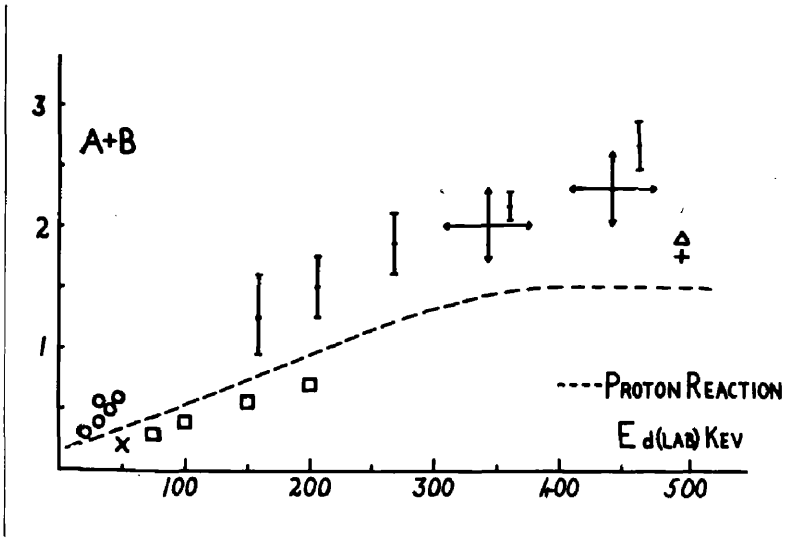

Fig.12.

$\frac{\sigma(0°)}{\sigma(90°)} - 1 = A + B$, plotted as a function of bombarding energy.

- □ Bartholdson (1950.
- × Baker and Waltner (1952).
- o Elliot et al (1953)
- △ Hunter and Richards (1949)
- \+ Bennet et al (1946)
- ‡ Preston et al (1954)
- ✣ Values obtained by author.

CHAPTER 4.

The Reactions $^3H(d,n)^4He$ and $^3H(d,\gamma)^5He$.

This chapter is devoted to a discussion of the reaction $^3H(d,n)^4He$ and a description of an experiment designed to give information on the mode of the reaction at low deuteron energies.

The angular distributions in the reactions $^3H(d,n)^4He$ have been measured for different values of the reaction energy (E_r in centre of mass coordinates) by Bretcher and French (1949), Argo et al (1952), Hemmendinger and Argo (1955), Stratton et al (1952) and Brolley et al (1951), at E_r 100 Kev, 152, 228, 392, 480 Kev, 600 Kev, 1.32 Mev and 6.3 Mev respectively. These measurements show that for values of $E_r < 300$ Kev the angular distribution is isotropic to within 10%, but as E_r increases above this value more neutrons are emitted in the direction of the incident deuteron beam. The two measurements above 1 Mev indicate that $\sigma(0^o)/\sigma(180^o) \sim 3 : 1$ for neutron emission in centre of mass. An angle of 0^o refers to neutrons emitted along the direction of the incident deuterons. At $E_r = 6.3$ Mev (Brolley et al) the angular distribution shows a secondary

maxima at 90° and the curve has been fitted fairly well by the deuteron stripping theory (as compared with triton stripping) of Butler (1950) by Butler (1951).

The integrated yield curve has been measured by Arnold et al (1954) and Conner et al (1952) over the range E_r = 6 Kev to 1·02 Mev, and at E_r = 6·3 Mev (Brolley et al). The curve of yield versus energy E_r shows a peak at E_r = 110 Kev. The value of the cross section at this energy is 5 barns, and is 2·0 barns at E_r = 55 Kev and 250 Kev. The shape of the yield curve in the energy region $E_r < 500$ Kev has been fitted very exactly by the single level resonance formula multiplied by the Gamow Coulomb function. The yield at energies $E_r > 500$ Kev and, in particular, at E_r = 6.3 Mev, appears to deviate above the value expected from the single level formula which fits so well at $E_r < 500$ Kev. Although an alternative explanation has been put forward by Flowers (1951), these results for the yield curve indicate the existence of a very strong compound nucleus level in $^5He^*$ at E^* 16·7 Mev. This would also appear

to follow from a comparison of these angular distributions and those which have been measured for the reaction $^2H + {}^2H \rightarrow {}^3He + n$ (Preston et al 1954, and others described in chapter 3). While at high energies above the Coulomb barrier both reactions can be fitted fairly well by deuteron stripping theory, at energies below the Coulomb barrier the latter reaction is still very much peaked in the forward direction. The lack of excited levels of $^4He^*$ at bombarding energies $E_d <$ barrier height suggests that the angular distributions in the deuteron reaction will indicate the degree of smoothing out of the nuclear angular distribution by Coulomb effects alone. The degree of isotropy observed and the very high yield in the tritium reaction cannot be reconciled with the residual anisotropy and yield in the deuterium reaction if any attempt is made to explain isotropy and yield in the former reaction entirely in terms of the effects of the Coulomb barrier. These are strong arguments in favour of describing the reaction $^3H(d,n)^4He$ at $E_d <$ 500 Kev in

terms of the formation and decay of a single level in the compound nucleus $^5He^*$.

The observed isotropy and the energy range of E_r involved indicate s wave deuteron interaction. Conservation of total spin and parity show that the intermediate state of $^5He^*$ must have even parity, since the observed large value for the yield at resonance can only be explained if the level involved has total spin $J = 3/2$. (Conner et al and Arnold et al).

On the basis of these existing results, it was thought that the final proof for the existence of this level and thereby proof that the most prolific of all d-n reactions in light nuclei is not due to a stripping mode but to the decay of a compound nucleus would be the detection of a yield of gamma radiation from this level consistent with the above parameters. The yield of gamma radiation expected on the basis of these parameters and an experimental confirmation of such a yield is described below.

An analysis of all available data on the nucleus ^5He (Ajzenberg and Lauritsen, 1955) shows

that there is a slight indication of a level in $^5He^*$ at $E^* = 2.6$ Mev. The level width may be ~ 3 Mev. If this level is the $P_{\frac{1}{2}}$ state predicted by the Shell Model then the parity is negative. The ground state of $^5He^*$ has been shown to be $^2P_{3/2}$ by an analysis of the scattering of fast neutrons. The parity is odd, and the width is ~ 0.8 Mev (Ajzenberg and Lauritsen). These values of spin and parity are those predicted by the Shell Model, and the width is due to the transition $^5He \rightarrow ^4He + n$ $Q = 0.95$ Mev.

Figure 13 shows the possible transitions in $^5He^*$. Estimates of the partial widths associated with the transitions are made using the radiation transition formula of Weisskopf, (Wilkinson 1953) and the usual selection rules. These calculations show that the existence of this level in $^5He^*$ at 16.6 Mev will result in the emission of several gamma rays, the most intense being γ_1, the electric dipole transition to the ground state. This transition is the only one which need be considered here. The partial width Γ_γ of the level can be

identified with the emission of γ_1 , without introducing any error > 20%.

The analysis of the yield curve for the reaction at energies near the resonance by Conner et al (1952) and by Argo et al (1952) shows that $\Gamma_n \simeq \Gamma_t$. Γ_n and Γ_t are the observed partial widths for the decay of the level by neutron emission and by triton emission (elastic nuclear scattering). The observed total width of the level Γ is, therefore, given by

$$\Gamma \simeq 2\Gamma_n \quad \text{and} \quad \Gamma_\gamma = \Gamma_n \cdot Y_\gamma/Y_n .$$

and where Y_γ/Y_n is the ratio of the observed gamma ray and neutron integrated yields at the resonance. Since the observed neutron yield near resonance is explained on the basis of s wave deuteron interaction and the possible gamma transition is electric dipole, the angular distribution of the 16.6 Mev gamma ray should be isotropic. Therefore,

$$\Gamma_\gamma = \Gamma/2 \cdot \frac{N_\gamma}{N_n}$$

where N_γ/N_n equals the ratio of 16.6 Mev gamma rays to 14 Mev neutrons observed at 90° in centre of mass.

The theoretical expression given by Weisskopf (Blatt and Weisskopf, p.627) for an electric dipole transition reduces to

$$\Gamma_\gamma = 0.11\ E^3_{(\mathrm{Mev})}\ A^{2/3}\ S,$$

where A is the atomic weight of the nucleus. S is a statistical weight factor equal to 1/5 for the values of spin change involved in this transition (see Hughes, 1954, and Wilkinson, 1954). However, there is sufficient data available on electric dipole transitions now (Wilkinson, 1953) to indicate that this theoretical value is too large and should be reduced by a factor of the order 0.05. If this is done the "theoretical" gamma width of this level for the electric dipole transition γ_1 is $\Gamma_\gamma = 15$ e.v. (to within a factor of two). Since the observed total width $\Gamma = 80$ Kev, (centre of mass) a measurement of $\frac{N_n}{N_\gamma}$ gives an experimental value for Γ_γ given by

$$\Gamma_\gamma = 4\ \frac{N_\gamma}{N_n}\ 10^4 \text{ e.v.}$$

The experiment described here consisted of measuring $\frac{N_\gamma}{N_n}$ at $E_d = 200$ Kev.

A thin (50 Kev) tritium-zirconium target was bombarded by 200 Kev deuterons and the number of 14 Mev neutrons and ~17 Mev gamma rays emitted from the target were measured simultaneously.

The neutron counter was a thin stilbene crystal in the vacuum of the deuteron accelerator. Stilbene was used in preference to sodium iodide because the non-linear response of hydrogeneous scintillators (Birks 1952) acts effectively as a mass spectrometer and widely separates the pulses from protons and alpha particles from the reactions $^{2}H(d,p)^{3}H$ and $^{3}H(d,n)^{4}He$ into two peaks in a pulse height distribution, even though the energies are so similar (E_p = 3 Mev, E_α = 2.5 Mev). The reaction $^{2}H(d,p)^{3}H$ appears as a result of deuterium build up in the tritium-zirconium target, and it was necessary to be sure that counts were not recorded during the experiment from this reaction rather than $^{3}H(d,n)^{4}He$. This was done by observing the pulse height distribution from the stilbene crystal, monitoring the tritium under deuteron bombardment, before and after the experiment. The position of the peak due to

2.5 Mev alpha particles was verified using alpha particles from polonium. After the experiment the effect of pulses corresponding to protons from the reaction $^{2}H(d,p)^{3}H$ was observed to be less than 5% of the counting rate during the experiment. In addition to ensuring that not too many spurious pulses were counted which were larger than those due to alpha particles from the tritium reaction, it was necessary to arrange a low energy cut off in the pulses counted. Towards lower energies in the spectrum there was a rising background, probably due to neutrons from the reaction $^{2}H(d,n)^{3}He$ and X-rays. The neutrons came from deuterium pile up on the slits and have an energy 2·5 Mev. The X-ray energy is probably low but is effectively enhanced by the non-linear response of the stilbene. By arranging that the pulse height distribution from the stilbene was gated by the output pulses from a discriminator fed in parallel, it was possible to find a bias on the discriminator which ensured that 90% of the pulses operating the

discriminator were due to alpha particles from the reaction $^{3}H(d,n)^{4}He$.

Applying reasonable corrections for loss of alpha particle pulses and gain of spurious pulses, it was reasonable to expect that the error due to all causes in counting alpha particles by counting the number of pulses from the discriminator was 10%. Assuming isotropy and correcting for centre of mass effects the neutron emission N_n from the target was calculated by measuring the geometry of the solid angle subtended by the stilbene crystal to the tritium target.

The gamma ray counter was a large (2" long by 1.75" diameter) sodium iodide crystal mounted on a photomultiplier. During the experiment the pulse height distribution from this crystal was observed for a measured number of counts on the discriminator counting neutrons. The gamma ray counter was calibrated by observing the pulse spectrum for gamma rays from the reaction $^{11}B(p, \gamma)^{12}C$. The gamma ray energies above 10 Mev from this reaction at E_d = 580 Kev are

16.4 Mev and 12 Mev (Ajzenberg and Lauritsen 1955). The observed pulse height spectrum is shown in figure 14.

Four runs of deuterons on tritium were made during the experiment and the pulse height distributions from the gamma ray counter were recorded separately for observed counts from the discriminator counting neutrons. Each of the four gamma ray spectra were plotted on graphs and showed the same shape and intensity corresponding to equal numbers of neutrons. The results of one run, including background, are shown in figure 14. The unscreened background in the sodium iodide crystal in position at the target was measured in the range 12 Mev — 20 Mev, for a time equal to that taken in the four runs, in between each run. This background observed in the energy region 12 — 20 Mev is also shown in figure 14, and was measured by moving the deuteron beam just off the tritium target. In addition, the background in the sodium iodide crystals was very carefully measured before the experiment and at intervals of days for

several months afterwards, over the energy range 20 Mev — 1 Kev. This was done in a heavily screened lead chamber.

The number of counts in the neutron counter was recorded for each measured gamma ray spectrum. From these readings it is possible to estimate the value of N_γ / N_n - the ratio of the number of 14 MeV neutrons to the number of 17 MeV gamma rays emitted at 90° (in centre of mass coordinates) from a tritium target under bombardment by 200 KeV deuterons. This calculation does however, require one assumption and involves factors which are somewhat uncertain. These are discussed below.

The assumption that is made here is outlined in the following discussion. It is clear from figure 14 that the gamma ray observed is not 16.6 Mev but is $\sim$ 17.5 Mev. It is assumed that this is due to the E^3 factor in the Weisskopf transition formula and that because the ground state of ^{5}He is unstable with a width $\sim$ 0.8 Mev the energy of gamma ray transitions actually observed will be larger

than the transition to the centroid of the ground state of ^5He as measured by the cross section for elastic scattering of low energy ($\sim$ 1 Mev) neutrons in ^4He. The centroid of gamma ray energies observed should be given by the factor $E_\gamma^3 B$, where B is the value of the Breit-Wigner formula for the ground state width. It is assumed here that an exact analysis in this way will give a value for $E_\gamma = 17.5$ Mev in agreement with the observed edge in figure 14. This difficulty has been recognised by Blair et al (1954) for the mirror transition $^5Li^* \rightarrow {}^5Li$ and will be discussed below.

To obtain accurately the number of gamma rays emitted from the target from the edge in the pulse spectrum in figure 14 requires a knowledge of the pulse shape for 17.5 Mev gamma rays in this size of sodium iodide crystals. Due allowance must also be made for solid angle, and gamma ray absorption. At the present time these corrections can only be made to within an error of 20%, the largest source of error being the shape of the pulse spectrum from a

single 17.5 Mev gamma ray. No single gamma ray of this energy was available. The shape of the pulse spectrum assumed here was that which would give a total number of pulses equal to one third of the product of the channel number at the edge and the number per channel on the plateau. This figure is suggested by the shape of the $^{11}B(p, \gamma)^{12}C$ spectra. The solid angle Ω of the crystal to the target was measured, and the gamma ray absorption calculated from the total cross sections for sodium and iodine. The result of these calculations were that the NaI crystal was 50% transparent to 17.5 Mev gamma rays, all the gamma rays absorbed produced pulses and the shape of the pulse spectrum was that described above. Thus N_γ is given by

$$N_\gamma = \frac{4\pi}{\Omega} \times (\text{number of } \underset{\text{Mev}}{17.5} \text{ pulses in the spectrum}) \times 2$$

Inserting the measured quantities into this equation and the similar one for N_n the value of N_γ/N_n measured is

$$N_\gamma/N_n = 15 \cdot 10^{-5} \ (\pm 7)$$

and since $\Gamma_\gamma = 4. \ \frac{N_\gamma}{N_n} \ 10^4$ e.v.

$\therefore \quad \Gamma_\gamma$(experimental) = 6 ± 3 e.v.

which can be compared with the "theoretical" value of Γ_γ (theoretical) = 15 e.v. (to within a factor of two).

Conclusions

While it is clear that both the theoretical and the experimental values given above are somewhat uncertain, it is, nevertheless, considered that they agree sufficiently well to prove that the level in $^5He^*$ at 16.6 Mev does exist and the gamma transition to the ground state has been observed. It is of interest to compare this result with that observed for the identical mirror transition $^5Li^* \longrightarrow {}^5Li$, by Blair et al (1954), using the mirror reaction $^3He(d, \gamma)^5Li$, who obtained a value for Γ_γ(experimental) = 11 ± 2 e.v. The observed gamma ray energy quoted by these authors is 16.6 MeV but analysis of their published spectra indicates that a value of 17 MeV can be obtained if a linear relation is assumed between pulse height and electron energy dissipated in their sodium iodide crystal the theoretical values are the same for $^5Li^*$ and $^5He^*$.

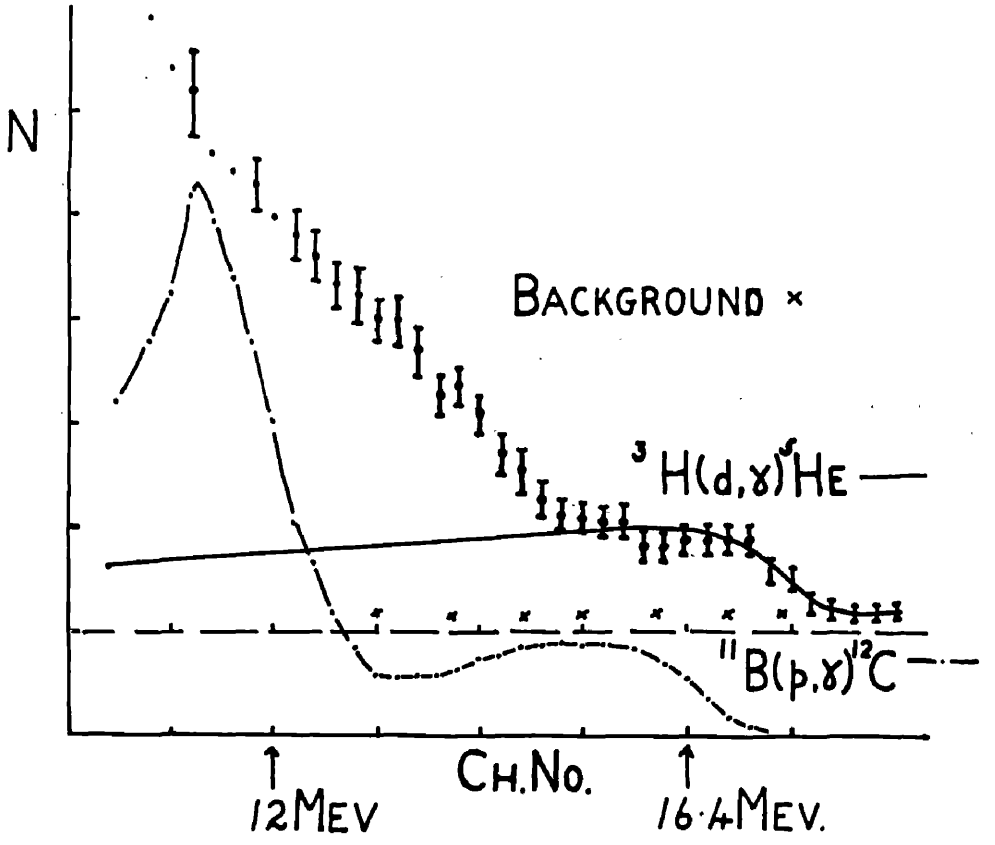

Fig.14.

Pulse height distributions from a sodium iodide crystal 2" x 1.5". Reactions $^{3}H(d,\gamma)^{5}He$ and $^{11}B(p,\gamma)^{12}C$.

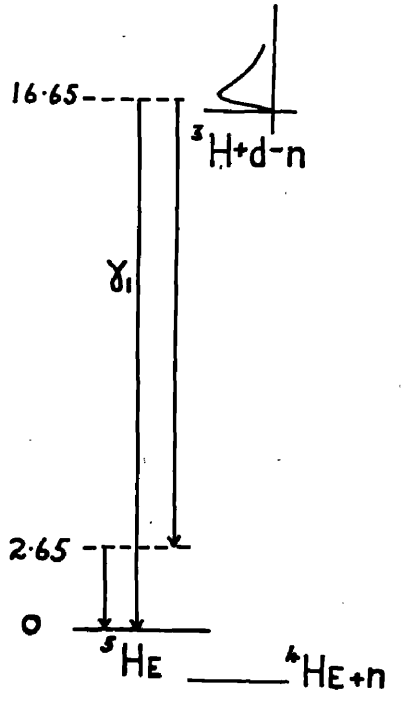

Possible gamma ray transitions in helium.

Fig.13.

CHAPTER 5.

Discussion of A(d,n)A + p Reactions in Light Elements at Deuteron Energies below the Coulomb Barrier.

$^{2}H(d,n)^{3}He$

The evidence for the view that at high deuteron energies, the neutrons which are observed from this reaction are "stripped" off by the interaction of nuclear forces, and that at low deuteron energies there is nothing to indicate compound nucleus formation and decay has been presented at the beginning of chapter 3.

At low deuteron energies the original Butler theory for (nuclear) deuteron stripping gives much too high (factor 5 - 10) an assymetry ratio, although the qualitative appearance of the angular distributions (peaked in the direction of the incident deuterons in centre of mass) suggests a form of deuteron stripping process. If this is accepted, there appear to be two alternatives, either the reaction mode is (nuclear) deuteron stripping greatly modified by Coulomb scattering of the colliding deuterons before the stripping occurs, or the stripping occurs due to the polarisation and eventual splitting of the

deuterons by the electric force between the protons in the two deuterons.

The latter has been examined quantitatively by Phillips and Oppenheimer (1935). As would be expected from the nature of the process (two protons pushing each other away), these calculations predict that the assymetry ratio in the angular distributions for the mirror reaction ($^2H(d,p)^3H$) and the integrated yield should be higher than those for the neutron reaction at the same deuteron energy. The results of the experiment by the author, described in chapter 3, support Preston et al (1954) and Elliot et al (1953) in showing that the observed assymetry ratios for the neutron reaction have significantly (30%) higher values than those for the proton reaction. In addition Preston et al (1954) and Booth (1955 private communication) have shown that the integrated yield is greater in the neutron reaction by 10 - 20%. Both of these results are in contradiction to what is expected if the reaction is described by the Phillips-Oppenheimer theory.

However, these results and the general

reduction observed in the assymetry ratio for both reactions as the deuteron energy decreases appear qualitatively at least to be consistent with the view that, as the deuteron energy falls below the Coulomb barrier, the deuterons suffer significant Rutherford scattering which smears out the well defined laboratory direction, before the nuclear (Butler) stripping occurs. Qualitatively the results observed are very similar to what would be expected if an extra angular width (varying with angle) were introduced experimentally.

In principle, the introduction of Coulomb scattering into Fairbairn's theory (i.e. Butler theory modified to allow for the identical reacting deuterons) is possible by considering the interference between the incident and scattered waves of deuterons. Unfortunately, a detailed calculation is very complicated and, at the time of writing, neither the author or anyone else has succeeded. It is not possible here to do more than suggest that results observed in the $^{2}H(d,n)^{3}He$ reaction are in qualitative agreement with those expected from

nuclear (Butler) deuteron stripping modified by Coulomb scattering. The additional small reduction in the assymetry ratio for the proton reaction may be due to Coulomb scattering of the emitted proton, just as the large reduction in the ratio for both reactions may be due to Coulomb scattering of the incident deuterons.

$^{3}H(d,n)^{4}He$

The conclusion reached above, that Coulomb scattering may smooth out the observed angular distributions due to 'nuclear' stripping, does not affect the interpretation of this reaction at low deuteron energies, since the angular distribution is isotropic. The evidence in the yield at low energies, and the shape of the angular distribution at high energies which leads to the view that the reaction mode at low energies is due to compound nucleus, was discussed in chapter 4. The observation of a yield of gamma radiation by the author, consistent with the life-time of the level of ^{5}helium involved, adds weight to the previous evidence.

It seems quite impossible to reconcile the degree of isotropy in this reaction with the residual anisotropy in the reaction $^{2}H(d,n)^{3}He$ at the same deuteron energy $\sim$ 200 Kev, on the basis that the reaction mode in the tritium reaction is deuteron stripping modified by Coulomb scattering, which is, indirectly, suggested by Flowers (1951). All the evidence suggests that at low deuteron energies approximately 98% of the observed neutron yield comes from the decay of a level in 5helium, and only 2% can be due to deuteron stripping. (These figures are obtained by comparing the observed cross sections in $^{3}H(d,n)^{4}He$ and $^{2}H(d,n)^{3}He$).

An interesting result, which can easily be deduced from the angular distribution at high energies but is rarely mentioned, is that since the neutrons are observed mainly in the direction of the deuteron in centre of mass, it is the deuteron which loses the neutron and not the triton. It is interesting to speculate whether a small increase at 180^{o} might be observed at high energies due to neutrons leaving the triton. The angular separation of neutrons from the

different nuclei in this way should provide an interesting comparison of the two possibilities. Both are, of course, $l = 0$ transitions, but are peaked in the initial direction of the nucleus they leave.

If it is accepted that this reaction is due to compound nucleus formation and decay at low deuteron energies, then it is clear that the existence of a strong level in the compound nucleus $(A + d)^*$ can easily cause the yield in the reaction to rise well above that due to deuteron stripping, and that the yield curve will show a pronounced resonance.

The two hydrogen reactions $^2H(d,n)^3He$ and $^3H(d,n)^4He$ appear to be examples of the extremes, predominantly deuteron stripping and compound nucleus reaction modes respectively.

$^{11}B(d,n)^{12}C$

The results shown in figure 8 of chapter 2 for the ground state transition in $^{11}B(d,n)^{12}C$, observed by the author, can be fitted fairly well by the simple Butler deuteron stripping curve plus an apparently incoherent isotropic background.

When this result at 600 Kev is compared with that of Ihsan (1955) at 870 Kev, also shown in figure 8, the effect of lowering the deuteron energy is apparently to increase the contribution of the isotropic background.

The curve in figure 9 for the angular distribution of neutrons leaving ^{12} carbon in the first excited state observed by the author at 600 Kev cannot be fitted by a Butler curve plus an incoherent isotropic background. Comparison with the results of Ihsan at 870 Kev suggests that the general shape of the curve fluctuates wildly in a manner similar to that expected from the formation of different levels of the compound nucleus ^{13} carbon.

However, the yield curves, shown in figure 7, for both neutron groups show no indication of a resonance and the curves are very similar. There is also a consistent agreement in the relative intensities of the neutron groups measured at higher energies (Gibson 1949 and Johnson 1952).

The author is very much indebted to

A.H.de Borde (private communication) for the following outline of a theoretical approach to this problem which appears to give a reasonable explanation of these results, which are very similar in their general characteristics to those observed by Green et al (1955) for the reactions $^{9}Be(d,n)^{10}B$ and $^{13}C(d,n)^{14}N$, using nuclear emulsion technique. At low deuteron energies the incident plane wave (e^{ikz}) of deuterons will suffer significant Coulomb scattering. If the plane wave is expressed as the sum of partial waves of angular momentum $l = 0, 1, 2 .....$, then only the contribution due to s waves is likely to interact with the target nucleus, and only the scattering of the s wave component need be considered. Thus the effect of Coulomb scattering can be represented approximately by a plane wave of incident deuterons and a spherically symmetrical wave of scattered deuterons. That is if $\psi_1 = e^{i\lambda}\psi_1$, where ψ_1 is the wave function of the emitted neutrons in the simple Butler deuteron stripping theory and ψ_1 is real,

and $\psi_2^0 = e^{i(\lambda+\phi)}\psi_2$ where ψ_2 is real and independent of θ corresponding to the s wave of scattered deuterons and ϕ is the phase shift between ψ_1^0 and ψ_2^0,

then $\psi^0 = \psi_1^0 + \psi_2^0 = e^{i\lambda}(\psi_1 + \psi_2 e^{i\phi})$

where ψ^0 is the total wave function for the emitted neutrons,

and $\psi^0 \cdot \psi^{0*} = \psi_1^2 + \psi_1\psi_2(e^{i\phi} + e^{-i\phi}) + \psi_2^2$

$\therefore \sigma(\theta) \propto \psi_1^2 + 2\psi_1\psi_2\cos\phi + \psi_2^2$

i.e. $\sigma(\theta) \propto f(\theta) + 2K^{1/2}\cos\phi[f(\theta)]^{1/2} + K$,

where $f(\theta)$ is the simple Butler deuteron stripping curve; K is independent of θ and decreases with incident deuteron energy; $\cos\phi$ may be either positive or negative, and is independent of θ, but may vary with deuteron energy and from one neutron group to another at the same deuteron energy.

In terms of this theory, the phase shift for the ground state transition in the reaction $^{11}B(d,n)^{12}C$ at 600 Kev is $\sim\pi/2$ since there is no indication of the interference term

$$2\,[K]^{1/2}\cos\phi\,[f(\theta)]^{1/2}$$

also $K/f(\theta) \sim 2, \quad \theta = 0^\circ$.

which indicates that the contribution from s wave scattered deuterons is large. The phase shift ϕ for the excited state transition cannot be such that $\cos\phi$ is zero, ~~and~~ since the curve rises in the back direction. . No attempt has been made to fit the results exactly by this theory, since it is hoped that further calculations (de Borde private communication) will give values for K and reduce the number of unknown variables to one instead of two. However, qualitatively, it can be seen that the value of K is fairly close to that for the ground state transition.

In addition to the theory by de Borde, outlined above, there have been three other attempts recently to derive the Coulomb correction in deuteron stripping.

Austern and Butler (1954) and Yoccoz (1954) have stated that the result of numerical calculations of the effect of Coulomb charge in deuteron stripping is to show that there is very little effect. No generalised formula or other reason for this statement is given, and the

results observed by the author and others, especially for the reaction $^{2}H(d,n)^{3}He$, are definitely not consistent with this view.

A recent attempt to include Coulomb charge effects in the original Butler deuteron stripping theory has been made by Grant, I.P. (1955) who gives a generalised formula involving two additional variable parameters. Unfortunately, the formula is extremely complicated, and it is stated that it is very tedious to compute results from it. It is interesting to note that the two results so far computed by Grant suggest that Coulomb charge effects can greatly modify the shapes of the curves.

Examination of the existing experimental results suggests that it may be possible to explain almost all of the angular distributions in reactions of the type A(d,n)A + p in light elements by the Butler deuteron stripping theory, modified by the addition of a coherent isotropic background, as suggested by de Borde. There may, however, be one or two cases in which strong levels of the compound nucleus $(A + d)^{*}$

contribute significantly, but where this occurs there should be evidence for the level in the yield curve for the reaction. It seems possible that further work along these lines will permit the development of a detailed mathematical theory for the Coulomb correction to deuteron stripping for partial width measurements at high energies, and to explain the results at low energies. This will, however, require many further measurements at different deuteron energies on different targets.

CHAPTER 6.

The Reaction $^{127}I(n,2n)^{126}I$.

During the experiment described in chapter 4, the sodium iodide crystal became radioactive. It is very unlikely that sodium iodide crystals will often be irradiated in this manner intentionally, but there will be occasions when, in the course of an experiment, an unavoidable activity will be built up in a sodium iodide crystal by fast neutrons. It is important to know the characteristics of the radioactivity produced. For this reason, the decay of the radioactivity produced in the crystal was observed over a period of one month. To assist in the identification of the activity in the crystal a sample of ordinary iodine (^{127}I) was irradiated with 14 Mev neutrons and the radioactivity produced was analysed and the decay observed over a similar length of time.

The pulse height spectrum from the sodium iodide crystal was measured at intervals of a few days, and a typical spectrum is shown in figure 15. A detailed analysis of the decay rate of each element in the spectrum was found

to have a large uncertainty due to statistical error, electronic drift and the large number of elements present. It seemed, however, from the curves that all the elements in the spectrum decayed with a half-life of the order 15 $\pm$ 3.5 days. The spectra taken soon after the initial irradiation clearly showed that whatever the radioactivity was, it decayed with the emission of a gamma ray of energy 675 $\pm$ 5 Kev, unaccompanied by an electron. This indicated that an electron capture process to an excited state was involved, and an examination of the very low energy pulse spectrum from the crystal showed that X-rays of energy 27 Kev were appearing in the crystal, unaccompanied by any other ionising radiation.

The energy of the X-ray was measured by comparison with the X-rays from a radium D source, E_X = 12 and 45 Kev. A typical spectrum is shown in figure 16. The rate of decay appeared to be consistent with a half life of 13 days. These observations suggested an electron capture process to a ground state.

In addition to the prominent gamma line

at 675 Kev, there appeared to be two low intensity gamma rays at 1.42 ± .01 Mev and 1.72 ± .01 Mev in the spectra of figure 15, which might also be due to electron capture to excited states of ^{126}Te.

The subtraction of pulses due to all three gamma rays in the spectra was possible using pulse spectrum shapes extrapolated from those observed using a ^{137}cesium source (E = 677 Kev) and ^{22}sodium source (E = 511 Kev and 1.27 Mev). When this was done, and the initial background was also subtracted, the shape of the remainder of the spectrum was rather uncertain, due to statistical error. However, on the assumption that it was due to an electron transition, it was possible to fix the maximum energy of the transition at a value of 1.3 Mev.

The radioactivity in the crystal was, therefore, attributed to the decay of ^{126}I, since it was known (Mitchell et al, 1949, and Perlman and Friedlander, 1951) that ^{126}I decays

with a half life of 13 days (Nuclear Data) through electron capture and beta decay to stable ^{126}Tellurium and ^{126}Xenon (see figure 17).

As a further check to this identification, a sample of normal iodine was irradiated with a very strong flux of 14 Mev neutrons, and the intense radioactivity produced was analysed using the same sodium iodide crystal. In this analysis only the gamma ray transitions were observed, since the radioactivity came from outside the crystal. The counting rates involved were of the order one hundred times that due to the residual activity in the crystal. Typical gamma ray spectra observed are shown in figure 18. Observations extended over a period of one month showed that the detailed shape of the pulse height distribution did not change, and the total radioactivity decayed with a half life 13 days. The gamma rays observed were, therefore, attributed to transitions in the decay of ^{126}I. The two prominent lines in figure 18 (E = 370 $\pm$ 10 Kev and E = 650 $\pm$ 10 Kev)

can be identified with gamma ray transitions in the beta emission and electron capture branches respectively. A gamma ray of energy 382 Kev has been observed by Perlman and Friedlander in coincidence with the 0.85 Mev beta spectrum of ^{126}I.

There is a significant difference between the observed gamma ray energies of the electron capture transition when it was observed from the iodine in the crystal ($E = 675 \pm 5$ Kev, figure 18) and from iodine outside the crystal ($E = 650 \pm 10$ Kev, figure 15). This difference in energy of ~ 25 Kev can be attributed to the addition in the crystal of a gamma ray of energy 650 Kev and a ^{126}Te X-ray of energy 23 Kev (see figure 16).

Conclusions.

These observations were sufficient to show that when a sodium iodide crystal is exposed to fast neutrons of energy near 14 Mev, the activity observed in the crystal for several months afterwards is essentially due to the

decay of ^{126}I with a half life of 13 days, formed in the reaction $^{127}I(n,2n)^{126}I$. The bulk of the decay products have an energy $\lesssim$ 1.3 Mev, plus two weak gamma lines at 1.42 Mev and 1.72 Mev. (but see note in proof.)

The other most likely reactions which might have contributed to the activity are:-

$^{23}Na(n,2n)^{22}Na$ σ = 13.8 $\pm$ mb. Prestwood (1955)
τ = 2.8 years Nuclear Data.

$^{23}Na(n,p)^{23}Ne$ σ = 34 mb. Paul and Clark (1953)
τ = 40 secs. Nuclear Data.

$^{23}Na(n,d)^{20}F$ σ = not observed probably 50 mb.
τ = 12 secs. Nuclear Data.

$^{23}Na(n,\gamma)^{24}Na$ σ = not observed at 14 Mev. probably very small.
τ = 15 hours Nuclear Data.

$^{127}I(n,p)^{127}Te$ σ = 231 mb. (Paul and Clark)
τ = 90 days Nuclear Data.

$^{127}I(n,\alpha)^{123}Sb$ σ = 18.4 mb. (Paul and Clark)
τ = 21 minutes Nuclear Data.

$^{127}I(n,\gamma)^{128}I$ σ = not observed at 14 Mev probably very small.
τ = 25 minutes Nuclear Data.

The only reaction which needs to be taken into account is apparently $^{127}I(n,p)^{127}Te$, which

will contribute approximately 5% to the observed activity in a sodium iodide irradiated with 14 MeV neutrons. The value of the cross section for the reaction $^{127}I(n,2n)^{126}I$ at 14 MeV is of ~ 1.5 barns, and accounts for 95% of the observed activity.

NOTE ADDED IN PROOF.

A recent measurement of the residual activity in the sodium iodide crystal shows that the two weak gamma lines at 1.42 MeV and 1.72 MeV in figure 15 cannot be attributed to the decay of ^{126}I with a half life of 13 days, since the intensity of these lines relative to the rest of the spectrum is now considerably higher. The relative intensities of the two lines has not changed.

CHAPTER 7.

Time of Flight Fast Neutron Spectrometer.

Nuclear emulsions as fast neutron spectrometers rapidly lose their value at neutron energies less than 3 Mev, due to lack of energy resolution from straggling in the small ranges and scattering of recoil protons by the heavy constituents in the emulsion. Measurements of pulse height distributions, due to recoil protons in organic scintillators, also have poor energy resolution in this region, which gets rapidly worse as the neutron energy decreases. Very recently a new technique, using a gas filled proportional counter with a high concentration of ^{3}helium, has been developed at A.E.R.E., Harwell (England). The basis of this technique is the observation of protons from the reaction $^3He(p,n)^3H$, Q = 770 Kev. Some preliminary details given at the 1955 Neutron Physics Conference at Harwell can be summarised here. Energy resolution 10%, mainly due to edge effects; the efficiency is a few per cent; the cost is £500,000, due to the current price of ^{3}helium; and at energies above 1 Mev the pulse height distribution includes

a comparable number of recoil ^{3}helium nuclei. While this instrument is an improvement over other techniques, the high cost is likely to limit severely its general application.

Time of flight technique exploiting the speed and efficiency of organic scintillators offers, in principle, good energy resolution in the energy region < 3 Mev. The time of flight t per metre of path for a neutron of energy E is given by $t = 72.1\ E^{-\frac{1}{2}} \cdot 10^{-9}$ secs. and the time resolution of scintillation counter coincidence circuits lies within 10^{-8} — 10^{-9} secs, depending on the required efficiency of coincidence detection and the photomultipliers.

The time of flight technique, described in this chapter, was developed primarily for use with the reaction $^3H(d,n)^4He$. Essentially, the technique consists of measuring the time delay between two pulses from separate photomultipliers. The first pulse is due to the recoil alpha particle from the tritium reaction detected in a thin stilbene crystal. The second pulse is due to a recoil proton in an

organic scintillator at the end of the neutron flight path. Apart from centre of mass effects, the neutron and alpha particle from a single reaction are emitted in opposite directions. The solid angle subtended by the stilbene crystal to the tritium target defines a solid angle for neutrons emitted in coincidence with detected alpha particles. A "target" placed within this "beam" of neutrons causes the beam to be scattered. Gamma rays, and neutrons resulting from the scattering processes in the "target" are emitted, and can be detected by the second organic scintillator, which is placed at a position out of the "beam" of 14 Mev neutrons. The distance between the scattering "target" and the second scintillator is the effective flight path for measurements on the scattering products. By measuring the time delay spectrum between the pulses from the two scintillators it is possible to calculate the neutron energy distribution, if two factors are known accurately. These factors are:-

(1) the n-p scattering cross section in the second scintillator,

(2) the energy of recoil proton in the second scintillator which just fails to operate the time delay measuring device (coincidence unit).

The first factor is known very accurately, and is discussed in chapter 1. The second factor can be measured experimentally by observing the pulse height distribution in the second scintillator, in coincidence with output pulses from the coincidence unit. This is done by operating the coincidence unit from the collectors of both multipliers and measuring the pulse height distribution appearing on earlier dynodes stages. To achieve linearity in the observed pulse spectrum, the third or fourth dynode stage has been found suitable.

Using the known response curve for organic scintillators, discussed in chapter 1, it is possible to measure the cut off using coincidences from annihilation radiation. The use of gamma ray sources is of considerable help, and is strongly advised in setting up apparatus before experiments on neutrons which

require the operation of deuteron accelerators, and the use of costly tritium targets with dangerous neutron fluxes.

The circuit of the simple coincidence unit developed by the author to allow simultaneous measurements of time delays over the region 0 - 10^{-7} sec. in steps of 10^{-9} sec. is given, and its operation explained, in the Appendix. For convenience, it is called here — the time converter. The basis of this method of multichannel time delay analysis is that a single output pulse is produced by the time converter for each pair of delayed pulses from the two scintillation counters. The height (in volts) of the single output pulse is linearly related to the time delay (in millimicroseconds) between the pair of input pulses, and a trivial pulse output is observed when this time delay is greater than 10-7 sec. (The value of 10-7 quoted here is easily changed if required). Thus the time delay spectrum in the pairs of pulses from the two photomultipliers is converted into

a pulse height distribution which can be analysed by pulse height analysers. The Hutchinson-Scarrot (1951) pulse height analyser was used by the author to obtain 100 channels, each channel corresponding to a time delay of 10^{-9} sec. over the range 0 - 10^{-7} sec. This technique was developed following preliminary measurements of time delays by the author, using a simple high speed time base on an oscilloscope (see Appendix)

Time Calibration

In the Appendix it is shown that the pulse output V from the time converter and the time delay t of neutrons in the flight path are related by the equation

$$V \propto T_0 - t,$$

where T_0 is a time depending on the distances of the scattering "target" and the stilbene crystal to the source of 14 Mev neutrons, and on the length of the delay cable inserted between the collector of the photomultiplier used to detect neutrons and the corresponding input to the time converter.

Using coincidences produced by the effectively instantaneous double gamma transition in ^{60}cobalt detected in two liquid (xylene + terphenyl) scintillators (2" x 2" x 2") the linearity of V as a function of T_o was measured. Figure 19 shows the pulse height distribution from the time converter for a fixed value of T_o, and the variation of the mean pulse height for different lengths of inserted cable, giving different values of T_o. The cable employed here was insulated by polythene and had a velocity of propagation of 2.10^{10} cms./sec. at the frequencies involved.

Using this calibration curve, the velocity of gamma rays, from the positron source ^{22}sodium, was measured. The two liquid scintillators were separated by about two metres and the shift in the peak on the pulse height analyser produced by shifting the source from one scintillator to the other was compared with that produced by a known length of inserted delay cable. Figure 20 shows the peaks observed. The value of C for gamma rays obtained in this way by careful statistical analysis is

$3.09 \pm .23\ 10^{10}$ cms./sec. The large error is due to the poor statistics.

Using the reaction $^3H(d,n)^4He$ and detecting recoil ^{4}helium nuclei and emitted 14 Mev neutrons at different distances to the target the velocity v_n of 14 Mev neutrons and v_α of 3.5 Mev alpha particles was measured to establish whether the delay cable propagation constant could be used with confidence to establish a convenient standard time scale. The values of v_n and v_α observed agreed within an error of one or two per cent (almost the statistical error) with the value of the cable velocity quoted above. In addition, the delay observed for two positions of the neutron detector appeared to indicate that V varied linearly with t. The peak observed for neutron-alpha coincidences at a fixed value of T_o and t, with the neutron detector in the coincidence "beam" is shown in an inset of figure 22 in the following chapter.

Time Resolution

The time resolution in the peak in figure 22 and of that produced by gamma ray coincidences, shown in figure 19, is of the order 10^{-8}sec. By selecting pulses within a limited range of height on each of the two collectors and arranging that coincidences were counted only when they were due to pulses within this range the resolution was improved only at the expense of a drastic reduction in the overall efficiency of coincidence counting. It seems probable that the resolution observed here would be improved without sacrificing efficiency by using R.C.A. 5819 photomultipliers and external distributed amplifiers for extra gain before the time converter, and that the observed width for E.M.I. tubes is due to their characteristic bandwidth for high frequencies being $\lesssim$100 megacycles.

After the conclusion of the work described in this chapter and the next, O'Neill (1954) published an account of an independent development and application of an almost

identical technique. The term time chronometer is used by O'Neill instead of time converter, and the principle of converting time delays to pulse heights is not used for time measurements. Only 9 channels are available with a time resolution of $4 \cdot 7 \cdot 10^{-9}$ sec. each, in O'Neill's method, in contrast with 100 channels and 10^{-9} sec. in the method described here by the author.

Recently, Snyder and Parker (1954) have measured neutron time delays over a flight path of ten metres by pulsing the deuteron beam in a Cockcroft-Walton accelerator at a frequency of two megacycles and with a pulse duration of 10^{-8} sec. The technical problem of measuring neutron energies is essentially the same and the results obtained in the course of the research described here are of interest in connection with using reactions of the type A(d,n)A + p with pulsed deuteron sources, as well as with the particular reaction $^{3}H(d,n)^{4}He$, in which there is a convenient recoil particle to indicate time zero. The main drawback to using recoil particles is that only one neutron

is emitted for each time zero pulse, while only a small fraction of emitted or scattered neutrons are detected. This drawback is overcome using a pulsed intense beam of deuterons, and it seems likely that further developments will be made along these lines.

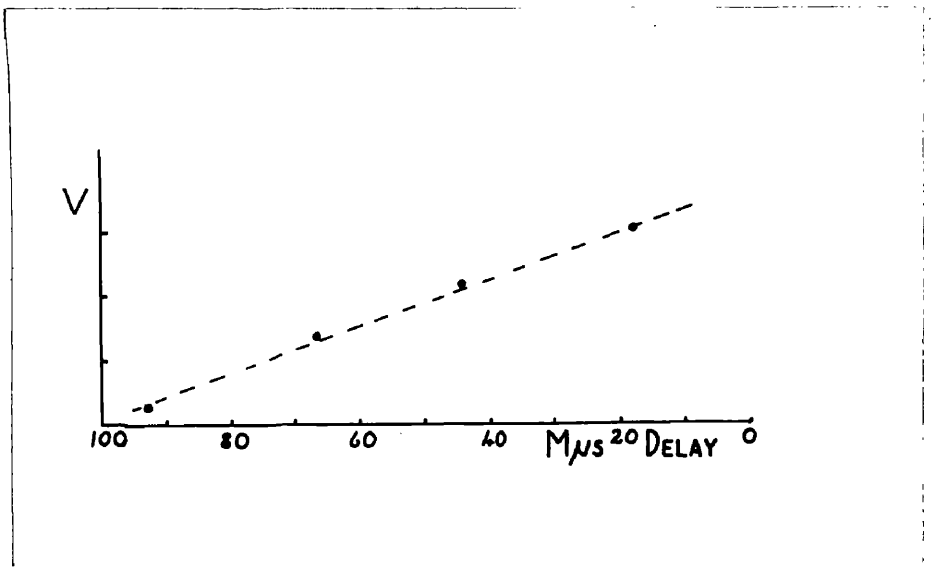

Fig.19.

Mean pulse height versus inserted delay, time converter.

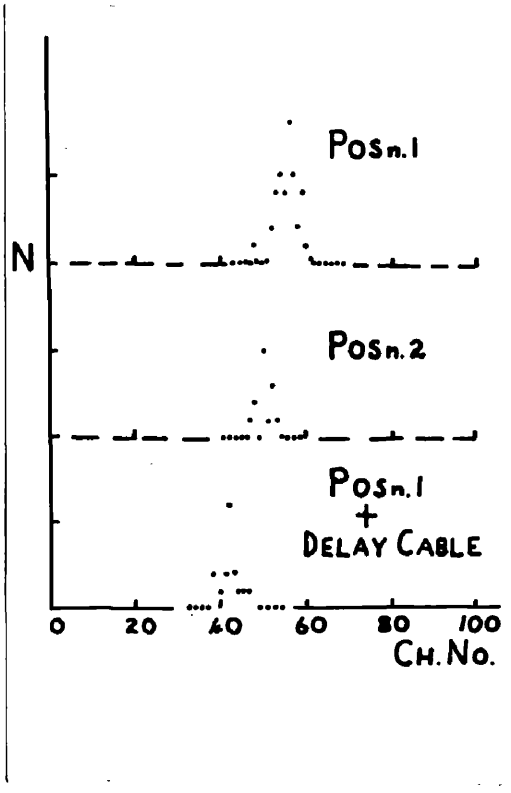

Fig.20.

Velocity of Gamma rays.

Shift in mean pulse height due to time of flight compared with shift due to inserted delay

CHAPTER 8.

The Energy Spectrum of Neutrons following Scattering of 14 Mev Neutrons in Aluminium.

Gittings et al (1949) and Phillips et al (1952) have used threshold detectors to estimate crudely the energy distribution of neutrons following the scattering of 14 to 15 Mev neutrons in several elements, including aluminium. They estimate that most of the inelastic neutrons are scattered with energies less than 3 Mev. This result is confirmed by observations of Stelson and Goodman (1950), and Whitmore and Dennis (1951) using nuclear emulsions.

The emission of inelastically scattered neutrons has been studied theoretically by Weisskopf (Blatt and Weisskopf, p.366) who have shown that on the basis of the Evaporation model and under the conditions of a very large number of levels in the final nucleus, the energy spectrum of emitted neutrons should be given by

$$\frac{dn}{dE} \propto E \quad e^{-E/T}.$$

T is called the nuclear temperature of the final nucleus (in the case of neutron scattering, the final nucleus is the target nucleus) and its

value is uncertain in the theory due to the lack of data on energy levels at high excitation energies. The available information (Ajzenberg and Lauritsen 1952, 1955) on the level structure at high energies suggests that even in medium and fairly light nuclei the level density may be sufficiently large for the equation given above to hold for inelastic neutron emission following the scattering of 14 Mev neutrons. The equation is only expected to be followed where either the levels overlap or the energy resolution is not sufficiently good to resolve discrete levels.

The purpose of the experiment described in this chapter was to discover whether it is practical to measure the inelastic neutron spectrum following the scattering of 14 Mev neutrons in aluminium using the time of flight technique described in the previous chapter, and if possible to relate the low energy distribution to the predictions of the Weisskopf evaporation model.

Neutron "Beam"

The intensity contours of the 14 Mev neutron "beam" formed by observing coincidences between recoil alpha particles and emitted neutrons from a thick tritium target bombarded by 200 Kev deuterons are shown in figure 21, together with the angular size of the alpha particle and neutron detector used.

Aluminium "Target"

The target consisted of two pieces of aluminium, each one centimetre thick, placed in the position indicated in figure 21. This thickness was chosen to be less than the mean free path of emitted neutrons.

Neutron Detector

The neutron detector was a glass bottle 2" x 2" x 2", containing a xylene-terphenyl mixture, mounted on a 14-stage E.M.I. photomultiplier type number 6262.

The neutron detector was placed at an angle of 45^{o} to the target in the plane of the neutron "beam" and the coincidence time spectrum

measured with "target" in and "target" out. The background with target out was of the order of 20% of the true scattered counting rate, and is attributed to scattering of the "beam" in the room and chance coincidences between alpha particles and neutrons from the target. The observed pulse height distribution from the time converter is shown in figure 22. To convert this time spectrum into an energy spectrum it is necessary to know the variation of n-p cross section with neutron energy and the proton energy which, dissipated in the scintillator, just fails to operate the time converter. This is measured by observing the pulse height distribution in the neutron detector gated by coincidence between it and an identical liquid scintillator for gamma rays from Na^{22}. The value of the cut off in proton energy, using the electron-proton response curves of chapter 1, was 450 Kev. By combining this with the n-p cross section and angular distribution data of Blatt and Jackson (1949), and assuming that the inelastic neutrons in

the energy region 1 — 3 Mev have a continuous distribution, the neutron energy spectrum is obtained. An inset of figure 22 shows a plot of

$$\log_e \frac{1}{E} \cdot \frac{dN}{dE}$$

as a function of E. The gradient of this graph defines the quantity T. The region of time delays involved is indicated by the arrows in figure 22.

Diffraction Peak in the Angular Distribution of Elastically Scattered Neutrons.

A discriminator and scaler biased off to count only pulses from the time converter corresponding to the elastically scattered neutron peak in figure 21 was used to investigate the variation of $\sigma_{el}(\alpha)$ in the region $\alpha = 55^{\circ}$ — 85°. The observed variation of the counting rate in the scaler is shown in figure 23. For these measurements the solid angle of the alpha particle detector to the tritium target was reduced by moving it further away, and a thin 50 Kev tritium target was bombarded at

200 Kev to form a coincidence neutron "beam" considerably narrower than that used in the energy distribution experiment. The angles at which measurements were taken were selected because of the difficulty in making measurements at small angles to the incident neutron "beam" and because a simple calculation on the basis of diffraction of a neutron wave by a spherical nucleus of radius R indicated that the second maximum in the diffraction pattern should appear in this region. The angular resolution due to the angular size of the neutron "beam" and the solid angle subtended by the neutron detector are shown in the figure.

Discussion of Results

Probably the most significant result of this experiment is that a new technique for detecting fast neutrons scattered out of a neutron "beam" is seen to be capable of giving quantitative results.

The measurements of the angular variation of $\sigma(\alpha)_{el}$ are only significant in indicating

the apparatus was functioning properly and in confirmation of the extensive accurate measurements of Coon et al (1955 private communication). The curve in figure 23 is drawn using the recent theory of Fernbach et al (1955 unpublished report), which is discussed in chapter 9. The method used by Coon et al is very similar to that described in chapter 1, and is much superior to time of flight methods for measurements of elastic scattering at this neutron energy (14 Mev).

The results observed by Graves and Rosen (1953), using nuclear emulsions, and O'Neill (1954), using time of flight, are shown in the inset of figure 22 on the log plot for the nuclear temperature. The values of T observed are of the same order of magnitude as is expected from the Evaporation Model, which does not claim precision due to lack of data on level densities. A possible contribution from the (n,2n) reaction has been ignored. However, the results observed add support to the concept of the Evaporation Model and indicate that time of flight technique is capable of at least giving

results as good as those obtained using nuclear emulsion technique. As confidence in techniques employing scintillation counters increases, it seems probable that time of flight will be used over considerably longer flight paths, with subsequent improvement in energy resolution, which will allow more detailed examination of low energy neutron spectra.

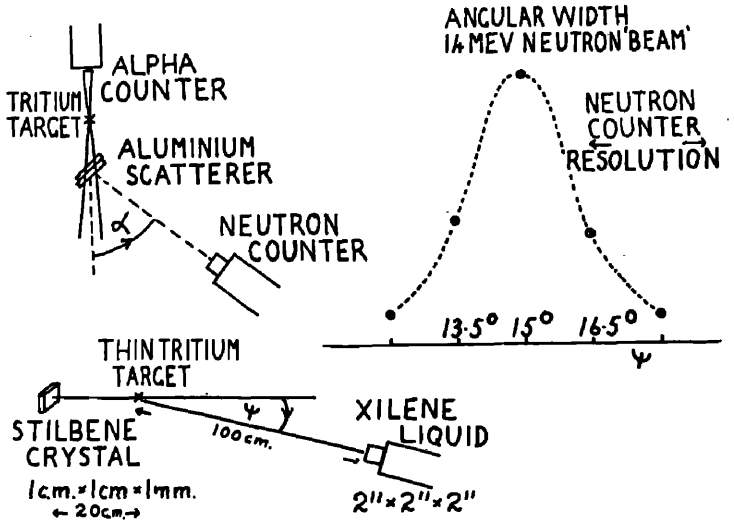

Fig.21.

Formation and angular width of 14 Mev neutron "beam" used in scattering experiments.

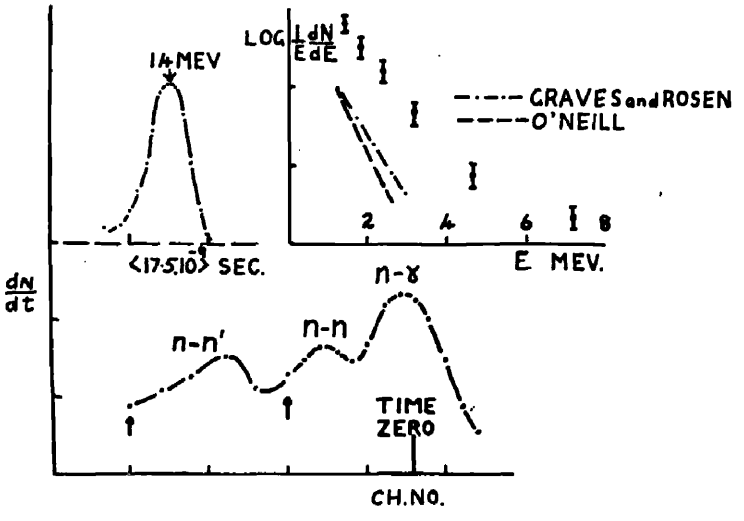

Fig.22.

Inelastic scattering of 14 MeV neutrons in Aluminium.

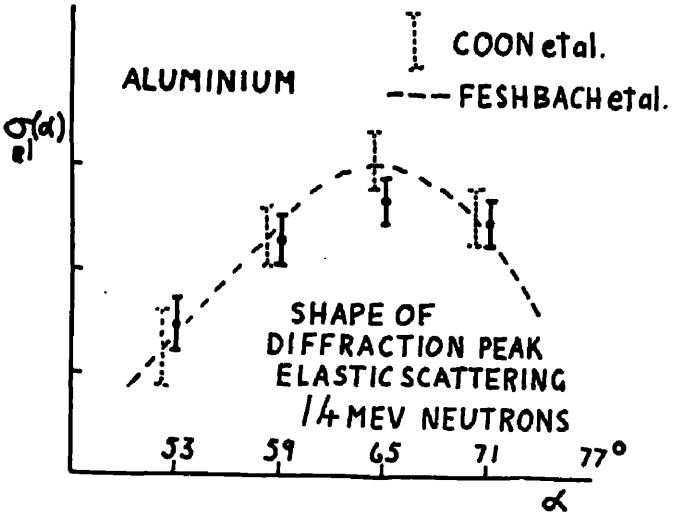

Fig.23.

Elastic scattering of 14 Mev neutrons in Aluminium.

CHAPTER 9.

Reactions of the Type A(d,n)A + p in Light Elements as a Source of Fast Neutrons for Scattering and Absorption Experiments.

The purpose of this chapter is to outline some recent developments in the interpretation of fast neutron experiments and to suggest how the reactions listed in the Introduction, together with the scintillation counter and other techniques developed in the course of the research by the author, can be used with advantage in future investigations.

The original interpretation of elastic scattering and reaction cross sections for fast neutrons is due to Feshbach (1949), and is based on the concept of the compound nucleus (N. Bohr) discussed in the Introduction. The early theory (1949) can be stated as follows - incident fast neutrons are represented statistically by a plane wave which is partially reflected at the surface of the target nucleus A. A neutron corresponding to the fraction of the wave transmitted through the surface is assumed to share its energy with the nucleons and form a compound

nucleus immediately. The decay of the compound nuclei thus formed can occur through any energetically possible exit channels, resulting in elastic and inelastic neutrons. The elastic scattering cross section is expected to be mainly due to neutrons reflected at the nuclear surface (potential scattering) plus a usually small contribution due to the decay of compound nuclei. The theory was an attempt to predict total cross sections, reaction and elastic cross sections for fast neutrons. It was not concerned with a study of individual levels but with the gross structure problem of the mean effective potential V_0 in a nucleus of radius R for incoming fast neutrons. It is, therefore, expected to be more applicable to medium and heavy target nuclei and that results showing sharp resonances due to levels in the compound nucleus $(A + n)^*$ must be smoothed out before comparison with the predictions of the theory.

The measurements of Barschall et al (1952) and others of total neutron cross sections in the range 1 — 15 Mev show that the smoothed out values varied slowly and continuously as a

function of atomic weight and neutron energy as expected from the theory but showed a low rise and fall instead of the expected monotonic variation. Since the right order of magnitude of elastic and reaction cross sections was predicted, and the observed total cross section is continuous for both varying atomic weight and neutron energy, it does not seem probable that the fault in the interpretation is due to the relatively narrow resonances in the compound nuclei formed. As a result of these measurements Feshbach et al (1954) have proposed that the early theory be modified by the introduction of the concept of a nuclear absorption coefficient for fast neutrons transmitted through the nuclear surface. Instead of the immediate and inevitable formation of a compound nucleus $(A + n)^*$ it is proposed that the fast neutron can collide with individual nucleons and knock them out of the nucleus (or be scattered out itself) during a finite time before the formation of the compound nucleus by less energetic collisions. This modification appears in the theory as a change

in the potential well describing the nucleus. Instead of a completely real potential V_o, the potential V which the neutron "sees" within the nuclear surface at radius R is complex and represented by

$$V = V_o(1 + i \epsilon).$$

This change results in a scattered coherent wave from within the nucleus which interferes with the surface scattered wave and introduces an absorption into the transmitted wave before the formation of a compound nucleus.

A comparison of calculations based on this Complex Potential well model with the total cross sections measured by Barschall et al and others shows that the theory can reproduce the results very precisely over the energy range 1 - 15 Mev and in the range 0 - 3 Mev in particular for values of V_o = 42 Mev, and ϵ = .03, which corresponds to a mean free path of fast neutrons in nuclear matter (before formation of a compound nucleus) of 24.10^{-13}cms. (Fernbach et al 1954). Experimental results for the elastic angular distributions and

reaction cross sections are not very plentiful, due to the limitations and delays in experimental techniques. Phillips et al (1952) and Walt and Barschall (1954) have measured reaction cross sections at 14 Mev and 1 Mev respectively. The results at 14 Mev can be interpreted in terms of the early theory, suggesting that the mean free path is very small at this energy. The results at 1 Mev are not in good agreement with those predicted by the Complex Potential well theory, but the characteristic oscillatory shape of the variation with atomic weight is reproduced. Feshbach et al (1954) interpret these results to indicate that the nuclear mean free path varies significantly in the energy region 1 - 5 Mev. The few existing measurements of angular distributions are not very well fitted by the Complex well theory or by the earlier theory. However, a very recent (1955 unpublished) report by Fernbach et al shows that the introduction of a degree of rounding off of the nuclear surface is sufficient to fit the result of Coon et al (1955 unpublished) at

14 Mev. It is expected that the combination of a complex potential well and rounded nuclear surface will fit angular distributions at lower energies. In this report some predictions of 14 Mev neutron polarisations following elastic scattering in medium and heavy nuclei are made, by the introduction of a spin-orbit term ($\alpha \underline{l} . \underline{s}$) into the potential well. At some angles the predicted polarisation is of $\sim$ 100%.

The concept of a nuclear absorption coefficient implies that nucleons and groups of nucleons may be observed from nuclei by direct collision processes preceeding the formation of a compound nucleus. Paul and Clarke (1953) have observed values for reactions of the type A(n,p), A(n, α) and A(n,2n) at 14 Mev, which are much higher than those predicted by the Evaporation Model based on the value of the reaction cross section using the early theory (Feshbach 1949). While the recent developments described above apply to medium and heavy nuclei, there are also advances being made in the interpretation and significance of experiments involving discrete

levels of light nuclei. Satchelor (1955 private communication) has shown that the concept of direct collision processes in medium and heavy nuclei discussed above has a parallel in light nuclei which can be termed nucleon stripping. This theory is very similar to Butler's deuteron stripping theory in concept, the nature of the calculations and the numerical results. Nucleon stripping is an immediate process in competition with the formation and decay of compound nuclei $(A + n)^*$ formed by neutron capture. The relative contributions of the two reaction modes can be found by measurements of the angular distribution and correlations in experiments of the type $A(n,n^1)A^*$. The final nucleus can be any discrete levels of the target nucleus. The same theory applies to the nuclear effects observed in fast proton scattering experiments. Although Coulomb charge effects are very difficult to allow for, the recent experiments of Schrank (1954) on inelastic scattering of 17 Mev protons in iron suggest that the contribution to the reaction mode from nucleon

stripping may be large.

Some measurements of polarisation of neutrons have been made for the reaction $^{2}H(d,n)^{3}He$ at low deuteron energies, although they are not in very good agreement with each other, they can be compared with the theory of Blin-Stoyle (1951, 1952 and private communication). It seems probable that the polarisation of neutrons from the reaction $^{2}H(d,n)^{3}He$ at deuteron energies less than 300 Kev will be of the order 50% at some angles. This reaction is, therefore, a most convenient source of polarised neutrons for future scattering experiments (Blin-Stoyle, 1951). It seems probable that high deuteron beam current (10 m.a.) Cockcroft-Walton accelerators of a few hundred Kev will be very convenient and powerful sources of fast neutrons using the reactions listed in the Introduction. The Q values for these reactions cover the range of neutron energy in which many interesting developments are appearing. The difficulty in using the reactions as sources of neutrons in the energy range 1 - 15 Mev is mainly that they are roughly isotropic and, apart from the

hydrogen reactions, they do not emit single neutron lines, and they do emit gamma rays. While many further developments in technique will appear, and previous techniques such as nuclear emulsions still have value, an attempt is made here to try to suggest how significant and purposeful research can be done, which is closely related to the apparent trends in this field very briefly reviewed above, using these sources and the techniques developed in the course of the research described in the thesis.

Discrete Neutron Groups

The plastic scintillator as a fast neutron spectrometer, described in chapter 1, can probably be used for angular distribution measurements of elastically scattered neutrons and for inelastic neutrons corresponding to low lying levels of the target nucleus. A practical arrangement for these measurements is to use cylindrical scatterers and a neutron absorber as a shield between the neutron source and the plastic scintillators. As different neutron

energies are used (different targets and centre of mass effects) different thicknesses of plastic scintillator can be selected to avoid gamma rays. Another method which would avoid gamma ray effects completely would be to gate the pulse height distribution of proton recoils in the plastic by a delayed coincidence with a sharp machine pulse. The big increase in technology required for this may be justified in some cases where several inelastic groups can be measured at once. The best method of pulsing the machine is probably to shift the beam with a self-running oscillator at the ion source where the deuteron energy is low. A pulse at time zero, for coincidence gating, could be produced by arranging that the deuteron beam struck a piece of quartz, viewed by a photomultiplier, immediately before it fell upon the target.

Low Energy Continuous Distributions

Apart from direct measurements of low energy neutron distributions from the reactions themselves, which has not been done to any great extent, it seems probable that measurements of inelastic neutron spectra can be made accurately

by Time of Flight. If the machine can be pulsed with a pulse duration of the order of a few times 10^{-9} sec, and long flight paths are used, the energy resolution achieved will be better than any other technique. It seems probable that the spectra will consist of sharp lines corresponding to the decay of compound nuclei and perhaps a continuous distribution due to direct collision processes. The lack of efficiency will result in long machine times being required, but this is quite feasible using such a simple accelerator, which should be capable of running night and day by itself without servicing for several weeks. In this way the spectra can be measured at different angles. These results will be of great value in extending our knowledge of direct collision processes.

Polarisation Experiments

These experiments will be aimed at measuring the polarisation of the neutrons from the reactions A(d,n)A + p, especially the D-D reaction, and the use of the partially polarised

beams for scattering experiments of the type described above. It is expected that there will be advances in theoretical interpretation as a result of preliminary experiments, and that further experiments will be guided by theory. Another type of experiment will be the production or enhancement of polarisation. The experimental arrangement for polarisation experiments of all types will probably use double scattering which should become feasible using high neutron fluxes and high efficiency plastic scintillators, with or without machine pulsing.

Production of Isotopes

The production of isotopes using the intense neutron fluxes from these reactions and the analysis of their decay schemes should allow a considerable amount of very useful research. Although the experiment using iodine, described in the thesis, involved no very short half lifes, it seems probable that very short lived isotopes can be produced and their decay analysed by linking the analysing apparatus to the

accelerator. In some cases this will mean simply repeatedly blocking off the beam for a minute or so, with a mechanical shutter, but measurements can be extended to times of the order of 10^{-8} by pulsing the accelerator and observing decay products in between pulses.

Background from the D-D Reaction

At very high deuteron beam currents, deuterium build up in slits and in targets will rapidly result in a background of neutrons from the reaction $^{2}H(d,n)^{3}He$. Slits should be made of thin metal and heated to over 600°C to keep them clean of deuterium. Targets should be rotated to expose fresh surfaces uncontaminated by deuterium build up in experiments in which a background of 2.5 Mev neutrons will be troublesome. A convenient type of deuterium target is made of a cylinder with deuterium inserted into the surface by bombardment using the technique described in the Appendix, and rotated slowly with a lateral movement to obtain a very large surface area. Centre of

mass effects are very large in the D-D reaction, and the neutron energy observed at 0° from reactions in deuterium inserted to form a target may be 1 Mev higher than that of neutrons from deuterium build up in the target during an experiment.

APPENDIX
Section 1

The Production of Thin Deuterium Targets

Gas targets of deuterium are unsuitable for experiments using the reaction $^{2}H(d,n)^{3}He$ at deuteron energies of a few hundred Kev. The thickness of window required to separate the vacuum of the accelerator and the target is too thin at these deuteron energies, and produces large energy straggling and is mechanically difficult to maintain. When no window is used, and the pressure difference is maintained by the impedance of a long narrow canal down which the incident deuterons travel before reaching the target volume, the background of neutrons from reactions in the canal is extremely high, and gas targets of this type are only suitable for experiments in which recoil ^{3}helium and tritium nuclei are detected. (Arnold et al 1954, Preston et al 1954).

Solid deuterium ice targets are, in practice, thick targets and the background can be considerable from evaporated deuterium.

Thin hydrogen targets can be prepared by adsorption on zirconium, but this technique of producing targets of a specified thickness is something of a fine art for stopping powers of the order of 25 KeV.

At the moment only tritium-zirconium targets are supplied by Harwell, and these are usually thick to several hundred Kev deuterons.

The method used here to produce thin deuterium targets consisted of bombarding silver with 50 Kev deuterons. There are several references to this method of preparing "solid" targets of materials, normally gaseous, in the literature (Siegbahn 1951).

This method of preparing thin targets relies on the ability of a metal to trap gas atoms in the crystal lattice. The metal chosen must also satisfy the criteria of clean reproducible surfaces and good thermal conductivity. Silver appears to be the best choice of metal to satisfy these requirements. The blocks of silver used in the experiments of chapter 3 were 2 mm. x 1 cm. x 3 cm. and were carefully turned, then

polished with the finest emery cloth available; then mounted on a target holder with a very flat thin metal surface. Immediately below this surface a circulating water supply kept the target backing cool.

The deuterons were accelerated in a column which was made of glass to provide insulation and allow the target surface to be observed during the bombardment. Figure 24 shows the electrode design which was finally arrived at. The metal screens shown as dotted lines in figure 24 were essential to prevent the accelerating voltage short circuiting down the glass walls. The accelerating column was immediately above a 2" oil diffusion pump (backed by a small rotary pump). It was found to be unnecessary to use a liquid air trap. With clean oil in the diffusion pump it required thirty minutes to lower the vacuum in the chamber from atmospheric pressure to operating pressure. For convenience in supplying the ion source with gas, magnet current, and probe voltage, the ion source was at ground

potential and the target at -50 Kev. An isolated water supply was used for target cooling. The high voltage was obtained from a conventional Cockcroft-Walton power pack. No focussing electrode was used, but it is doubtful whether this was entirely satisfactory, as it was necessary to change the dimensions of the accelerating lens until the final required beam size on the silver target block was achieved. It was arranged that the beam focus point occurred above the target, and that the area of the diverging beam as it entered the silver block was 0.25 cm^2.

The targets were prepared by mounting the silver blocks at 45° to the deuteron beam. They were then transferred to the high tension accelerator and used at 45° to the bombarding high energy deuterons. The reason for this procedure was to avoid the effects of any irregularities in the surface of the silver. The effect of different preparation times T for a fixed target producing current was investigated by observing the yield of protons

from the reaction $^{2}H(d,p)^{3}H$ at a bombarding deuteron energy E_d = 500 Kev. It was observed that for a target deuteron current of 250μA at 50 Kev the yield of protons from the targets increased with T for values of T less than one hour, for a target area of 0.25 cm^2.

The targets used for investigation of the reaction $^{2}H(d,n)^{3}He$ were prepared at I= 200μA and T = one hour, area = 0.25 cm^2, E_d = 50 Kev. When bombarded for a short time at 500 Kev and then several days later bombarded again in the same position, the yield of protons from the target for the same bombarding current did not appear to change by more than 5% = the experimental error.

Although it should be possible to measure the characteristics (depth in the silver d and target thickness t) of targets produced in this way by precise matching of the two deuteron beams, and a measurement of the observed neutron or proton cross section for the incident bombarding energy, this was not done. To be of any practical use, such measurements would require

a long and detailed experimental programme, and the prime requirement at this time was simply the production of thin deuterium targets with characteristics known only to within the accuracy required by the experiment in view. The calculation of $\underline{d}$ and $\underline{t}$ was made as follows.

The empirical results for $\frac{dE}{dx}$ of protons in silver, reviewed by Allison and Warshaw 1953, end at a proton energy of 50 Kev. If the final gradient of the curve is extended linearly to zero energy and applied to the case of deuterons then

$$\frac{dE}{dx} = 50 + 0{\cdot}6\ E,$$

where E is the deuteron energy in Kev and dx is in mg./cm^2. The range R is given by

$$R = \int_0^{50\ \text{Kev}} \frac{dE}{50 + 0{\cdot}6\ E} = \frac{1}{0{\cdot}6} \log_e 50 + 0{\cdot}6\ E$$
$$= 0{\cdot}80\ \text{mg./cm}^2.$$

For deuterons in silver the Rutherford scattering formula reduces to

$$\frac{n(\theta)}{n_o} = \frac{1{\cdot}6}{2} \cdot 10^3 \frac{dx}{E^2\,\theta^2} \qquad \theta \quad \sin\theta$$
$$dx \text{ in mg./cm}^2.$$
$$E \text{ in Kev},$$

where $\frac{n(\theta)}{n_o}$ is the ratio of the number of deuterons scattered at angles greater than θ divided by the number of deuterons in the beam. Replacing dx by $\frac{dE}{50 + 0.6\,E}$, equating θ to unity

$$\frac{n(1)}{n_o} = \frac{1.6}{2} \cdot 10^3 \int_{50\ \text{Kev.}}^{E} \frac{dE}{E^2\,(50 + 0.6E)}$$

Numerical integration of this equation gives the result E = 16 Kev, when $\frac{n(1)}{n_o} = \frac{1}{2}$.

That is, assuming primary scattering only, the value of the deuteron energy in the silver at which one half of the incident deuteron beam has been scattered is $\sim$16 Kev, for an incident energy of 50 Kev, and this energy is reached at a distance of 0.40 mg./cm^2, which is identified with d.

On the basis of these simple calculations the values of t and d are

$$d \sim 0.4 \text{ mg./cm}^2$$

$$\text{and } t \sim 0.40 \text{ mg./cm}^2.$$

From the tables of Allison and Warshaw the values of $\frac{dE}{dx}$ in silver for deuteron energies of 500 and

400 Kev are 140 Kev per mg./cm^2. The effective reaction energies in these targets for incident bombarding energies of 500 and 400 Kev are, therefore, 445 $\pm$ 30 and 345 $\pm$ 30 Kev respectively.

The deuteron energy of 50 Kev, used for the production of targets, was chosen as a compromise between various factors. It was essential to get sufficient deuterium into the targets to achieve a high signal:background ratio during experiments using the targets. Since the effect to be investigated varied rapidly with deuteron energy, it was also essential to limit the depth of the deuterium in the silver. Also it was necessary to avoid intense overheating of the silver surface, and overloading the silver lattice with deuterium atoms. A figure of 10:1 silver atoms to deuterium atoms in the target region was chosen, and the deuteron charge Q for an area S = 0.25 cm^2 and thickness of silver t = 0.4 mg./cm^2 was calculated from the equation -

number of silver atoms = $5.5 .10^{23} . S.t = 10 \times Q.\frac{10^{19}}{1.6}$

= 10 x number of deuteron atoms,

i.e. Q = 0.9 Coulombs,

which corresponds to a current of 200μA x one hour.

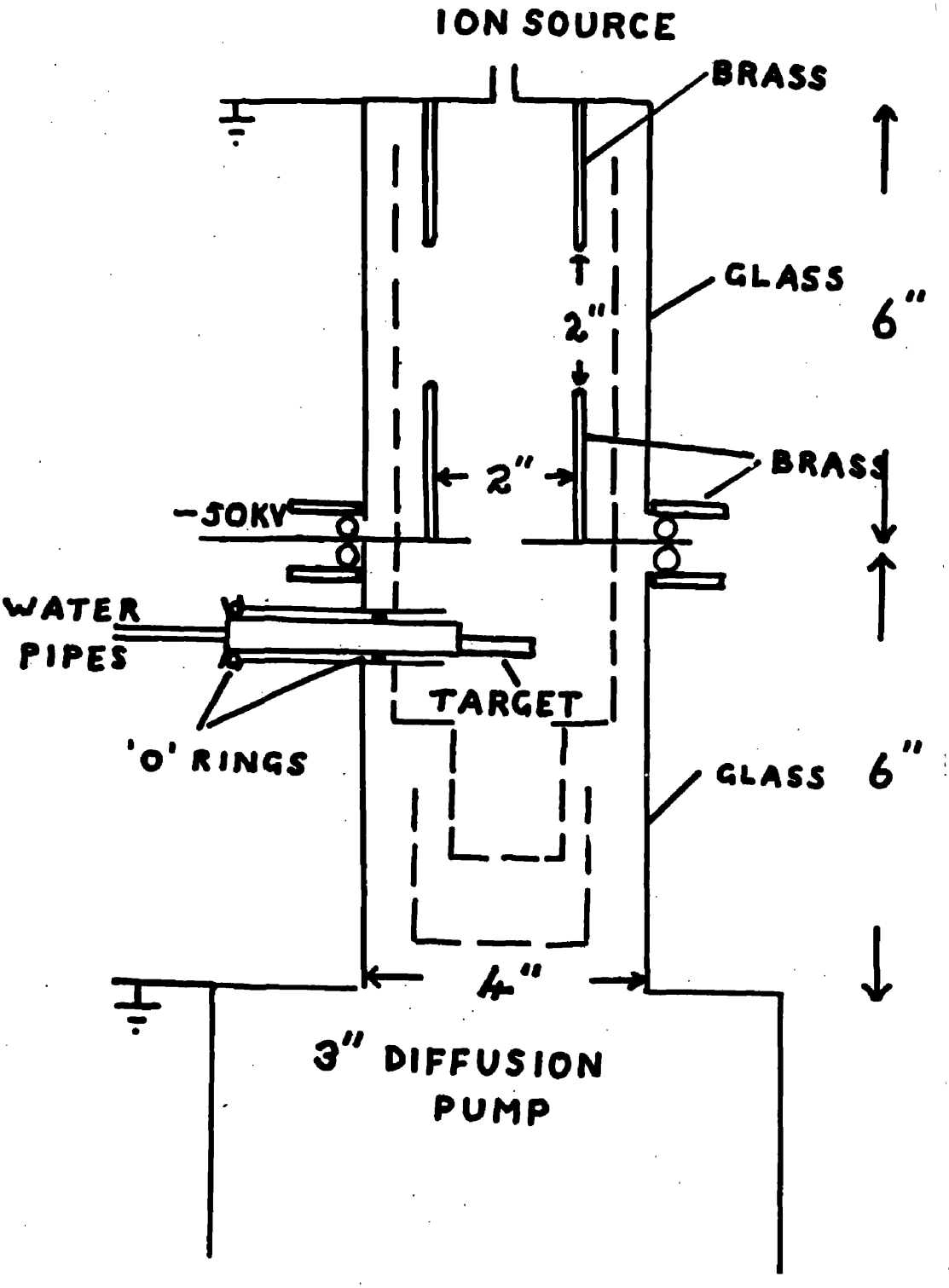

Fig.24.

Apparatus used for the production of thin deuterium targets by bombarding silver with 50 KeV deuterons.

APPENDIX

Section 2.

Time Delay - Voltage Converter

Fig.25 is the circuit diagram of a unit which linearly converts time delays into voltage pulses in the region 0 - 10^{-7} sec. Fig.26 shows the pulse waveforms at different points in fig.25.

The operation of the circuit shown in fig.25 is as follows. Consider a current pulse (16a) appearing on the collector K_1 of photo-multiplier 1. The voltage waveform produced by this on the grid of the pentode V_1 has the form shown in fig26b. The initial fast recovery is to approximately - 7.5 volts as C_s discharges through the clamping diode D_1. The almost linear rise to zero beyond this is due to C_s trying to discharge to earth potential through R_2. The holding diode D_2 helps to prevent V_{gk} from going positive. The purpose of these diodes D_1 and D_2 is to avoid excessive pulse pile up on the grid at high counting rates. A similar voltage

waveform appears on the grid of the pentode V_1^1 when a current pulse is produced by photo-multiplier $2(K_1^1)$.

When a current pulse appears on the collector of only one photo-multiplier the shape of the voltage waveform at the anode of V_1 is as shown in fig.26c. The effect of the delay cable L_D is to displace this waveform to the right when the current pulse appears on K^1. The amount of the displacement T_D is given by the time taken by the pulse to travel down L_D. The duration of the pulse $\underline{T}$, is twice the time taken by a pulse to travel from the anode of V_1 to the shorted end of the cable L_S: $T = 10^{-7}$ sec. in the tests described in chapter 7. When V_1 is shut off at time $t = o$ and V_1^1 a time $\underline{t}$ later, the voltage waveform on the anode of V_1 is as shown in fig.26d. The duration of the step or overlap is $T - (T_D + t)$.

The cathode of the germanium crystal diode D_3 is biased by V through R_{10}, R_9, R_8 and R_7 to a positive voltage slightly larger

than the height of the voltage waveform in fig.26c. This diode only conducts appreciably during the overlap shown in fig.26d. The time constant $R_8 C_A$ is adjusted to be much longer than the maximum duration of overlap. The voltage pulse V_A on C_A is, therefore, a linear function of $T - (T_D + t)$. V_A is amplified by an external amplifier and fed to a multichannel pulse height analyser. A change in pulse height recorded by the pulse height analyser clearly corresponds to a shift in time delay between the original very fast photomultiplier pulses.

Occasionally, the pulse recorded by the pulse height analyser can be much smaller than it should be to correspond to the time delay between the original events producing the coincidences. The output from the point B in fig.25 is employed for this purpose; fig.26f shows the voltage waveform at this point. When a waveform, such as is shown in fig.26d, is amplified without discrimination by a slow amplifier the size of the output voltage pulse

is proportional to the area of the original fast waveform, that is the output is reasonably insensitive to the position of the step or overlap in fig.26d. The condition that must be satisfied is that 1/T is much greater than the bandwidth of the amplifier. The network R_5, C_B, R_6 satisfies these conditions for $T = 10^{-7}$ sec. The amplifier feeds a discriminator which is biased so that it only delivers an output pulse when two standard pulses of the type shown in fig.26f have appeared at the anode of V_1 inside a time less than 10^{-6} sec. The output from this discriminator is used to gate the pulse height analyser; a conventional circuit can be used for this purpose. The 100 channel pulse height analyser used by the author (Hutchinson and Scarrott) has a built in coincidence gate circuit. The reason why the pulse output from the time converter is sometimes smaller than it should be is probably due to the clipping valves being partly shut off before the real coincidence pair of pulses arrive at the grids. It is essential in any practical application of

this circuit, or similar circuits, to choose photomultipliers with low noise, and to avoid excessive background of small pulses if the number of coincidences discarded by the operation of the gate is to be kept small. Since the number of noise pulses from photomultipliers increases rapidly at very high gain it is an improvement to use distributed amplifiers (Electronic Engineering 1952) between the collector of the photomultiplier and the input to the coincidence unit, thus allowing smaller voltages on the photomultipliers.

It can be seen from fig.25 that the valves V_1 and V_1^1 have no feedback or negative grid bias, therefore their standing currents I and I^1 are sensitive to changes in heater voltage. To avoid drift it is preferable to provide the heating current for these valves from "trickle" charged accumulators and to monitor visually I and I^1. The positive line is at earth potential to avoid 50 cycle hum. Excessive temperature changes in the time converter should be avoided by allowing the air to circulate freely as the characteristics

of the diodes change with temperature. The bias on the gate discriminator should be monitored as the efficiency depends on its value. Without distributed amplifiers the photo-multipliers (14-stage E.M.I. 6262) are run at approximately + 2 KV on the collectors. The power packs supplying the - 150 V are carefully stabilised and the mains voltage applied to all the electronics is monitored visually by a meter on the output of a "Variac" transformer.

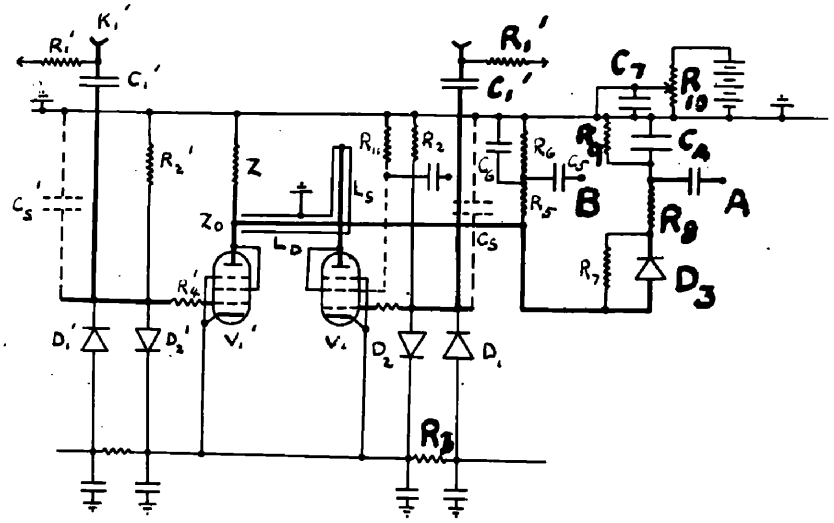

Fig.25.

Time Converter Circuit.

K_1, K_1^1 ; E.M.I.6262.

D_1, D_2, D_3 ; GEX/45.

V_1, V_2 ; 6 X CV138.

$Z = 6852 = Z_o$.

$L_o = 20.10^{-9}$ sec.

$L_s = 10^{-7}$ sec.

E = 6 volts.

$R_1 = R_1^1 = 100$ K.

$R_2 = R_2^1 = 470$ K.

$R_3 = R_3^1 = 75\ \Omega$.

$R_4 = R_4^1 = 12\ \Omega$.

$R_5 = 470$ K.

$R_6 = 82$ K.

$R_7 = 100$ K.

$R_8 = 2$ K.

$R_9 = 22$ K.

$R_{10} = 500\ \Omega$.

$R_{11} = 70\ \Omega$.

$C_1 = C_1^1 = 100$ pf.

$C_2 = C_2^1 = .01 \mu F$.

$C_3 = C_3^1 = 0.1 \mu F$.

$C_4 = C_5 = C_6 = C_7 = .01 \mu F$.

$C_A = 500$ pf.

$C_B = 20$ pf.

$C_S = C_S^1 = 50$ pf.

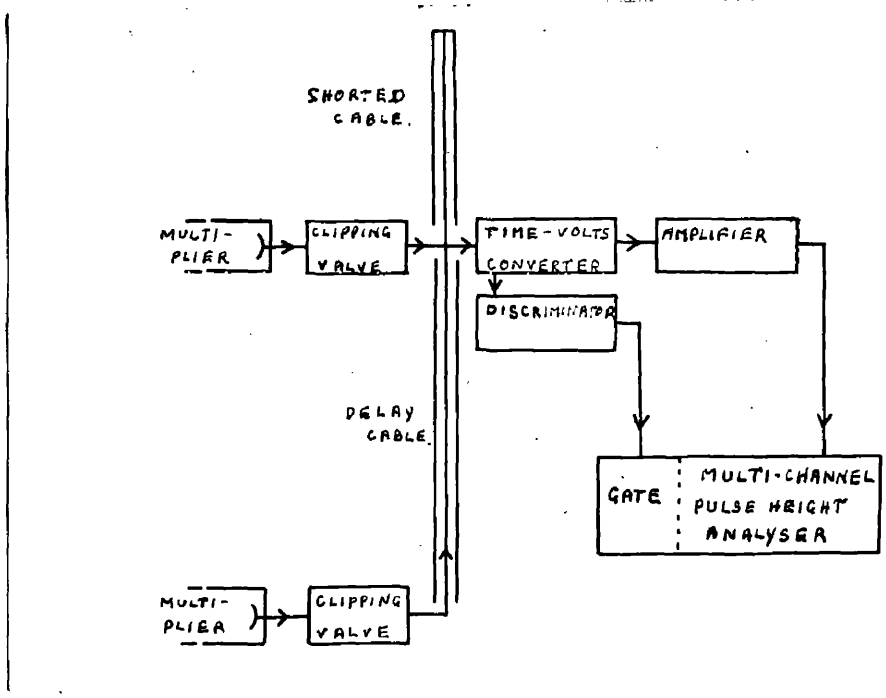

Fig.25(a).

Arrangement for measuring millimicrosecond time delays by pulse height analysis.

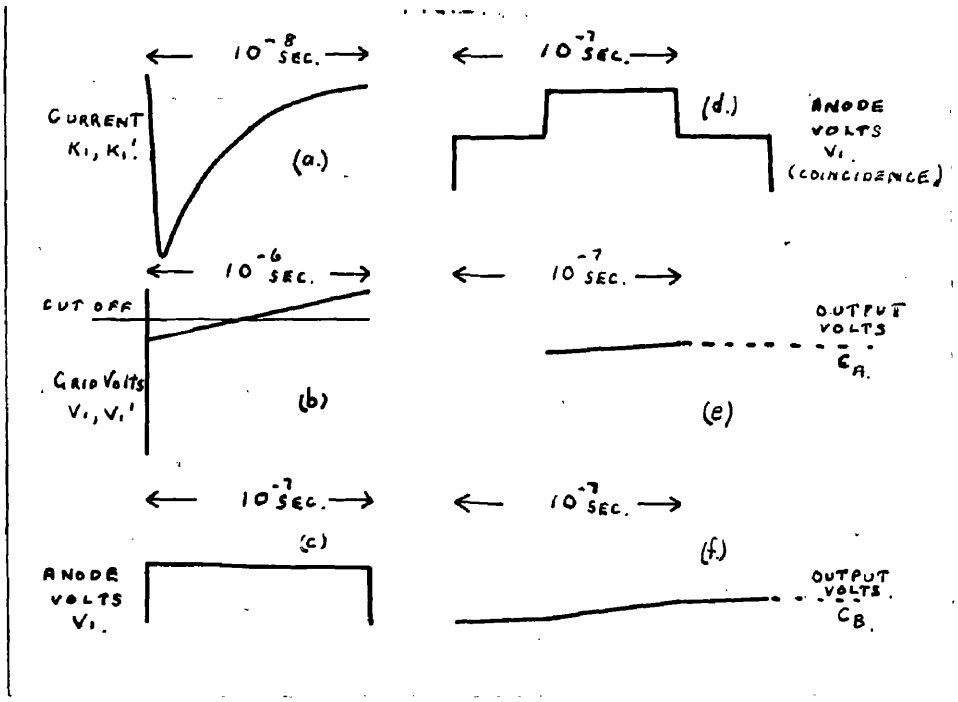

Fig.26.

Pulse shapes at different points in Fig.25.

APPENDIX

Section 3.

Low Level Fast Discriminator and High Speed Time Base.

Figure 27 shows the circuit diagram of a fast discriminator developed by the author to operate from fast pulses as small as 0.2 volts. It is essentially a blocking oscillator, in which a biased-off diode in the loop line reduces the loop gain to less than unity, thus allowing the oscillator valve (6CH6) to carry a normal current and provide amplification of the incoming pulse before the trigger action.

A negative input pulse to the grid of the first valve (CV138) is reversed by this valve and fed to the grid of the oscillator valve through the input diode. Since the oscillator valve is running, the pulse is amplified at the anode and is reversed by the ferrox-cube transformer and appears across the biased-off diode in the loop line. A sufficiently large input pulse causes this diode to conduct and the loop gain rapidly becomes greater than unity, strong feedback occurs

and the circuit then behaves as a normal blocking oscillator. The purpose of the input diode is to avoid loss of current through resistances in parallel with the grid to cathode path during the positive swing of the grid in the blocking oscillator action. The initial bias of the oscillator valve is supplied by a cathode follower (6AM6) to allow fast recovery after a pulse.

The characteristics of the output pulse from the circuit given here are a current of one ampere turned on for 10^{-7} sec. with a leading edge of 2.10^{-8} sec. The oscillator will operate from pulses as low as 0.2 volts by adjusting the bias of the grid of the oscillator valve. The ferrox-cube transformer was wound with eight turns on the primary and eight turns on the secondary.

The circuit shown in figure 28 is a simple high speed time base which can be operated by the output pulse from the discriminator described above. A positive pulse at the input appears on the grid of the oscillator

valve which is normally held off by about - 10 volts. An input pulse larger than 15 volts causes the oscillator valve to conduct sufficiently for blocking action. The output pulse of current in the cathode load of the oscillator valve has a duration of $\sim 2.10^{-7}$ sec. and rises to 1.5 amps in 10^{-8} sec. The ferrox-cube feedback transformer was wound with eight turns on the primary and secondary. The output voltage pulse on the cathode is amplified and fed to the X deflection plates of an oscilloscope through the step up transformer (ferrox-cube core) which had five turns on the primary and thirty on the secondary.

It is important to remember that at these frequencies the cathode load of the oscillator valve is the capacity of the X plates multiplied by the square of the turns ratio of the step up transformer. The oscilloscope used must have low capacity deflection plates to avoid integration of the sweep and the capacity of wiring on the secondary must be kept to a minimum.

Figure 2g shows the linearity and speed of the sweep observed on a high speed oscilloscope

tube type number VCRX 357A when a sine wave was applied to the Y deflection plates. Figure 30 shows a display of delayed double pulses with leading edges of 10^{-8} sec. for a slower time base speed obtained by increasing the capacity on the secondary of the step up transformer. The double pulse generator used to provide these pulses was a simple extension by the author of a circuit for a single pulse generator designed by Hutchinson (1953). In this extension two blocking oscillators biased off by variable amounts were triggered by essentially the same leading edge generated by a Miller time base. By varying the bias on each oscillator the time delay between the output pulses was varied.

The high speed circuitry described above was used extensively by the author for the development and testing of high speed circuitry and preliminary experiments on the feasibility of using millimicrosecond spectroscopy for measurements of neutron energies by time of flight. Figure 31 shows a graph of the line observed on the high speed oscilloscope time

base due to 14 Mev neutrons detected over a flight path of five metres. The arrangement used to obtain this line is shown in figure 21. The results obtained using this simple technique in which the position of pulses on the time base was recorded by eye led to the development of the time delay - voltage converter method described in the thesis in which the time delays are measured by pulse height analysers.

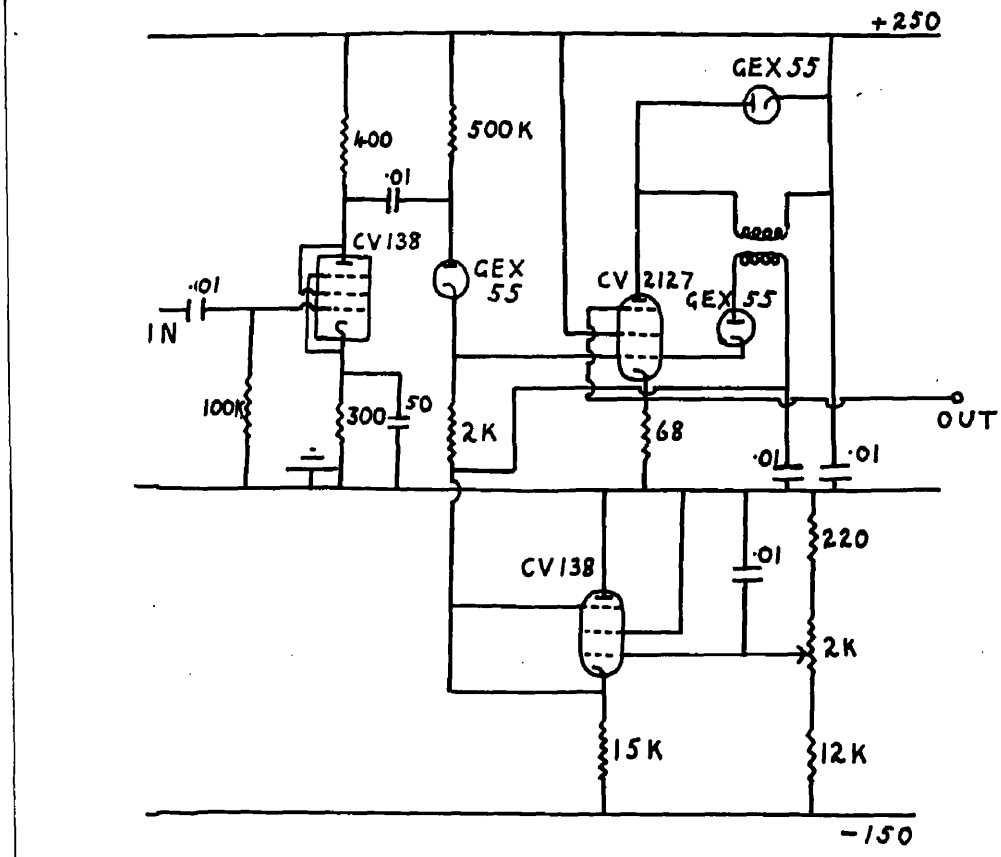

fig. 27.
Fast low level discriminator circuit.

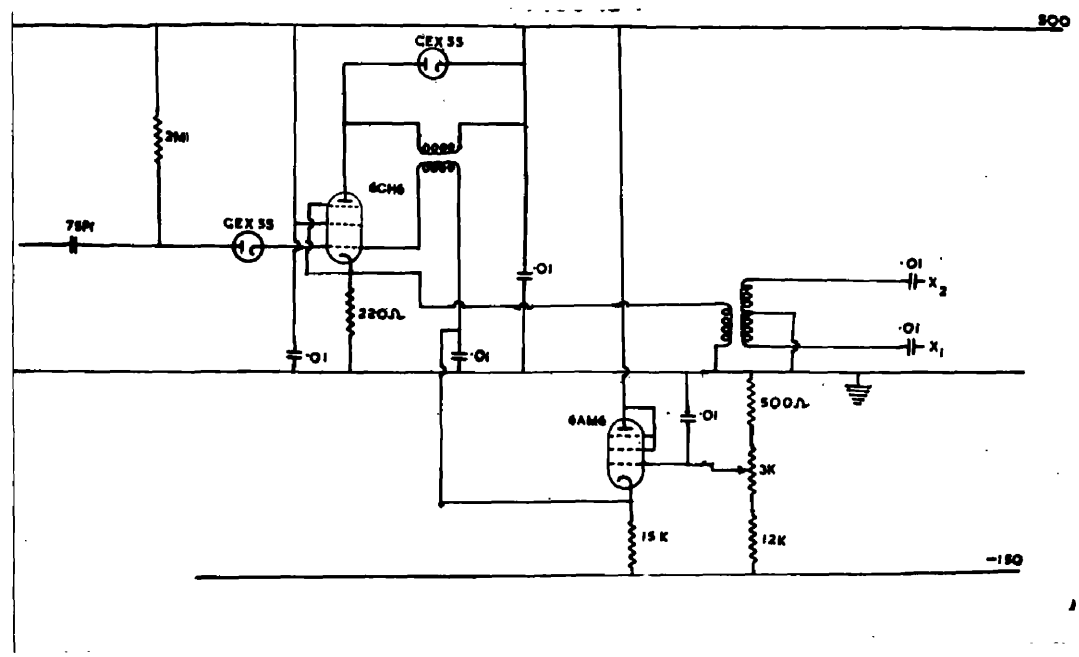

fig. 28
High speed time base circuit.

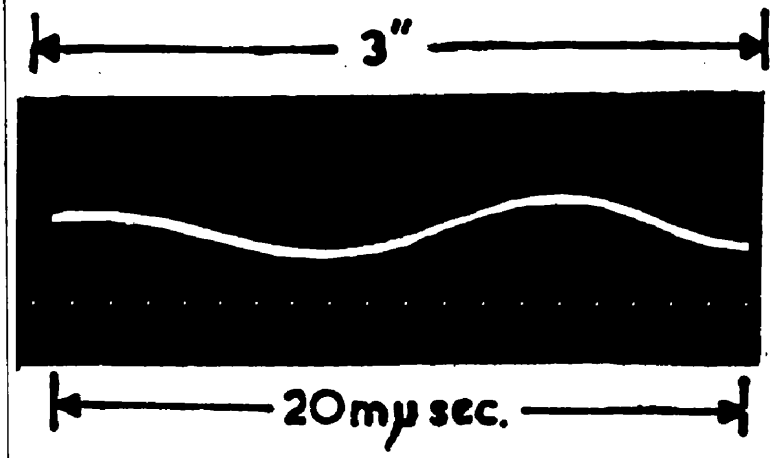

Fig.29.

High speed time base linearity and speed.

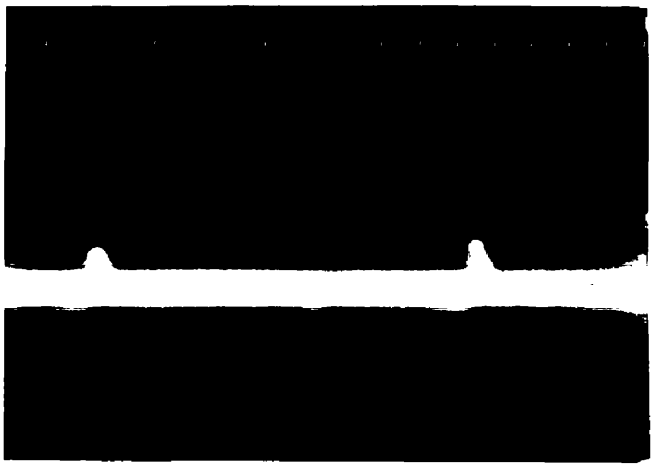

Fig.30.

Delayed double pulses.

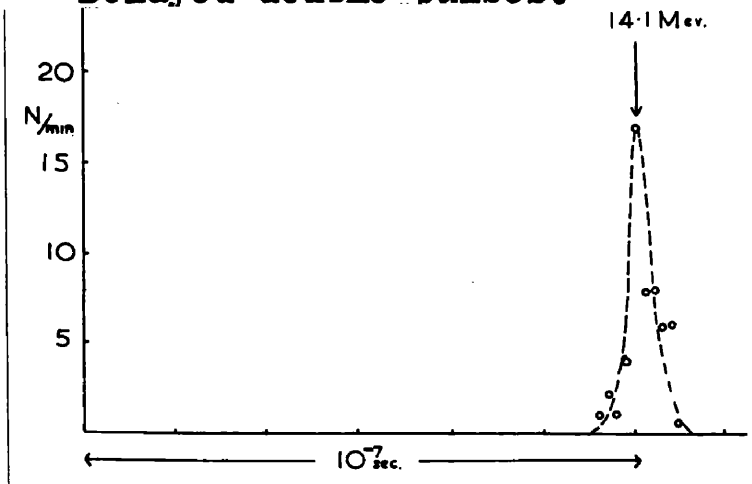

Fig.31.

14 MeV neutron line on high speed oscilloscope.

REFERENCES

Armstrong, A.H. et al (1953), Phys. Rev. 90, 340.

Aaron, W.A. et al (1949), A.E.C.U. - 663.

Ajzenberg, F. and Lauritsen, J. (1952, 1955), Rev. Mod. Phys. 27, 7.

Allison, S.K. and Warshaw (1953), Rev. Mod. Phys. 25,792.

Argo, H.Y. et al (1952), Phys. Rev. 87, 612.

Arnold, W.R. et al (1954), Phys. Rev. 93, 483.

Austern, N. and Butler, S.T. (1954), Phys. Rev. 93, 355.

Baker, P. and Waltner, A. (1952), Phys. Rev. 88, 1213.

Barschall, H.H. et al (1952), Phys. Rev. 86, 431.

Bartholdson, I. (1950), Ark. Fys. 2, 271.

Biedenharn, L.C and Rose, M.E (1949). SEE BLATT & WEISSKOPF.

Begbian, L.E. et al (1952), 86, 1044.

Birks, J.B. (1953), "Scintillation Counters", p.79, Pergamon Press, London.

Blatt, J.M. and Weisskopf, V.F. "Theoretical Nuclear Physics".

Boicourt, G.P and Brolley, J.E. (1954) Rev. Sci. Ins. 25, 1218.

Blatt, J.M. and Jackson, J.D. (1949), Phys. Rev. 76, 18.

Booth, D.L. (1955), Private Communication.

Bretcher, E and French, A.P (1949), Phys. Rev. 75,1154

Brolley, J.E. et al (1951), Phys. Rev. 82, 502.

Blair, J.M. et al (1954), Phys. Rev. 96, 1023.

Butler, S.T. (1950), Phys. Rev. 80, 1095.

Butler, S.T. (1951), Proc. Roy. Soc. A. 208, 559.

Butler, S.T. (1951), Phys. Rev. 83, 858.

Bohr, N. (1936, 1937) Nat. 137, 344; Kgl. Danoke Videnskab Selscab Mat-fys Medd 14, 10.

Bhatia, A.B. et al (1952), Phil. Mag. 43, 485.

Blin-Stoyle, R.J. (1951, 1952) Proc. Phys. Soc. ALXIV, 700 ; ALXV, 949.

(1955 Private Communication).

Burke, W.H. et al (1954), Phys. Rev. 93, 188.

Bennett, W.E. et al (1946), Phys. Rev. 69, 418.

Butler, S.T. and Austern, N., Phys. Rev. 93, 355 L(1954).

Coon, J. et al (1955), Private Communication.

Conner, J.P. et al (1952), Phys. Rev. 88, 468.

Curran, S.C. and Craggs, J.D. (1949), "Counting Tubes", (London, Butterworths Scientific Publications, p.45).

de Borde, A.H. (1955), Private Communication.

Elliot, E.A. et al (1953), Proc. Roy. Soc. A.216, 57.

Electronic Engineering (1952), Cormack, A. 24, 144.

Freemantle (see Fairbairn 1954).

Fairbairn, W.M. (1954), Proc. Phys. Soc. A.67, 990.

Fields, R.E. et al (1953), 89, 908A.

Fernbach, S. et al (unpublished report U.C.R.L. 4436, LY29) Radiation Lab. Univ. of California.

Flowers, B.H (1951), Proc. Roy. Soc. 204A, 503.

Fermi, E. and Marshall, L. (1947), Phys. Rev. 72, 1139.

Feshbach, H. (1949), Phys. Rev. 76, 1550.

Feshbach, H. et al (1954), Phys. Rev. 96, 448.

Foldy, L.L. (1951), Phys. Rev. 83, 688; 87, 693.

Green, A.E. and Schopper, E. (1952), Z. Naturf. 6a, 698 - 700.

Gittings, H.T et al (1949), Phys. Rev. 75, 1610.

Graves, E.R. and Rosen, L. (1953), Phys. Rev. 89, 343.

Gibson, W.M. (1949), Proc. Phys. Soc. A62, 586.

Grant, I.P. (1955), Proc. Phys. Soc. A68, 244.

Green, L.L. et al (1955), Proc. Phys. Soc. 86, 390.

Heintz, N.M. (1954), Phys. Rev. 93, 924 A.

Hunter, G.T. and Richards, H.T. (1949), Phys. Rev. 76, 1445.

Harrison, G.R. et al (1948), "Practical Spectroscopy", p.172, Blackie and Son, Glasgow.

Harwell (1955), "Neutron Physics Conference", Phys. Soc. Spring Meeting, A.E.R.E. (England).

Hutchinson, G.W. (1953), Nucleonics, No.11, 76.

Hutchinson, G.W. and Scarrott, G.G. (1951), Phil. Mag. 42, 792 (1951).

Hamilton, (1949) PROC. PHYS. SOC. 61 A. 12.

Hafner, E.M. et al (1953), Phys. Rev. 89, 204.

Heitler, W. (1944), "Quantum Theory of Radiation", 2nd Ed., University Press, Oxford.

Hemmendinger, A. and Argo, H.V. (1955), Phys. Rev. 98, 70.

Hughes, D.J. (1954), "Progress in Nuclear Physics", 4, 339.

Huby, R. (1953), "Progress in Nuclear Physics", 3, 177.

Havens, W.W. et al (1949, 1951), Phys. Rev. 75, 1295; 82, 345A.

Ihsan, M.A. (1955), Proc. Phys. Soc. 86, 393.

Johnson, V.R. (1949), Phys. Rev. 86, 302.

Mitchell, A.C.G et al (1949), PHYS. REV 76 1450

Mott, N.F. and Massey, H.S.W. (1949), "Theory of Atomic Collisions", Oxford, Clarendon Press, 2nd edn. p.283.

Mattauch, J. and Fluegge, S. (1946), "Nuclear Physics Tables ... "Interscience Pub. Inc., New York.

"Nuclear Data" (1950), John Smith & Son (Glasgow).

Nereson, N. and Darden, S. (1953), Phys. Rev. 89, 775.

O'Neill, G.K. (1954), Phys. Rev. 95, 1235.

Phillips, D.D. et al (1952), Phys. Rev. 88, 600.

Perlman, M.L. and Friedlander, (1951), Phys. Rev. 82, 449.

Prestwood, R.J. (1955), Phys. Rev. 98, 47.

Paul, E.B. and Clarke, R.L. (1953), Canad. Journal Phys. 31, 267.

Preston, G. et al (1954), Proc. Roy. Soc. A.226, 206.

Phillips, M. and Oppenheimer, J.R. (1935), Phys. Rev. 48, 500.

Perlman, M.L. and Welker, (1954), J. Phys. Rev. 95, 134.

Rose, et al (1952) SEE BLATT & WEISSCOPF

Rutherglen, J.G. et al (1954), Proc. Phys. Soc. A67,101

Remley, M.E et al (1953), Phys. Rev. 89, 1195.

Satchelor G.R. (1955), Private Communication.

Schrank, G. (1954), Phys. Rev. 96, 1156.

Snyder, C.W. and Parker, V.E. (1954), Bull. Am. Phys. Soc. 29, No.4.

Siegbahn, M. (1951), Almqvist and Wiksells, Boktrikeri A.B. Uppsala.

Storro, C.L. et al (1953), Phys. Rev. 90, 339.

Storey, R.S. (1955), Private Communication.

Stratton, T.F. et al (1952), Phys. Rev. 88, 261.

Schwinger, J. (1948), Phys. Rev. 73, 407.

Stelson, P.H. and Goodman, C. (1950), Phys. Rev. 82, 69.

Weisskopf, V.F. (1952), Blatt and Weisskopf "Theoretical Nuclear Physics".

Wilkinson, D.H.(1954).

Wilkinson, D.H.(1953), Phil. Mag. 44, 450.

Whitmore, B.G. and Denis, G.E. (1951), Phys. Rev. 84,296

Walt, M. and Barschall, H.H. (1953), Phys. Rev. 90, 714.

Wright, G.T. (1953), Phys. Rev. 91, 1283.

Ward, A. (1954), Nat. 173, 771.

Ward, A. (1954), Proc. Phys. Soc. A67, 841.

Ward, A. and Grant, P.J., Proc. Phys. Soc. A68, 637.

Yoccoz, J. (1954), Proc. Phys. Soc. A67, 813.